The intestinal epithelium during damage and regeneration

Cell type-specific responses in experimental colitis and after cytostatic drug treatment

The intestinal epithelium during damage and regeneration:
Cell type-specific responses in experimental colitis and after cytostatic drug treatment
Ingrid B. Renes

Thesis, Erasmus University - with references - with a summary in Dutch
ISBN 90-6734-017-0

Printed by Optima Grafische Communicatie , Rotterdam, The Netherlands (www.ogc.nl)
© 2002 Ingrid B. Renes, Rotterdam, The Netherlands.
All Rights reserved. No part of this thesis may be reproduced or transmitted in any form, by any means, electronic or mechanical, without prior written permission of the author.

The intestinal epithelium during damage and regeneration

Cell type-specific responses in experimental colitis and after cytostatic drug treatment

Het darmepitheel gedurende schade en regeneratie

Cel type-specifieke responsen in experimentele colitis en na cytostatica behandeling

Proefschrift

ter verkrijging van de graad van doctor aan de
Erasmus Universiteit Rotterdam
op gezag van de Rector Magnificus
Prof.dr.ir. J.H. van Bemmel
en volgens besluit van het College voor Promoties

De openbare verdediging zal plaatsvinden op
woensdag 20 november 2002 om 15.45 uur

door

Ingrid Brunhilde Renes

Geboren te Zeist

Promotie commissie

Promotor:	Prof.dr. H.A. Büller
Overige leden:	Prof.dr. E.J. Kuipers
	Prof.dr. D. Tibboel
	Dr.ir. H.W. Verspaget
Copromotoren:	Dr. A.W.C. Einerhand
	Dr. J. Dekker

Publication of this thesis was financially supported by:
Sectie Experimentele Gastroenterologie van de
Nederlandse Vereniging voor Gastroenterologie
Nutricia Nederland B.V.
AstraZeneca B.V.

The work described in this thesis was performed at the Laboratory of Pediatric Gastroenterology & Nutrition of the Academic Medical Center, Amsterdam, The Netherlands and at the Laboratory of Pediatrics, Pediatric Gastroenterology & Nutrition, of the Erasmus MC, Rotterdam, The Netherlands. Part of this project was financially supported by Numico BV, Zoetermeer, The Netherlands.

Contents

Chapter 1

Introduction

Introduction

The intestinal epithelium

The intestinal mucosa is covered by a continuous monolayer of epithelial cells, which are connected via tight junctions. This monolayer of epithelial cells separates the mucosa from the intestinal lumen, which is in continuity with the external environment. The intestinal epithelium exerts many physiological functions including digestion and absorption of nutrients, secretion and absorption of electrolytes and water, and defense against pathogens and noxious agents within the intestinal lumen. Each of these functions is conducted by specialized cells, which together form the intestinal epithelium. These specialized cells arise from progenitors located in the intestinal crypts [1]. As cells migrate upwards and out of the crypts or downwards to the bottom of the crypts they differentiate, and thus acquire the specific modalities, which enables them to exert their specific functions. Finally, at the end of their lifespan, *i.e.* 3-5 days, the upwards migrating cells reach the tips of the villi (in the small intestine) or the surface epithelium (in the colon), where they undergo apoptosis and/or are shed into the lumen [2]. The downwards migrating cells differentiate to Paneth cells, undergo apoptosis at the end of their lifespan at approximately 3 weeks, and are subsequently phagocytosed.

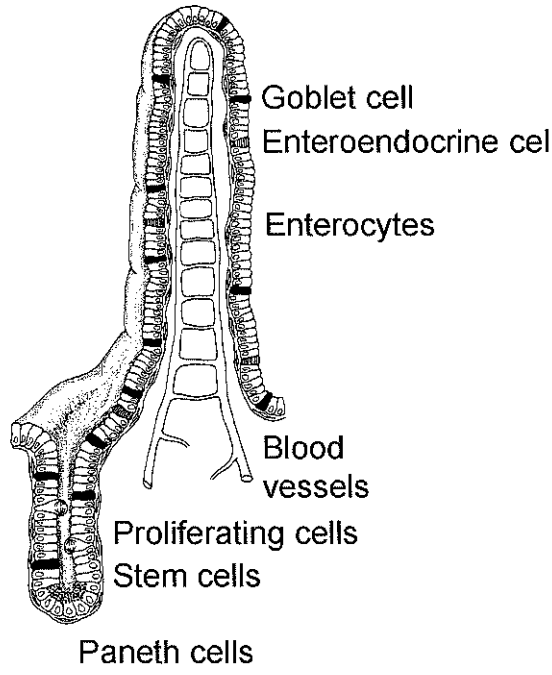

Figure 1. Schematic representation of the small intestinal epithelium (as published by Dekker *et al.* 2002[3]). The small intestinal epithelium contains four differentiated cell types: enterocytes, goblet cells, enteroendocrine cells, and Paneth cells.

The small intestinal epithelium, which is organized into crypts and villi, contains at least 4 distinct specialized cell types: enterocytes, goblet cells, enteroendocrine cells, and Paneth cells (Fig. 1). The enterocytes, goblet cells and enteroendocrine cells are located in the upper crypts and along the villi. Paneth cells reside at the crypt base. The colonic epithelium is organized into crypts and surface cuffs instead of villi and consists of 3 distinct specialized cell types: the enterocytes, goblet cell and enteroendocrine cells. In the small intestine, the enterocytes play a critical role in the degradation, uptake and transport of nutrients by expressing, *i.a.* the sugar degrading enzymes lactase and sucrase-isomaltase (SI), the glucose and fructose transporters 2 and –5 (Glut2 and –5), and the fatty acid binding proteins (FABPs) [3-5]. The colonic enterocytes are specialized in electrolyte and water absorption [6], therefore they express gene products like carbonic anhydrase I and -IV (CA I and IV), and the sodium hydrogen exchanger 2 and -3 (NHE2 and -3) [7-10]. Both the enterocytes in the small intestine and in the colon appear to be involved in the epithelial defense by the expression of alkaline phosphatase (AP) at their apical membranes, which has detoxifying capacities [11, 12]. Enteroendocrine cells are specialized in the mucosal secretion of hormonal peptides, which mediate for example motility in the gastrointestinal tract. Paneth cells are exclusively present in the small intestine and have a critical role in the epithelial defense by the synthesis of antimicrobial peptides [13]. Goblet cells synthesize the secretory mucin MUC2, which is the most important structural component of the intestinal mucus layer [14]. This mucus layer serves as a barrier to protect the epithelium from mechanical stress, noxious agents, bacteria, viruses and other pathogens [15, 16]. Goblet cells are also known to synthesize and secrete trefoil factor 3 (TFF3), a bioactive peptide which is involved in epithelial repair [17, 18].

Under normal conditions, *i.e.* in health, epithelial proliferation, differentiation and apoptosis are tightly regulated and are therefore in balance. Yet, during intestinal diseases or after treatment with cytostatic drugs epithelial damage occurs and the homeostasis in proliferation, differentiation, and apoptosis is disturbed leading to alterations in epithelial cell functions and thus alterations in intestinal functions.

Inflammatory bowel diseases and the intestinal epithelium

The inflammatory bowel diseases (IBDs), ulcerative colitis (UC) and Crohn's disease (CD), are characterized by chronic inflammation of parts of the gastrointestinal tract. The intestinal epithelium is severely damaged, and crypt distortions, crypt abscesses, depletion of mucins from goblet cells, and loss of epithelium (in particular ulcerations) are observed in both types of disease. IBD patients can suffer from body weight loss, loose and bloody stools, and diarrhea. Therapies are aimed at alleviating the symptoms, induction of remission, and reducing the number and severity of relapses by down-regulation of the inflammatory response. Despite the fact that the etiology of UC and CD is unknown, it is clear that the cause and course of these diseases is multifactorial with both environmental and genetic components, involving the immune system, microbial factors, and the epithelium together with its associated mucus-layer. As the epithelium with its associated mucus-layer forms a

physical barrier between the immune cells in the lamina propria and the bacteria in the intestinal lumen, it is more than likely that the epithelium plays a central role in UC and CD. The central role of the epithelium and in particular its associated mucus layer in IBD is reviewed in detail in chapter 2 of this thesis [19].

Still, relatively little is known about enterocyte functions, goblet cell functions and the epithelial functions in general during these inflammatory diseases. Focussing on UC, aberrations in Na^+ and Cl^- absorption and secretion were observed [20, 21], however, information on the (regulation of) expression levels of the genes that are directly or indirectly involved in these processes, like NHE2, NHE3, CA I, and CA IV is lacking. Another limitation of these studies in human tissue is that only the sigmoid colon is investigated, and that mostly only active colitis is compared with control, *i.e.* UC in remission was not studied.

In contrast, much more is known about goblet cell-specific MUC2 expression levels and alteration in the structure of MUC2 during health and in UC. MUC2 expression was extensively studied, as it is the predominant structural component of the protective mucus layer [14]. Therefore it was reasoned that changes in MUC2 levels and structure could play a role in the pathogenesis of UC. These studies demonstrated that MUC2 synthesis, sulfation and secretion is decreased in active UC, but restored while UC is in remission [22, 23]. This implies altered mucosal protection in active UC, and more importantly that alterations in MUC2 synthesis, sulfation and secretion are not the underlying primary defect in the onset of UC. But what consequences does the altered protective efficacy of the intestinal mucus-layer have during active UC? Does it result in an increased association of luminal bacteria with the epithelium? Does it result in damage to the protected epithelium? And how does the epithelium respond to this? In other words; do enterocyte functions, goblet cell functions and epithelial functions in general alter during the different phases of UC? It is difficult, or in some cases even impossible, to address these questions in human patients with UC. For example, in UC, patients biopsy specimens are generally taken from the distal colon and not from the proximal colon, as it is a too heavy burden for the patient to take biopsies from the proximal colon. Therefore, information about the epithelium in the proximal colon is very difficult to obtain. Additionally, the onset of UC is often devoid of symptoms, thus when patients visit their physician the disease is already established and has entered an already more chronic phase. In other words, the initial acute phase of UC is not easily studied in humans. Furthermore, patients undergo anti-inflammatory therapy, which may complicate interpretation of the results. Therefore, in the first part of this thesis a rat model was used to analyze enterocyte-specific functions, goblet cell-specific functions, and general epithelial functions during health and dextran sodium sulfate (DSS)-induced colitis (Chapters 3-5).

Cytostatic drug treatment and the intestinal epithelium

Among the cytostatic agents, the application of the folate antagonist methotrexate (MTX) either alone or in combination regimens to treat cancer has been extensively described. MTX alone is highly effective in the treatment of choriocarcinoma, as 50% of the patients bearing this tumor appear to be cured after MTX treatment. MTX is used in combination regimens to

treat acute lymphoblastic leukemia, lymphoma, advanced breast cancer, bladder cancer, and cancer of the head and neck [24, 25]. In combination with leucovorin 'rescue', high doses of MTX are used as adjuvant therapies for breast cancer and osteosarcoma [25].

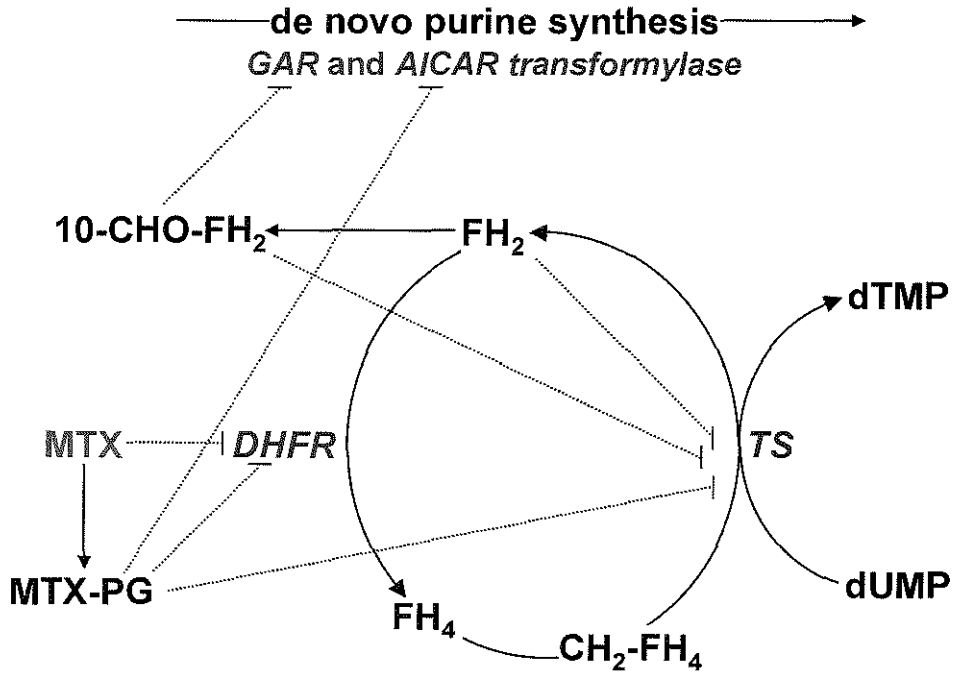

Figure 2. Mechanisms of action of methotrexate. Methotrexate (MTX) inhibits the enzyme dyhydrofolate reductase (DHFR). Moreover, MTX is polyglutamated (MTX-PG) intracellularly. MTX-PG is a potent inhibitor of DHFR, thymidylate synthetase (TS), and of aminoimidazole carboxamide ribunucleotide (AICAR) transformylase. Dihydrofolate (FH2) which accumulates due to inhibition of DHFR, is converted to folate byproduct 10-formyl-FH2 (10-CHO-FH2). 10-CHO-FH2 is an inhibitor of glycinamide ribonucleotide (GAR) transformylase. FH4, tetrahydrofolate; CH_2-FH_4, N5,N10-methylene tetrahydrofolate; dUMP, deoxyuridylate; TMP, thymidyne monophosphate.

The mechanism of action of MTX is based on its ability to bind to the key enzyme in the thymidylate cycle, dihydrofolate reductase (DHFR) (Fig. 2, [24, 25]). DHFR is responsible for the formation of the co-enzyme tetrahydrofolate, which in turn is necessary for the thymidylate and purine biosynthesis. In rapidly proliferating tissues the binding of MTX to DHFR results in the inhibition of tetrahydrofolate formation, and hence thymidylate biosynthesis. This in turn, leads to a decrease in thymidine triphosphate pools, a decrease in DNA synthesis, and eventually to cell death. Additionally, MTX, its metabolites, and the folate byproducts (dihydrofolate and 10-formyldihydrofolate), which are formed by the

inhibition of DHFR can also inhibit de novo purine synthesis (Fig. 2, [24, 25]). Thus MTX treatment can lead to the inhibition of DNA and RNA synthesis and even to inhibition of protein synthesis in tumor tissue as well as normal tissue.

Because of the actions on thymidylate biosynthesis and thus DNA synthesis, MTX and other folate antagonists are extremely toxic to rapidly proliferating tissues like tumor tissue, bone marrow and the small intestinal epithelium. It is this toxic effect of cytostatic drugs that often limits the clinical application. Many cytostatic regiments have severe gastrointestinal side effects. Insight in the mechanism and possible prevention of gastrointestinal damage will be of paramount importance in the treatment of cancer patients. The effects of methotrexate (MTX) on the small intestinal epithelium of human and rat are well described. MTX is known to inhibit epithelial proliferation and induce apoptosis in the proliferative compartment of the small intestine, the crypts [26]. Furthermore, MTX is known to induce loss of crypts, crypt atrophy, and villus atrophy [26-29]. In rat and mice small intestine MTX treatment induced a down-regulation of SI and lactase enzyme activities [26]. Collectively these data demonstrate that MTX treatment results in impairment of small intestinal epithelial functions in general. However, it is unclear how MTX treatment affects specific enterocyte functions, goblet cell functions, and Paneth cell functions. In other words, does MTX affect enterocyte specific -, goblet cell specific -, and Paneth cell specific RNA and protein synthesis? Moreover, knowledge of region-specific variation in MTX-sensitivity within the small intestine is also lacking. Specifically, it is not clear whether there is a difference in MTX sensitivity between; 1) the epithelium of the duodenum, jejunum and ileum, 2) the epithelium located near lymphoid nodules within the small intestinal mucosa, *i.e.* the Peyer's patches (PPs). Hence, in the second part of this thesis (Chapters 6-7), a rat-MTX model was used to analyze cell type-specific functions and region-specific variations in MTX sensitivity.

Aims and outline of this thesis

In the first part of this thesis the role of the colonic epithelium and in particular its associated mucus-layer during IBD and in several experimental colitis models is discussed (Chapter 2). In Chapter 3-5 our investigations regarding the colonic epithelium in rat during the different phases of DSS-induced acute colitis are described. Studied are:

A. clinical symptoms, morphology, proliferation and apoptosis (Chapter 3).
B. enterocyte-specific gene expression, goblet cell-specific gene expression, and the Muc2 - and TFF3 secretion capacity of goblet cells, as a measure of enterocyte and goblet cell functioning (Chapters 4 and 5).
C. goblet cell-specific Muc2 biosynthesis, Muc2 sulfation, and Muc2 secretion (Chapter 5).

These parameters were studied in conjunction during the onset of disease, active disease and the regenerative phase of DSS-induced colitis, in the proximal and distal colon to obtain insight in the specific colonic functions during damage and regeneration.

In the second part of this thesis the small intestinal epithelium after treatment with the cytostatic drug MTX is investigated. Described are:

A. clinical symptoms, morphology, proliferation, apoptosis, and enterocyte-, goblet cell-, and Paneth cell specific gene expression in the 'normal' small intestinal epithelium, *i.e.* the epithelium distant from the Peyer's Patches (Chapter 6).
B. the above described parameters in the PP-associated epithelium, and compared these with alterations seen in the small intestinal located more distantly from PP (Chapter 7).

These parameters were studied on various days after MTX-treatment in the duodenum, jejunum, ileum, and colon to obtain a complete picture of the epithelial functions during MTX-induced damage and regeneration.

Finally, by comparing the DSS-induced colonic damage with the MTX-induced small intestinal damage, the obtained insight in the types of damage and damage control in the colon and small intestine are discussed (Chapter 8).

References

1. Potten CS, Loeffler M. Stem cells: attributes, cycles, spirals, pitfalls and uncertainties. Lessons for and from the crypt. Development 1990;110:1001-20.

2. Hall PA, Coates PJ, Ansari B, Hopwood D. Regulation of cell number in the mammalian gastrointestinal tract: the importance of apoptosis. J Cell Sci 1994;107 (Pt 12):3569-77.

3. Dekker J, Einerhand AWC, Büller HA. Carbohydrate Malabsorption. In: Lifschitz CH, ed. Pediatric Gastroenterology and Nutrition in Clinical Practice. New York: Dekker, M., 2002:339-373.

4. Alpers DH. Digestion and Absorption:Digestion and Absorption of Carbohydrates and Proteins. In: Johnson LR, ed. Physiology of the Gastrointestinal Tract, 3rd Edition. Volume 2. New York: Raven Press, 1994:1723-1749.

5. Alpers DH, Bass NM, Engle MJ, DeSchryver-Kecskemeti K. Intestinal fatty acid binding protein may favor differential apical fatty acid binding in the intestine. Biochim Biophys Acta 2000;1483:352-62.

6. Binder HB, Sandle GI. Digestion and Absorption: Electrolyte Transport in the Mammalian Colon. In: Johnson LR, ed. Physiology of the Gastrointestinal Tract. Volume 2. New York: Raven Press, 1994:2133-2171.

7. Fleming RE, Parkkila S, Parkkila AK, Rajaniemi H, Waheed A, Sly WS. Carbonic anhydrase IV expression in rat and human gastrointestinal tract regional, cellular, and subcellular localization. J Clin Invest 1995;96:2907-13.

8. Sowden J, Leigh S, Talbot I, Delhanty J, Edwards Y. Expression from the proximal promoter of the carbonic anhydrase 1 gene as a marker for differentiation in colon epithelia. Differentiation 1993;53:67-74.

9. Bookstein C, DePaoli AM, Xie Y, Niu P, Musch MW, Rao MC, Chang EB. Na+/H+ exchangers, NHE-1 and NHE-3, of rat intestine. Expression and localization. J Clin Invest 1994;93:106-13.

10. Bookstein C, Xie Y, Rabenau K, Musch MW, McSwine RL, Rao MC, Chang EB. Tissue distribution of Na+/H+ exchanger isoforms NHE2 and NHE4 in rat intestine and kidney. Am J Physiol 1997;273:C1496-505.

11. Poelstra K, Bakker WW, Klok PA, Kamps JA, Hardonk MJ, Meijer DK. Dephosphorylation of endotoxin by alkaline phosphatase in vivo. Am J Pathol 1997;151:1163-9.

12. Poelstra K, Bakker WW, Klok PA, Hardonk MJ, Meijer DK. A physiologic function for alkaline phosphatase: endotoxin detoxification. Lab Invest 1997;76:319-27.

13. Ouellette AJ, Bevins CL. Paneth cell defensins and innate immunity of the small bowel. Inflamm Bowel Dis 2001;7:43-50.

14. Tytgat KMAJ, Büller HA, Opdam FJ, Kim YS, Einerhand AWC, Dekker J. Biosynthesis of human colonic mucin: Muc2 is the prominent secretory mucin. Gastroenterology 1994;107:1352-63.

15. Forstner JF, Forstner GG. Gastrointestinal mucus. In: R. JL, ed. Physiology of the Gastrointestinal Tract. Volume 2. New York: Raven, 1994:1255-1283.

16. Van Klinken BJW, Dekker J, Büller HA, Einerhand AWC. Mucin gene structure and expression: protection vs. adhesion. Am J Physiol 1995;269:G613-27.

17. Mashimo H, Wu DC, Podolsky DK, Fishman MC. Impaired defense of intestinal mucosa in mice lacking intestinal trefoil factor. Science 1996;274:262-5.

18. Wong WM, Poulsom R, Wright NA. Trefoil peptides. Gut 1999;44:890-5.

19. Einerhand AWC, Renes IB, Makkink MK, Van der Sluis M, Büller HA, Dekker J. Role of mucins in inflammatory bowel disease: Important lessons from experimental models. European Journal of Gastroenterology and Hepathology 2002; 14:757-65.

20. Charney AN, Dagher PC. Acid-base effects on colonic electrolyte transport revisited. Gastroenterology 1996;111:1358-68.

21. Ejderhamn J, Finkel Y, Strandvik B. Na,K-ATPase activity in rectal mucosa of children with ulcerative colitis and Crohn's disease. Scand J Gastroenterol 1989;24:1121-5.

22. Tytgat KMAJ, van der Wal JW, Einerhand AWC, Büller HA, Dekker J. Quantitative analysis of MUC2 synthesis in ulcerative colitis. Biochem Biophys Res Commun 1996;224:397-405.

23. Van Klinken BJW, Van der Wal JW, Einerhand AWC, Büller HA, Dekker J. Sulphation and secretion of the predominant secretory human colonic mucin MUC2 in ulcerative colitis. Gut 1999;44:387-93.

24. Allegra JA. Antifolates. In: Chabner BA, Collins JM, eds. Cancer chemotherapy: Principles and Practice. Philadelphia: Lippincott, 1990:110-153.

25. Kamen BA, Cole PD, Bertino JR. Chemotherapeutic Agents: Folate Antagonists. In: Bast Jr. RC, Kufe DW, Pollock RE, Weichselbaum RR, Holland JF, Frei E, eds. Cancer Medicine. 4 ed. Hamilton: B. C. Decker INc., 1997:907-22.

26. Taminiau JAJM, Gall DG, Hamilton JR. Response of the rat small-intestine epithelium to methotrexate. Gut 1980;21:486-92.

27. Pinkerton CR, Cameron CH, Sloan JM, Glasgow JF, Gwevava NJ. Jejunal crypt cell abnormalities associated with methotrexate treatment in children with acute lymphoblastic leukaemia. J Clin Pathol 1982;35:1272-7.

28. Altmann GG. Changes in the mucosa of the small intestine following methotrexate administration or abdominal x-irradiation. Am J Anat 1974;140:263-79.

29. Trier JS. Morphological alterations induced by methotrexate in the mucosa of human proximal intestine. Gastroenterology 1962:295-305.

Chapter 2

Role of mucins in inflammatory bowel disease:
Important lessons from animal models

Adapted from:
Alexandra W.C. Einerhand, Ingrid B. Renes, Mireille K. Makkink, Maria Van der Sluis, Hans A. Büller, Jan Dekker. Role of mucins in inflammatory bowel disease: *Important lessons from experimental models*. Eur. J Gastroenterol Hepathol 2002, 14:757-765.

Summary

Inflammatory bowel disease (IBD) is characterized by a chronically inflamed mucosa of the gastrointestinal tract, caused by an underlying immune-imbalance and triggered by luminal substances including bacteria. Mucus forms a gel-layer covering the gastrointestinal tract, acting as a semi-permeable barrier between lumen and epithelium. Mucins, the building blocks of the mucus-gel, determine the thickness and properties of mucus. In IBD in humans alterations in both membrane-bound and secretory mucins have been described involving genetic mutations in mucin genes, degradation of mucin, changes in mucin levels, and the degree of glycosylation and sulfation of the mucins. As mucins are strategically positioned between the vulnerable mucosa and the bacterial contents of the bowel, changes in mucin structure and/or quantity likely influence their protective functions and therefore constitute possible etiological factors in the pathogenesis of IBD. This hypothesis, however, is difficult to prove in humans. Animal models for IBD permit detailed analysis of those aspects of mucins necessary for protection against disease. These models revealed pertinent data as for how changes in mucins, in particular in MUC2, imposed by immunological or microbial factors, may contribute to the development and/or perpetuation of chronic IBD, and shed some light on possible strategies to counteract disease.

Mucins in IBD: A review

The tripartite cause of IBD; involvement of mucins

The two forms of chronic human inflammatory bowel disease (IBD), Crohn's disease (CD) and ulcerative colitis (UC), are diseases primarily characterized by chronic inflammation of parts of the gastrointestinal tract. These are complex diseases caused by multiple environmental and genetic factors involving: 1) the immune system, 2) microbial factors, and 3) the intestinal epithelial barrier. Existence of an **immune imbalance** is one of the critical factors in the manifestation of IBD. Proof for this comes from various animal models with altered T-cell populations or cytokine deficiencies that spontaneously develop colitis, as reviewed [1, 2]. **Microbial factors** are implicated in the initiation and/or perpetuation of disease. The development of colitis in many animal models can be prevented or attenuated if animals were maintained in a germ free environment or treated with oral antibiotics [3-5]. Considering that the epithelium and its associated mucus-layer forms a physical barrier between bacteria and cells of the immune system, it is more than likely that **the epithelial barrier** plays an important role in IBD. In support of this are several animal models in which a primary change in integrity of the epithelium leads to IBD-like syndromes. For instance, transgenic mice expressing a dominant-negative mutant of cadherin on their small intestinal enterocytes spontaneously develop IBD, caused by breaching of the epithelial barrier [6]. In another model, mice deficient in the multi-drug resistant protein, which is normally found in the intestinal epithelium (mdr1a) spontaneously develop colitis. These IBD-like symptoms resolved under antibiotic treatment, indicating that bacteria critically affect the epithelium [16]. Mice carrying a homozygous knockout mutation in the trefoil factor-3 (TFF3) gene prove very sensitive to developing colitis, whereas supplementation of these knockout mice with TFF3 reverted the disease [17]. Each of these examples illustrates that many proteins expressed in intestinal epithelial cells are, directly or indirectly, involved in the protective epithelial barrier against IBD.

Mucins, as the primary constituents of extracellular mucus and the cellular barrier, are intimately associated with each of the three etiological factors of IBD. Mucins are important epithelial products of the intestine, essential for a proper epithelial barrier function, whereas both inflammatory mediators and bacterial factors are identified that influence the expression of the mucins. Moreover, mucins are very important in the contact of many microorganisms with the intestinal mucosa. Therefore a primary defect in mucins could breach the epithelial barrier or lead to altered mucosal-bacterial interactions. On the other hand, the changing effects of immunological or bacterial factors during initial or ongoing inflammation could influence the mucin-production, and have further adverse effects on these processes, sustaining the chronic character of IBD. Mucin expression and structure was influenced by cytokines, bacteria, and bacterial components in *in vitro* experiments on intestinal cell lines [18-22], which has contributed considerably to the interest in mucins as possible etiological factors in IBD.

MUC-type mucins in human intestine

Mucus forms a semi-permeable barrier between the intestinal lumen and the underlying epithelium, and is composed primarily of secretory gel-forming mucins, like MUC2 [23]. Other mucins exist in the intestine, like MUC3 found in intestinal microvilli, that are membrane-bound and form integral components of the apical side of the epithelial cells, but seem to be no part of the mucus-layer.

Biochemically, mucins are usually very large, filamentous molecules (molecular weight up to several millions). Mucins have very large regions within their polypeptides, which are comprised of relatively short tandemly repeated peptide domains, which are highly *O*-glycosylated [23, 24]. The *O*-linked carbohydrates form up to 80% of the molecular weight of the mucins. These very numerous, yet relatively short carbohydrate chains (2-20 monosaccharides), are very tightly packed along the polypeptide and are responsible for the overall filamentous structure of mucins. The addition of very large numbers of sulfate and sialic acid residues to the *O*-linked carbohydrates gives the mucins a highly negative surface charge.

Many of the known human mucin genes are presently assembled in the MUC gene family. The current nomenclature of the mucins is meanwhile challenged, as there appear to be large differences in primary sequence as well as function among the MUC-type mucins [25]. Functionally, MUC-type mucins can be subdivided into three classes: 1) secretory, gel-forming mucins, 2) membrane-bound mucins, and 3) small soluble mucins.

Ad. 1. Secretory, gel-forming mucins are widely acknowledged as important players in the defense of the gastrointestinal epithelium, and are produced in specialized mucous cells of glandular tissues and goblet cells of gastrointestinal tract [23, 26-28]. These mucins are produced as disulfide-linked oligomers [29], which proves essential for their ability to form viscoelastic mucus-gels. There are four members to this group, MUC2, -5AC, -5B, and -6, and these are well characterized [30, 31]. In the healthy human colon MUC2 is the predominant mucin produced by all goblet cells, and MUC5B is expressed in minor quantities in a subset goblet cells in the lower colonic crypts [27, 28, 32]. MUC5AC and MUC6 are normally confined to gastric epithelium [33], and are not expressed in the healthy intestines, but these MUCs appear in the colon in IBD [34, 35].

Ad. 2. The membrane-bound mucins have been shown to be involved in epithelial cell-signaling, adhesion, growth, and modulation of the immune system [26, 36-40]. Membrane-bound mucins are not covalently bound, and are made in serous cells or epithelial cells, like enterocytes [24, 39]. Of the membrane-bound mucins MUC1, MUC3A, MUC3B, MUC4 have been extensively studied, and their expression was also analyzed in IBD [34, 41, 42].

Ad. 3. So far only one small soluble human mucin has been identified (MUC7), which is found in saliva [43]. As MUC7 was not studied in IBD, it will not be discussed further. Other genes have been assigned to the MUC family (MUC8, -11, -12, -13, and -16) [44-47]. Although some of these are expressed in the intestine [45, 46], their involvement in IBD has not yet been analyzed.

Genetic deviations in human MUC3A are associated with IBD

For long it is known that IBD has a certain genetic predisposition, and therefore many investigators have sought to identify chromosomal loci in the human genome that predispose for IBD. Among the different susceptibility loci identified for IBD is 7q22, which harbors MUC3A, MUC3B, MUC11 and MUC12 [45, 48-51]. Further analysis has demonstrated an association of IBD with the intestinal membrane-bound mucin gene MUC3A (Table 1) [50, 51]. It was only recently shown that the gene originally designated MUC3 in fact consists of two genes MUC3A and MUC3B [49, 50, 52-56]. The entire structures of both MUC3A and MUC3B, in particular their N-termini are still unknown, because cloning of sequences containing long stretches of tandem repeats remains difficult. However both genes encode membrane-bound mucins with two EGF-like motifs, a membrane-spanning and a cytoplasmic domain at their C-terminal ends [25, 50].

Table 1. ***Summary of pathological changes in colonic mucin expression found in patients with ulcerative colitis (UC) and Crohn's disease (CD))***[A]

Characteristic	UC	CD	Reference
Mutations	altered VNTR	SNP in MUC3)[C]	50, 51
Mucus thickness	Reduced	unaltered	57
Goblet cells (numbers)	Depleted	unaltered	58
Sulfation	Reduced	unaltered	59, 60
Glycosylation	altered	altered	61, 62
MUC2 (protein-level)	decreased	n.d.)[D]	63, 64
MUC1, -3, -4, -5B (mRNA-levels)	unaltered	reduced	42
MUC2 (mRNA-levels)	unaltered	unaltered	34, 64
MUC5AC, -6 (mRNA-levels)	n.d.	increased	34
Anti-MUC auto-antibodies	present	absent	65
Number of bacteria in mucus	increased	n.d.	66

)[A] In Crohn's disease focus was on effects on colonic mucin. Only in this way the effects could be made comparable with the effects of ulcerative colitis, as the latter disease only occurs in the colon.

)[B] VNTR, variable number of tandemly repeated sequences

)[C] SNP, single nucleotide polymorphism

)[D] n.d., not determined

The possession of one or two rare alleles of the MUC3A gene, which have an unusual number of 51-bp repeat units, was associated with UC [51]. It could well be that these unusual forms of MUC3A negatively affect the barrier function within the intestine, conferring a genetic predisposition to UC. Furthermore, it was recently reported that non-synonymous single nucleotide polymorphisms within the cytoplasmic C-terminus of MUC3A, involving a tyrosine residue with a proposed role in epithelial cell signaling, may confer genetic predisposition to CD [50]. This indicates that genetic variants of the membrane-bound MUC3A may be involved in predisposition for UC and CD by dissimilar mechanisms. Whether other mucin genes on the 7q22 locus are associated with CD or UC still remains to be investigated.

To date none of the other mucin genes, have genetically been linked to the occurrence of UC or CD. In particular allelic variations of MUC2 were investigated, since MUC2 is the most prominent secretory mucin in the intestines [32], but no association with UC could be identified [67].

Changes in human and rodent intestinal mucins are associated with IBD: focus on MUC2

Alterations in mucin synthesis, maturation, secretion, and/or degradation in IBD are generally thought to be involved in the initiation or perpetuation of disease symptoms. The most important alterations in mucin in IBD were very recently summarized (Table 1) [68-70]. These quantitative and/or qualitative alterations in mucin synthesis may be related to mutations within mucin genes, as for MUC3A, or to changes in immunological or microbial factors that govern the mucin expression. The most pertinent data that help us understand the causes and consequences of these alterations comes however from studies in the mouse and rat, which will be an important focus of this review.

In the mouse, thus far six Muc-type genes have been identified (Table 2), and named after their human orthologues as Muc1, -2, -3, -4 (unpublished, GenBank; AF218265), Muc5ac, and Muc5b [71-75]. Members of the membrane-bound mucins were identified (Muc1, -3, and -4), as well as of the gel-forming mucins (Muc2, -5ac, and -5b, which are clustered on mouse chromosome 7), indicating that the mucosal defence and other functions of the mucins are preserved among man and mice. In the rat, Muc1, -2, -3, -4 and -5AC have been identified [76-80], which show high homology to the corresponding mucin genes of both mice and human. The *N*-terminus of Muc2 is highly conserved between species. Comparison of the *N*-terminus of rat, murine and human MUC2 showed 73% amino acid identity [73]. In rat intestine Muc2 appears to be the most prominent mucin [81]. The mouse is presently the most important model for studying IBD-like pathology. This animal can be genetically and environmentally manipulated enabling us to single out important pathogenic factors in IBD like the immune system, the enteric bacteria, and the role of mucins in the epithelial barrier.

Table 2. ***Mouse orthologues of human mucins***

Mucin	Expression	Mucin class	Chromo-some	Reference
Muc1	All epithelia	membrane-bound	3	74, 82
Muc2	Intestine, goblet cells	secretory	7	73
Muc3	Intestine, enterocytes	membrane-bound	5	71
Muc4	Virtually all epithelia	membrane-bound	n.d.	n.p.
Muc5a	Stomach, surface epithelium	secretory	7	72
Muc5b	Trachea, submucosal glands	secretory	7	75

n.d., not determined

n.p., not published; GenBank; AF218265.

The colonic mucus layer is thinner in UC [57], therefore a deficiency of secretory, gel-forming mucins is conceivable. MUC2, as the most prominent secretory mucin in the intestine, seems very important for maintenance of the mucus-layer. It was shown that MUC2 synthesis, secretion and sulfation is decreased in active UC [60, 63, 64], implying diminished mucosal protection in active disease (Table 1). Most importantly in mice, like humans and rats [32, 81], Muc2 is the most prominent, heavily sulfated mucin in mouse intestine, expressed and secreted by all enteric goblet cells [73]. We will present a working model, furnished with recent data, to show that MUC2 may play a critical role in development of IBD.

Bacteria and mucins in IBD

Vast numbers of bacteria roam in the intestines, particularly in the colon, and it is obvious that they pose a serious thread to the intestinal mucosa and development of IBD. Much research effort was put on identifying effects of bacteria in the initiation or perpetuation of IBD. Higher numbers of bacteria have indeed been detected within the colonic mucus-layer of IBD patients [66]. Likely these bacteria have deteriorating effects on the mucins in the mucus-layer. For example, increased levels of fecal mucinase and sulfatase activity, likely of bacterial origin, were found in fecal extracts of patients with IBD, especially in UC [83, 84]. Changes in glycosylation of mucins have been shown to occur in UC [85, 86], and *in vitro* fecal anaerobic bacteria have been shown to be able to degrade mucus by producing extracellular glycosidases [87, 88]. Thus, partial degradation of the mucus may increase to exposure of the epithelium to bacteria, bacterial products and other luminal substances, and constitute a predisposing condition for IBD.

Altered protective efficacy of the intestinal mucus in IBD may result in an increased association of luminal bacteria with the epithelium. Such an increased association may enhance or sustain the inflammatory process during IBD by exposing the mucosal surface to bacterial products and antigens that otherwise would not have been able to pass the mucus barrier. However, it is unknown to what extent luminal enteric bacteria are able to degrade the mucus *in vivo*. Furthermore, no correlation was found between the number of bacteria in the mucus-layer of rectal biopsy specimens and the degree of inflammation [66]. An association between the presence of specific bacterial species and IBD has been suggested, but results of numerous studies are inconclusive as has been recently reviewed [5]. Thus, it seems that the normal commensal enteric bacteria are sufficient to drive the inflammation once it has established itself, and that IBD, as far as we know, is not caused by a specific pathogen.

In humans it is extremely difficult to establish if changed bacterial colonization in IBD is either cause or consequence of inflammation. Therefore, the presence of bacteria as pathogenic factor in IBD was studied in germ free animals, which do not carry any microorganisms, by introduction of normal enteric bacteria (NEB). Germ free wild type mice do not develop signs of inflammation upon introduction of NEB [4, 13]. Moreover, germ free mice produce normal amounts of Muc2 compared to mice harboring NEB, indicating that the presence of bacteria does not lead to an altered mucus thickness per se (Fig. 1A and B) [10, 11]. Introduction of NEB into germ free mice induced an increase in the sulfation of *de novo* synthesized Muc2.

Normally colonic mucins are highly sulfated, and sulfated mucins are generally considered to be more resistant to bacterial degradation. A colonic mucus-layer composed of less sulfated mucins is deemed less protective, and was closely associated with IBD in humans [32, 59, 60, 84, 89-91].

When mice and rats colonized by NEB were treated with luminal dextran sulfate sodium (DSS), a toxic sulfated polysaccharide, colitis develops ([92, 93] and Chapter 3 of this thesis). DSS initially inhibits proliferation, whereas prolonged DSS-treatment results in an induction of hyperproliferation and enhanced apoptosis (Fig. 1C)[92-94]. Despite the increased turnover of the epithelium and crypt elongation, high expression levels of Muc2 were however maintained, whereas the degree of sulfation of the Muc2 molecules decreased (Fig. 1C) ([9, 12] and Chapters 3 and 5 of this thesis). Introduction of NEB in germ free mice that are highly susceptible to developing colitis, like interleukin 10 knockout ($IL10^{-/-}$) mice, rapidly develop severe and chronic colitis upon contact with NEB, which is also accompanied by a loss of sulfation of newly synthesized Muc2 molecules (Fig. 1D and E). This indicates that NEB are only able to elicit colitis in a compromised host (e.g. the DSS-treated or $IL10^{-/-}$ mice), but not in the healthy mouse. Decreased levels of sulfation of *de novo* formed Muc2 is a consistent finding in NEB-associated colitis, which suggests that NEB influences the structure, and possibly the functions, of Muc2 during synthesis. The decreased sulfation in these compromised hosts correlates with the inflammation, and therefore seems a secondary effect of introducing NEB into the colon (Fig. 1A-E).

Recently a very interesting example was found of a potential therapeutic intervention that could increase the MUC2 synthesis in IBD [95]. The probiotic *agents Lactobacillus plantarum* 299v and *L. rhamnosus* GG quantitatively inhibited the adherence of an entero-pathogenic *Escherichia coli* to intestinal epithelial cells. These bacteria increased MUC2 and MUC3 mRNA synthesis in these cells, and media containing both these mucins inhibited the binding of E. coli to intestinal cells. Thus, it can be hypothesized that these probiotic bacteria increase the epithelial barrier function by inducing increased synthesis of these important intestinal mucins.

Immunological influence on mucins

A number of rodent models of colitis were recently developed in which chronic intestinal inflammation occurs as a consequence of alterations in the immune system, leading to a failure of normal immuno-regulation in the intestine [2]. These animal models are very suitable for identifying the effects of the immune system on mucin expression. One of these animal models is the $IL10^{-/-}$ mouse, which spontaneously develop enterocolitis when maintained in conventional conditions, develop colitis when kept in specified pathogen-free environments, but shows no evidence of colitis when kept germ free (Fig. 1D) [8, 13]. In germ free $IL10^{-/-}$ mice at least 10-fold less Muc2 is produced than in germ free wild type mice (Fig. 1A and D) [10, 11]. Although the mucus-layer is most likely much thinner as consequence the decreased Muc2 synthesis, colitis does not occur, because of the absence of a bacterial-derived trigger from the lumen.

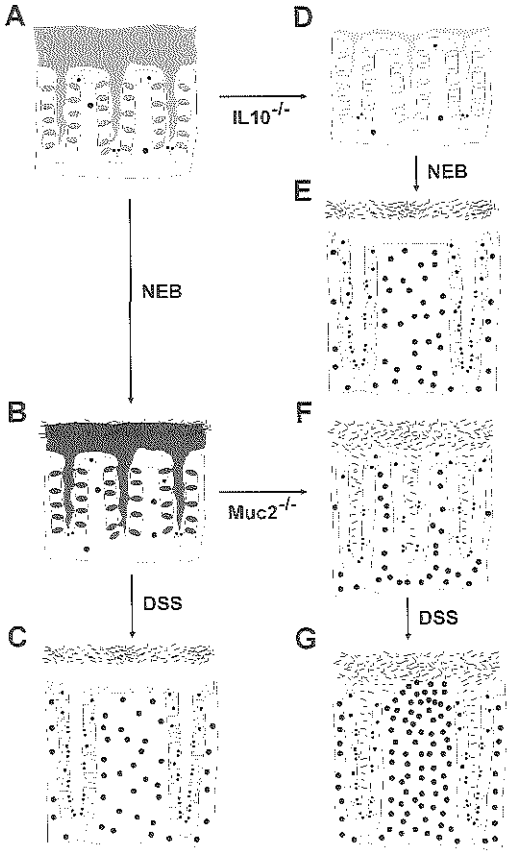

Figure 1. Effects of interleukin 10, bacteria, Muc2 and dextran sulfate sodium (DSS) on development of colitis in the mouse. This figure schematically depicts the work of others and our work on diverse IBD models that were developed in mice. [3-5, 7-15]. It summarizes the evidence that both bacteria and damaging agents (like the cytotoxic DSS) are particularly detrimental to the colonic mucosa when Muc2 synthesis (the major colonic gel-forming mucin) is low or absent. The models shown are: 1. Wildtype mice under germ free conditions (panel A) that were infected by normal enteric bacteria (NEB, panel B), 2. Wildtype mice with NEB, treated with DSS (panel C), 3. Interleukin 10 knockout mice ($IL10^{-/-}$, panel D) that were infected with NEB (panel E), and 4. Muc2 knockout mice ($Muc2^{-/-}$, panel F) that were treated with DSS (panel G). Mice were kept under specified pathogen free conditions. The effects of NEB and DSS are depicted as these occur after one week a of treatment, except for the $Muc2^{-/-}$ mice treated with DSS (panel G), which were shown after 2 days. *De novo* Muc2 production was measured under each of these circumstances. The thickness of the extracellular mucus-layer signifies the amounts of Muc2 that are produced (gray), while the gray-scale indicates the degree of sulfation of Muc2. When Muc2 is depicted in a lighter shade of gray, the degree of sulfation of Muc2 has declined. Changing of Muc2-producing goblet cell morphology in colitis is depicted as the slimming of the goblet cells (gray ellipses). The extent of the inflammation is indicated by the influx of immune cells (black circles). The proliferation is indicated by the occurrence of mitoses in the epithelium (), and the apoptosis in the epithelium is indicated by apoptotic cells (). Severe ulceration (overt rectal bleeding) and rectal prolaps occurred in $Muc2^{-/-}$ mice treated by DSS for 1 day, indicated by the focal absence of epithelium (panel G). Indicated are further the epithelium (white), the mucosa (stippled), and enteric

Upon introduction of NEB, the $IL10^{-/-}$ mice rapidly develop symptoms of colitis by showing infiltration of immune cells and induction of pro-inflammatory mediators such as IL12 [11]. The mucosa was thickened and the turnover of epithelial cells is much higher, because of increased proliferation in the crypts and apoptosis in the epithelium. Goblet cells become smaller

and less apparent (Fig. 1C and E), which is often referred to as goblet cell depletion. Goblet cell depletion is considered a characteristic feature in IBD and in many of the experimental animal models [1, 96-98]. However, it is our speculation that the apparent goblet cell depletion might (at least partly) be due to goblet cells losing their characteristic goblet-like shape, rather than a true loss of goblet cells. Thus, the immune-imbalance present in the $IL10^{-/-}$ mice leads to a primary down-regulation of the Muc2 synthesis that is not related to inflammation. The diminished Muc2 levels leave the epithelium barely protected against the influences of NEB. Interestingly, the decreased sulfation in the germ free $IL10^{-/-}$ mice exists without any signs of inflammation, and is also a primary effect of this immune-imbalance, instead of the secondary decrease in sulfation that is induced by NEB.

The mechanism by which Muc2 synthesis is down-regulated in $IL10^{-/-}$ mice remains obscured, yet the finding demonstrates that certain immune-regulators directly or indirectly influence mucin production. Participation of cytokines in the regulation of mucin gene expression was implicated in UC through analogy to results obtained with human colorectal cell lines. Exposure of human colonic goblet cell-like cells, LS180, to the pro-inflammatory cytokines interleukin 1 or -6, or tumor necrosis factor-α resulted in an increased synthesis of MUC2 and other secretory mucins, while addition of each cytokine also resulted in reduced and altered glycosylation [22]. Whereas IL10 has thus far not been tested directly on cell lines, is seems likely that immune-regulators are able to direct mucin expression levels as well as mucin structure.

Muc2 knockout mice are very susceptible to IBD

To directly address the question whether MUC2 is involved in epithelial protection, Muc2 deficient ($Muc2^{-/-}$) mice were generated, through genetic inactivation of the murine Muc2 gene, in the laboratory of Anna Velcich and Leonard Augenlicht (Einstein college, New York) [99]. In $Muc2^{-/-}$ mice the intestinal goblet cells are seemingly absent. However, expression of trefoil factor 3, another intestinal goblet cell marker, was still present in a high number of epithelial cells in the colon of the $Muc2^{-/-}$ mice. Apparently, goblet cells in absence of Muc2 loose their characteristic goblet-like shape in histology, indicating that Muc2 is the major phenotypic determinant of goblet cells. $Muc2^{-/-}$ mice spontaneously develop mild colitis when colonized by NEB under specified-pathogen-free conditions (Fig. 1F) [7]. Moreover, $Muc2^{-/-}$ mice frequently develop adenomas in the small intestine that progressed to invasive adenocarcinoma, as well as rectal tumors [99]. The $Muc2^{-/-}$ mice are extremely susceptible to cytotoxic luminal agents like DSS. Treatment with DSS led to very fulminant colitis within days, which was much more severe in each aspect than in wild type mice treated with DSS (Fig. 1G) [7], indicating that Muc2 plays an essential role in epithelial protection. These findings lend further credibility to the theory that the (partial) deficiency of Muc2 in $IL10^{-/-}$ mice predisposes for the development of inflammation. Thus, (partial) deficiency of Muc2 might be an etiological factor in the onset and/or perpetuation of IBD.

Conclusions

As evidence is fragmentary, we still await the formidable task to elucidate the involvement of mucin in the pathogenesis of IBD. Yet, so far there are two highlights in this field. The state of the art shows that the two most abundant intestinal mucins, the membrane-bound MUC3 and the secretory MUC2, are clearly implicated in the pathogenesis of IBD. So far MUC3 is the only human mucin of which particular alleles could be linked to IBD. This linkage of IBD to a genetic predisposition could not be established for MUC2. However, there are now compelling data to suggest that lowered abundance of MUC2 in humans and in experimental animals increases the sensitivity towards IBD. Although it may be still early days for full appreciation of mucins as predisposing factors in IBD, these results are highly encouraging.

Acknowledgements

Our work on mucins over the years has been made possible through grants from the Netherlands Digestive Diseases Foundation (Nieuwegein), the Irene Foundation (Arnhem), ASTRA/Zeneca (Zoetermeer), the Netherlands Foundation for Scientific Research (the Hague), the Sophia Foundation for Scientific Research (Rotterdam), the Jan Dekker/Ludgardine Bouman Foundation (Amsterdam), the Gastrostart Foundation (Haarlem), all based in the Netherlands, and from Nestec, Lausanne, Swiss.

References

1. Elson CO, Sartor RB, Tennyson GS, Riddell RH. Experimental models of inflammatory bowel disease. Gastroenterology 1995;109:1344-67.

2. Fedorak RN, Madsen KL. Naturally occuring and experimental models of inflammatory bowel disease. In: Kirsner JB, ed. Inflammatory bowel disease. 5th ed. Philadelphia: Saunders, 2000:113-143.

3. Sartor RB. Review article: Role of the enteric microflora in the pathogenesis of intestinal inflammation and arthritis. Aliment Pharmacol Ther 1997;11 Suppl 3:17-22.

4. Sartor RB. The influence of normal microbial flora on the development of chronic mucosal inflammation. Res Immunol 1997;148:567-76.

5. Sartor RB. Microbial factors in the pathogenesis of Crohn's disease, ulcerative colitis, and experimental intestinal inflammation. In: Kirsner JB, ed. Inflammatory Bowel Disease. 5th ed. Philadelphia: Saunders, 2000:153-178.

6. Hermiston ML, Gordon JI. Inflammatory bowel disease and adenomas in mice expressing a dominant negative N-cadherin. Science 1995;270:1203-7.

7. Van der Sluis M, Makkink MK, Sutmuller M, Büller HA, Dekker J, Augenlicht LH, Velcich A, Einerhand AWC. Muc2 mucin knockout mice are more susceptible to dextran sulfate sodium-induced colitis. Gastroenterology 2002;122:P194, T946

8. Kuhn R, Lohler J, Rennick D, Rajewsky K, Muller W. Interleukin-10-deficient mice develop chronic enterocolitis. Cell 1993;75:263-74.

9. Makkink MK, Schwerbrock NJM, Mähler M, Wagner S, Einerhand AWC, Büller HA, Hedrich HJ, Enss LM, Dekker J. Colon of interleukin 10 deficient mice shows highly specific changes in epithlial gene expression during inflammation. Gastroenterology 2000;118:A808.

10. Makkink MK, Schwerbrock NJM, Van der Sluis M, Büller HA, Sartor RB, Einerhand AWC, Dekker J. Interleukin 10 deficient mice are defective in colonic Muc2 synthesis both before and after induction of colitis by commensal bacteria. Gastroenterology 2002;122:P26, 254.

11. Schwerbrock NMJ, Li F, Büller HA, Einerhand AWC, Sartor RB, Dekker J. Altered Muc2 synthesis and sulfation in bacterial induced colitis in IL-10-/- mice. Gastroenterology 2001;120:A696.

12. Renes IB, Boshuizen JA, Van Nispen DJPM, Bulsing NP, Büller HA, Dekker J, Einerhand AWC. Alterations in Muc2 biosynthesis and secretion during dextran sulfate sodium-induced colitis. Am J Physiol 2002:in press.

13. Sellon RK, Tonkonogy S, Schultz M, Dieleman LA, Grenther W, Balish E, Rennick DM, Sartor RB. Resident enteric bacteria are necessary for development of spontaneous colitis and immune system activation in interleukin-10-deficient mice. Infect Immun 1998;66:5224-31.

14. Sartor RB. Pathogenesis and immune mechanisms of chronic inflammatory bowel diseases. Am J Gastroenterol 1997;92:5S-11S.

15. Sartor RB. Probiotics in chronic pouchitis: restoring luminal microbial balance. Gastroenterology 2000;119:584-7.

16. Panwala CM, Jones JC, Viney JL. A novel model of inflammatory bowel disease: mice deficient for the multiple drug resistance gene, mdr1a, spontaneously develop colitis. J Immunol 1998;161:5733-44.

17. Mashimo H, Wu DC, Podolsky DK, Fishman MC. Impaired defense of intestinal mucosa in mice lacking intestinal trefoil factor. Science 1996;274:262-5.

18. Van Seuningen I, Pigny P, Perrais M, Porchet N, Aubert JP. Transcriptional regulation of the 11p15 mucin genes. towards new biological tools in human therapy, in inflammatory diseases and cancer? Front Biosci 2001;6:D1216-34.

19. Campbell BJ, Rowe GE, Leiper K, Rhodes JM. Increasing the intra-Golgi pH of cultured LS174T goblet-differentiated cells mimics the decreased mucin sulfation and increased Thomsen- Friedenreich antigen (Gal beta1-3GalNac alpha-) expression seen in colon cancer. Glycobiology 2001;11:385-93.

20. Gouyer V, Wiede A, Buisine MP, Dekeyser S, Moreau O, Lesuffleur T, Hoffmann W, Huet G. Specific secretion of gel-forming mucins and TFF peptides in HT-29 cells of mucin-secreting phenotype. Biochim Biophys Acta 2001;1539:71-84.

21. Gratchev A, Siedow A, Bumke-Vogt C, Hummel M, Foss HD, Hanski ML, Kobalz U, Mann B, Lammert H, Stein H, Riecken EO, Hanski C, Mansmann U. Regulation of the intestinal mucin MUC2 gene expression in vivo: evidence for the role of promoter methylation. Cancer Lett 2001;168:71-80.

22. Enss ML, Cornberg M, Wagner S, Gebert A, Henrichs M, Eisenblatter R, Beil W, Kownatzki R, Hedrich HJ. Proinflammatory cytokines trigger MUC gene expression and mucin release in the intestinal cancer cell line LS180. Inflamm Res 2000;49:162-9.

23. Strous GJ, Dekker J. Mucin-type glycoproteins. Crit Rev Biochem Mol Biol 1992;27:57-92.

24. Gendler SJ, Spicer AP. Epithelial mucin genes. Annu Rev Physiol 1995;57:607-34.

25. Dekker J, Rossen JWA, Büller HA, Einerhand AWC. The MUC family: An orbituary. Trends Biochem Sci 2002:in press.

26. Van Klinken BJW, Dekker J, Büller HA, Einerhand AWC. Mucin gene structure and expression: protection vs. adhesion. Am J Physiol 1995;269:G613-27.

27. Van Klinken BJW, Dekker J, Büller HA, de Bolos C, Einerhand AWC. Biosynthesis of mucins (MUC2-6) along the longitudinal axis of the human gastrointestinal tract. Am J Physiol 1997;273:G296-302.

28. Van Klinken BJW, Dekker J, van Gool SA, van Marle J, Büller HA, Einerhand AWC. MUC5B is the prominent mucin in human gallbladder and is also expressed in a subset of colonic goblet cells. Am J Physiol 1998;274:G871-8.

29. Van Klinken BJW, Einerhand AWC, Büller HA, Dekker J. The oligomerization of a family of four genetically clustered human gastrointestinal mucins. Glycobiology 1998;8:67-75.

30. Desseyn JL, Aubert JP, Porchet N, Laine A. Evolution of the large secreted gel-forming mucins. Mol Biol Evol 2000;17:1175-84.

31. Moniaux N, Escande F, Porchet N, Aubert JP, Batra SK. Structural organization and classification of the human mucin genes. Front Biosci 2001;6:D1192-206.

32. Tytgat KMAJ, Büller HA, Opdam FJ, Kim YS, Einerhand AWC, Dekker J. Biosynthesis of human colonic mucin: Muc2 is the prominent secretory mucin. Gastroenterology 1994;107:1352-63.

33. Van den Brink GR, Tytgat KMAJ, Van der Hulst RW, Van der Loos CM, Einerhand AWC, Büller HA, Dekker J. H pylori colocalises with MUC5AC in the human stomach. Gut 2000;46:601-7.

34. Buisine MP, Desreumaux P, Leteurtre E, Copin MC, Colombel JF, Porchet N, Aubert JP. Mucin gene expression in intestinal epithelial cells in Crohn's disease. Gut 2001;49:544-51.

35. Longman RJ, Douthwaite J, Sylvester PA, O'Leary D, Warren BF, Corfield AP, Thomas MG. Lack of mucin MUC5AC field change expression associated with tubulovillous and villous colorectal adenomas. J Clin Pathol 2000;53:100-4.

36. Agrawal B, Gendler SJ, Longenecker BM. The biological role of mucins in cellular interactions and immune regulation: prospects for cancer immunotherapy. Mol Med Today 1998;4:397-403.

37. Wesseling J, van der Valk SW, Vos HL, Sonnenberg A, Hilkens J. Episialin (MUC1) overexpression inhibits integrin-mediated cell adhesion to extracellular matrix components. J Cell Biol 1995;129:255-65.

38. DeSouza MM, Surveyor GA, Price RE, Julian J, Kardon R, Zhou X, Gendler S, Hilkens J, Carson DD. MUC1/episialin: a critical barrier in the female reproductive tract. J Reprod Immunol 1999;45:127-58.

39. Carraway KL, Price-Schiavi SA, Komatsu M, Idris N, Perez A, Li P, Jepson S, Zhu X, Carvajal ME, Carraway CA. Multiple facets of sialomucin complex/MUC4, a membrane mucin and erbb2 ligand, in tumors and tissues (Y2K update). Front Biosci 2000;5:D95-D107.

40. Komatsu M, Jepson S, Arango ME, Carothers Carraway CA, Carraway KL. Muc4/sialomucin complex, an intramembrane modulator of ErbB2/HER2/Neu, potentiates primary tumor growth and suppresses apoptosis in a xenotransplanted tumor. Oncogene 2001;20:461-70.

41. Louvet B, Buisine MP, Desreumaux P, Tremaine WJ, Aubert JP, Porchet N, Capron M, Cortot A, Colombel JF, Sandborn WJ. Transdermal nicotine decreases mucosal IL-8 expression but has no effect on mucin gene expression in ulcerative colitis. Inflamm Bowel Dis 1999;5:174-81.

42. Buisine MP, Desreumaux P, Debailleul V, Gambiez L, Geboes K, Ectors N, Delescaut MP, Degand P, Aubert JP, Colombel JF, Porchet N. Abnormalities in mucin gene expression in Crohn's disease. Inflamm Bowel Dis 1999;5:24-32.

43. Bobek LA, Tsai H, Biesbrock AR, Levine MJ. Molecular cloning, sequence, and specificity of expression of the gene encoding the low molecular weight human salivary mucin (MUC7). J Biol Chem 1993;268:20563-9.

44. Shankar V, Pichan P, Eddy RL, Jr., Tonk V, Nowak N, Sait SN, Shows TB, Schultz RE, Gotway G, Elkins RC, Gilmore MS, Sachdev GP. Chromosomal localization of a human mucin gene (MUC8) and cloning of the cDNA corresponding to the carboxy terminus. Am J Respir Cell Mol Biol 1997;16:232-41.

45. Williams SJ, McGuckin MA, Gotley DC, Eyre HJ, Sutherland GR, Antalis TM. Two novel mucin genes down-regulated in colorectal cancer identified by differential display. Cancer Res 1999;59:4083-9.

46. Williams SJ, Wreschner DH, Tran M, Eyre HJ, Sutherland GR, McGuckin MA. Muc13, a novel human cell surface mucin expressed by epithelial and hemopoietic cells. J Biol Chem 2001;276:18327-36.

47. Yin BW, Lloyd KO. Molecular cloning of the CA125 ovarian cancer antigen: identification as a new mucin, MUC16. J Biol Chem 2001;276:27371-5.

48. Satsangi J, Parkes M, Louis E, Hashimoto L, Kato N, Welsh K, Terwilliger JD, Lathrop GM, Bell JI, Jewell DP. Two stage genome-wide search in inflammatory bowel disease provides evidence for susceptibility loci on chromosomes 3, 7 and 12. Nat Genet 1996;14:199-202.

49. Pratt WS, Crawley S, Hicks J, Ho J, Nash M, Kim YS, Gum JR, Swallow DM. Multiple transcripts of MUC3: evidence for two genes, MUC3A and MUC3B. Biochem Biophys Res Commun 2000;275:916-923.

50. Kyo K, Muto T, Nagawa H, Lathrop GM, Nakamura Y. Associations of distinct variants of the intestinal mucin gene MUC3A with ulcerative colitis and Crohn's disease. J Hum Genet 2001;46:5-20.

51. Kyo K, Parkes M, Takei Y, Nishimori H, Vyas P, Satsangi J, Simmons J, Nagawa H, Baba S, Jewell D, Muto T, Lathrop GM, Nakamura Y. Association of ulcerative colitis with rare VNTR alleles of the human intestinal mucin gene, MUC3. Hum Mol Genet 1999;8:307-11.

52. Gum JR, Hicks JW, Swallow DM, Lagace RE, Byrd JC, Lamport DT, Siddiki B, Kim YS. Molecular cloning of a novel human intestinal mucin gene. Biochem Biophys Res Commun 1990;171:407-15.

53. Crawley SC, Gum JR, Jr., Hicks JW, Pratt WS, Aubert JP, Swallow DM, Kim YS. Genomic organization and structure of the 3' region of human MUC3: alternative splicing predicts membrane-bound and soluble forms of the mucin. Biochem Biophys Res Commun 1999;263:728-36.

54. Gum JR, Jr., Ho JJ, Pratt WS, Hicks JW, Hill AS, Vinall LE, Roberton AM, Swallow DM, Kim YS. MUC3 human intestinal mucin. Analysis of gene structure, the carboxyl terminus, and a novel upstream repetitive region. J Biol Chem 1997;272:26678-86.

55. Van Klinken BJW, Van Dijken TC, Oussoren E, Buller HA, Dekker J, Einerhand AWC. Molecular cloning of human MUC3 cDNA reveals a novel 59 amino acid tandem repeat region. Biochem Biophys Res Commun 1997;238:143-8.

56. Williams SJ, Munster DJ, Quin RJ, Gotley DC, McGuckin MA. The MUC3 gene encodes a transmembrane mucin and is alternatively spliced. Biochem Biophys Res Commun 1999;261:83-9.

57. Pullan RD, Thomas GA, Rhodes M, Newcombe RG, Williams GT, Allen A, Rhodes J. Thickness of adherent mucus gel on colonic mucosa in humans and its relevance to colitis. Gut 1994;35:353-9.

58. Rhodes JM. Mucins and inflammatory bowel disease. Qjm 1997;90:79-82.

59. Raouf AH, Tsai HH, Parker N, Hoffman J, Walker RJ, Rhodes JM. Sulphation of colonic and rectal mucin in inflammatory bowel disease: reduced sulphation of rectal mucus in ulcerative colitis. Clin Sci (Colch) 1992;83:623-6.

60. Van Klinken BJW, Van der Wal JW, Einerhand AWC, Büller HA, Dekker J. Sulphation and secretion of the predominant secretory human colonic mucin MUC2 in ulcerative colitis. Gut 1999;44:387-93.

61. Parker N, Tsai HH, Ryder SD, Raouf AH, Rhodes JM. Increased rate of sialylation of colonic mucin by cultured ulcerative colitis mucosal explants. Digestion 1995;56:52-6.

62. Campbell BJ, Finnie IA, Hounsell EF, Rhodes JM. Direct demonstration of increased expression of Thomsen-Friedenreich (TF) antigen in colonic adenocarcinoma and ulcerative colitis mucin and its concealment in normal mucin. J Clin Invest 1995;95:571-6.

63. Tytgat KMAJ, Opdam FJ, Einerhand AWC, Büller HA, Dekker J. MUC2 is the prominent colonic mucin expressed in ulcerative colitis. Gut 1996;38:554-63.

64. Tytgat KMAJ, van der Wal JW, Einerhand AWC, Büller HA, Dekker J. Quantitative analysis of MUC2 synthesis in ulcerative colitis. Biochem Biophys Res Commun 1996;224:397-405.

65. Hayashi T, Ishida T, Motoya S, Itoh F, Takahashi T, Hinoda Y, Imai K. Mucins and immune reactions to mucins in ulcerative colitis. Digestion 2001;63:28-31.

66. Schultsz C, Van Den Berg FM, Ten Kate FW, Tytgat GN, Dankert J. The intestinal mucus layer from patients with inflammatory bowel disease harbors high numbers of bacteria compared with controls. Gastroenterology 1999;117:1089-97.

67. Swallow DM, Vinall LE, Gum JR, Kim YS, Yang H, Rotter JI, Mirza M, Lee JC, Lennard-Jones JE. Ulcerative colitis is not associated with differences in MUC2 mucin allele length. J Med Genet 1999;36:859-60.

68. Corfield AP, Myerscough N, Longman R, Sylvester P, Arul S, Pignatelli M. Mucins and mucosal protection in the gastrointestinal tract: new prospects for mucins in the pathology of gastrointestinal disease. Gut 2000;47:589-94.

69. Corfield AP, Carroll D, Myerscough N, Probert CS. Mucins in the gastrointestinal tract in health and disease. Front Biosci 2001;6:D1321-57.

70. Shirazi T, Longman RJ, Corfield AP, Probert CS. Mucins and inflammatory bowel disease. Postgrad Med J 2000;76:473-8.

71. Shekels LL, Hunninghake DA, Tisdale AS, Gipson IK, Kieliszewski M, Kozak CA, Ho SB. Cloning and characterization of mouse intestinal MUC3 mucin: 3' sequence contains epidermal-growth-factor-like domains. Biochem J 1998;330:1301-8.

72. Shekels LL, Lyftogt C, Kieliszewski M, Filie JD, Kozak CA, Ho SB. Mouse gastric mucin: cloning and chromosomal localization. Biochem J 1995;311:775-85.

73. Van Klinken BJW, Einerhand AWC, Duits LA, Makkink MK, Tytgat KMAJ, Renes IB, Verburg M, Büller HA, Dekker J. Gastrointestinal expression and partial cDNA cloning of murine Muc2. Am J Physiol 1999;276:G115-24.

74. Vos HL, de Vries Y, Hilkens J. The mouse episialin (Muc1) gene and its promoter: rapid evolution of the repetitive domain in the protein. Biochem Biophys Res Commun 1991;181:121-30.

75. Chen Y, Zhao YH, Wu R. In silico cloning of mouse muc5b gene and upregulation of its expression in mouse asthma model. Am J Respir Crit Care Med 2001;164:1059-66.

76. DeSouza MM, Mani SK, Julian J, Carson DD. Reduction of mucin-1 expression during the receptive phase in the rat uterus. Biol Reprod 1998;58:1503-7.

77. Ohmori H, Dohrman AF, Gallup M, Tsuda T, Kai H, Gum JR, Jr., Kim YS, Basbaum CB. Molecular cloning of the amino-terminal region of a rat MUC 2 mucin gene homologue. Evidence for expression in both intestine and airway. J Biol Chem 1994;269:17833-40.

78. Khatri IA, Forstner GG, Forstner JF. The carboxyl-terminal sequence of rat intestinal mucin RMuc3 contains a putative transmembrane region and two EGF-like motifs. Biochim Biophys Acta 1997;1326:7-11.

79. Wu K, Fregien N, Carraway KL. Molecular cloning and sequencing of the mucin subunit of a heterodimeric, bifunctional cell surface glycoprotein complex of ascites rat mammary adenocarcinoma cells. J Biol Chem 1994;269:11950-5.

80. Inatomi T, Tisdale AS, Zhan Q, Spurr-Michaud S, Gipson IK. Cloning of rat Muc5AC mucin gene: comparison of its structure and tissue distribution to that of human and mouse homologues. Biochem Biophys Res Commun 1997;236:789-97.

81. Tytgat KMAJ, Bovelander FJ, Opdam FJ, Einerhand AWC, Büller HA, Dekker J. Biosynthesis of rat MUC2 in colon and its analogy with human MUC2. Biochem J 1995;309:221-9.

82. Spicer AP, Parry G, Patton S, Gendler SJ. Molecular cloning and analysis of the mouse homologue of the tumor- associated mucin, MUC1, reveals conservation of potential O-glycosylation sites, transmembrane, and cytoplasmic domains and a loss of minisatellite-like polymorphism. J Biol Chem 1991;266:15099-109.

83. Dwarakanath AD, Campbell BJ, Tsai HH, Sunderland D, Hart CA, Rhodes JM. Faecal mucinase activity assessed in inflammatory bowel disease using 14C threonine labelled mucin substrate. Gut 1995;37:58-62.

84. Tsai HH, Dwarakanath AD, Hart CA, Milton JD, Rhodes JM. Increased faecal mucin sulphatase activity in ulcerative colitis: a potential target for treatment. Gut 1995;36:570-6.

85. Jacobs LR, Huber PW. Regional distribution and alterations of lectin binding to colorectal mucin in mucosal biopsies from controls and subjects with inflammatory bowel diseases. J Clin Invest 1985;75:112-8.

86. Rhodes JM. Unifying hypothesis for inflammatory bowel disease and associated colon cancer: sticking the pieces together with sugar. Lancet 1996;347:40-4.

87. Hoskins LC, Agustines M, McKee WB, Boulding ET, Kriaris M, Niedermeyer G. Mucin degradation in human colon ecosystems. Isolation and properties of fecal strains that degrade ABH blood group antigens and oligosaccharides from mucin glycoproteins. J Clin Invest 1985;75:944-53.

88. Corfield AP, Wagner SA, Clamp JR, Kriaris MS, Hoskins LC. Mucin degradation in the human colon: production of sialidase, sialate O-acetylesterase, N-acetylneuraminate lyase, arylesterase, and glycosulfatase activities by strains of fecal bacteria. Infect Immun 1992;60:3971-8.

89. Nieuw Amerongen AV, Bolscher JG, Bloemena E, Veerman EC. Sulfomucins in the human body. Biol Chem 1998;379:1-18.

90. Corfield AP, Myerscough N, Bradfield N, Corfield C, Gough M, Clamp JR, Durdey P, Warren BF, Bartolo DC, King KR, Williams JM. Colonic mucins in ulcerative colitis: evidence for loss of sulfation. Glycoconj J 1996;13:809-22.

91. Robertson AM, Wright DP. Bacterial glycosulphatases and sulphomucin degradation. Can J Gastroenterol 1997;11:361-6.

92. Dieleman LA, Ridwan BU, Tennyson GS, Beagley KW, Bucy RP, Elson CO. Dextran sulfate sodium-induced colitis occurs in severe combined immunodeficient mice. Gastroenterology 1994;107:1643-52.

93. Renes IB, Verburg M, Buller HA, Dekker J, Einerhand AWC. Epithelial proliferation and function during experimental colitis. Epithelial proliferation, cell death, and gene expression in experimental colitis. *Alterations in carbonic anhydrase I, mucin Muc2, and trefoil factor 3 expression.* Int J Colorectal Dis 2002,17(5):317-26.

94. Tessner TG, Cohn SM, Schloemann S, Stenson WF. Prostaglandins prevent decreased epithelial cell proliferation associated with dextran sodium sulfate injury in mice. Gastroenterology 1998;115:874-82.

95. Mack DR, Michail S, Wei S, McDougall L, Hollingsworth MA. Probiotics inhibit enteropathogenic E. coli adherence in vitro by inducing intestinal mucin gene expression. Am J Physiol 1999;276:G941-50.

96. Theodossi A, Spiegelhalter DJ, Jass J, Firth J, Dixon M, Leader M, Levison DA, Lindley R, Filipe I, Price A, et al. Observer variation and discriminatory value of biopsy features in inflammatory bowel disease. Gut 1994;35:961-8.

97. Nostrant TT, Kumar NB, Appelman HD. Histopathology differentiates acute self-limited colitis from ulcerative colitis. Gastroenterology 1987;92:318-28.

98. McCormick DA, Horton LW, Mee AS. Mucin depletion in inflammatory bowel disease. J Clin Pathol 1990;43:143-6.

99. Velcich A, Yang W, Heyer J, Fragale A, Nicholas C, Viani S, Kucherlapati R, Lipkin M, Yang K, Augenlicht L. Colorectal cancer in mice genetically deficient in the mucin Muc2. Science 2002;295:1726-9.

Chapter 3

Epithelial proliferation, cell death and gene expression in experimental colitis: *Alterations in carbonic anhydrase I, mucin Muc2, and trefoil factor 3 expression*

Published as:
Ingrid B. Renes, Melissa Verburg, Daniëlle J.P.M. Van Nispen, Jan A.J.M. Taminiau, Hans A. Büller, Jan Dekker, and Alexandra W.C. Einerhand. Epithelial proliferation, cell death, and gene expression in experimental colitis. *Alterations in carbonic anhydrase I, mucin Muc2, and trefoil factor 3 expression.* Int J Colorectal Dis 2002,17(5):317-26.

Summary

Background: To gain insight in intestinal epithelial proliferation, cell death and gene expression during experimental colitis, rats were treated with dextran sulphate sodium (DSS) for 7 days. **Methods:** Proximal- and distal colonic segments were excised on days 2, 5, 7 and 28. Epithelial proliferation, cell death, enterocyte gene expression (carbonic anhydrase I (CA I) and goblet cell gene expression (mucin (Muc2) and trefoil factor 3 (TFF3)) were studied immunohistochemically and biochemically. **Results:** Proliferative activity was decreased in the proximal and distal colon at the onset of disease (day 2). However, during active disease (days 5-7) epithelial proliferation was increased in the entire proximal colon and in the proximity of ulcerations in the distal colon. During DSS treatment the number of apoptotic cells in the epithelium of both colonic segments was increased. In the entire colon, surface enterocytes became flattened and CA I negative during active disease (day 5-7). Additionally, CA I levels in the distal colon significantly decreased during this phase. In contrast, during the regenerative phase (day 28) CA I levels were restored in the distal colon and up-regulated in the proximal colon. During all disease phases increased numbers of goblet cells were observed in the surface epithelium of the entire colon. In the distal colon TFF3 expression extended to the bottom of the crypts during active disease. Finally, Muc2 and TFF3 expression was increased in the proximal colon during disease. **Conclusions:** DSS affected the epithelium by inhibiting proliferation and inducing apoptosis. DSS-induced inhibition of CA I expression indicates down-regulation of specific enterocyte functions. Accumulation of goblet cells in the surface epithelium, up-regulation of Muc2 and TFF3 expression in the proximal colon underlines the importance of goblet cells in epithelial protection and repair, respectively.

Abbreviations: CA, carbonic anhydrase; DAB, 3,3-diaminobenzidine; DSS, dextran sulphate sodium; HE, hematoxylin; IBD, inflammatory bowel disease;Trefoil factor factor 3, TFF3; UC, ulcerative colitis.

Introduction

Since the beginning of the 1990s dextran sulphate sodium (DSS) has been widely used in a variety of animal models to induce colitis. Several clinical symptoms (*i.e.* diarrhea, bloody stools, and weight loss) and histopathological changes (*i.e.* inflammatory infiltrates, erosions, and crypt loss) that are induced by DSS, are similar to those observed in patients with ulcerative colitis (UC) [1-6]. Analogous to UC, DSS-induced colitis is mitigated by treatment with sulfasalazine [7], olsalazine [7], and cyclosporin [4], drugs that are widely used to treat inflammatory bowel diseases (IBD) [2].

The DSS-induced colitis model gives the opportunity to study the dynamic disease process from the onset of disease to complete remission. Such a study is not possible in humans, especially since the disease is usually diagnosed only during advanced stages. However, like in UC, the exact mechanisms underlying the DSS-induced pathology are largely unknown. Up to now, it was demonstrated that immune cells and bacteria do not play an essential role in the induction of DSS-induced colitis [8, 9]. Furthermore, DSS is known to inhibit epithelial cell proliferation *in vitro* [9, 10]. In vivo, the first signs of injury are seen in colonic crypt cells located at the crypt base [1, 5]. Previously, Tessner *et al.* reported that in mice, DSS induces a decrease in the proliferative activity in the cecal epithelium [11]. Collectively, these data suggest that the primary action of DSS on the epithelium is the inhibition of proliferation, thereby deranging epithelial homeostasis. Nevertheless, it is not known whether inhibition of proliferation is the only effect of DSS on the epithelium. As DSS induces diarrhea, it is also possible that DSS affects the expression of gene products of surface enterocytes, like carbonic anhydrases (CAs), which are involved in electrolyte transport, water absorption, and intracellular pH regulation [12-14]. Along the same line, we can not exclude the possibility that DSS alters the epithelial barrier function and epithelial repair capacity by affecting respectively mucin (Muc2) synthesis and trefoil factor 3 (TFF3). To help us understand the pathogenic mechanisms of colitis it is essential to unravel the primary effects of DSS on the epithelium and the ensuing response of the epithelium to the DSS-induced changes.

In this study, we used a rat model of DSS-induced colitis in which we investigated the successive changes in epithelial morphology, cell death, proliferation, and cell type-specific gene expression (as measure of cell function) in the proximal- and distal colon. In addition, clinical symptoms were evaluated during and after DSS administration. Epithelial proliferation and cell death were studied (immuno)histochemically. Cell type-specific gene expression was analyzed (immuno)histochemically as well as biochemically. CA I was used as marker for colonic enterocyte function. Muc2 the primary constituent of the colonic protective mucus layer and trefoil factor 3 (TFF3), a bioactive peptide that is involved in epithelial protection and repair, were used as markers for goblet cell function [15, 16]. By studying all these parameters in conjunction, we obtained a more complete picture of the complex pathogenic processes that occur during damage and regeneration in the different regions of the colonic mucosa during experimental colitis.

Materials & Methods

Animals

Eight-weeks-old, specified pathogen free, male Wistar rats (Broekman, Utrecht, The Netherlands) were housed at constant temperature and humidity on a 12 h light-dark cycle. One week prior to and during the experiment the rats were housed separately. The rats had free access to a standard pelleted diet (Hope Farms, Woerden, The Netherlands) and sterilized tap water (controls) or sterilized tap water supplemented with DSS. All the experiments were performed with the approval of the Animal Studies Ethics Committee of our institution.

Experimental Design

Rats were given 7% (w/v) DSS (37-40 kD, TdB Consultansy, Uppsala, Sweden) in their drinking water for 7 days, followed by a 21-day recovery period during which DSS was omitted from the drinking water. Fresh DSS solutions were prepared daily. To study proliferation of epithelial cells, 50 mg BrdU/kg body weight (Sigma, St. Louis, USA) was injected intra-peritoneally 24 h before decapitation. On day 0 (control), 2, 5, 7, and 28, four animals were sacrificed per day. Duplicate segments of 1 cm in length of the proximal colon (adjacent to the ileocecal valve) and of the distal colon (1 cm proximal from the rectum) were dissected. One set of segments (*i.e.* proximal- and distal colon) was washed in phosphate buffered saline (PBS), fixed in 4% (w/v) paraformaldehyde (Merck, Darmstadt, Germany) in PBS, and subsequently processed for light microscopy. The other set of segments was frozen in liquid nitrogen and stored in -70 °C till homogenization for biochemical analysis. Clinical symptoms *i.e.* weight loss, stool consistency, bloody stool, and presence of gross blood were scored during the course of the experiment.

Histology

Five μm thick sections were routinely stained with hematoxylin and eosin (HE) to study histological changes, *i.e.* distortion of crypt epithelium, erosions, inflammatory infiltrate, cell death and epithelial restitution during and after DSS-induced damage. The extent of crypt loss and ulcerations was estimated with a micrometer in 5 tissue sections per segment of each animal and the area involved was expressed as the percentage of the total surface area.

Immunohistochemistry

The 5 μm thick paraffin sections were deparaffinized through a graded series of xylol-ethanol. To visualize BrdU incorporation, sections were incubated with 2 N HCl for 1.5 h, washed in borate buffer (0.1 M $Na_2B_4O_7$, pH 8.5), incubated in 0.1% (w/v) pepsin in 0.01 M HCl for 10 min at 37 °C, and rinsed in PBS. Endogenous peroxidase activity was inactivated by 1.5% (v/v) hydrogen peroxide in PBS for 30 min, followed by a 30 min incubation with TENG-T (10 mM Tris-HCl, 5 mM EDTA, 150 mM NaCl, 0.25% (w/v) gelatin, 0.05% (w/v) Tween-20) to reduce non-specific binding. This was followed by overnight incubation with a 1:500

dilution of mouse anti-BrdU (Boehringer Mannheim, Mannheim, Germany). Then, the sections were incubated for 1 h with biotinylated horse anti-mouse IgG (diluted 1:2000, Vector Laboratories, England) followed by 1 h incubation with ABC/PO complex (Vectastain Elite Kit, Vector Laboratories) diluted 1:400. Binding was visualized after incubation in 0.5 mg/ml 3,3'-diaminobenzidine (DAB), 0.02% (v/v) H_2O_2 in 30 mM imidazole, 1 mM EDTA (pH 7.0). Finally, sections were counterstained with hematoxylin, dehydrated and mounted. Muc2, TFF3 and CA I expression was demonstrated according to the above described protocol with omission of the HCl incubation, washing with borate buffer, and pepsin treatment. To stain Muc2 and TFF3, sections were boiled in 0.01 M citrate buffer at pH 6.0 for 10 min prior to incubation with a Muc2-specific antibody (WE9, 1:500) [17] or TFF3-specific antibody (1:6000, Prof. Dr DK Podolsky). To detect CA I, rabbit anti-CA I (1:16000, Prof. Dr WS Sly) was used. Biotinylated goat anti-rabbit IgG (1:2000, Vector Laboratories) was used as secondary antibody to detect TFF3 and CA I.

To study differences in epithelial proliferation between control and DSS treated animals, the number of BrdU-positive cells in 6 well-oriented crypts was counted and expressed per crypt, per intestinal segment, per time point (± SEM). To determine the number of BrdU-positive cells per crypt in each intestinal region sections were judged twice by two independent and blinded observers.

Protein dot blotting

CA I -, TFF3 - and Muc2 expression was quantified as described previously [18, 19]. Briefly, segments of proximal- and distal colon were homogenized, protein concentration was measured, and 0.30 µg protein of each homogenate was dot-blotted. After blotting the blots were incubated with anti-CA I (1:4000) to detect CA I expression or with a MUC2 specific antibody (WE9, 1:100), to detect Muc2 expression [17, 20]. Thereafter, the blots were incubated with ^{125}I- labeled protein A (Amersham, Bucks, United Kingdom, specific activity 33.8 mCi/mg). Binding of ^{125}I-labeled protein A to anti-CA I, anti-TFF3 or WE9 was detected by autoradiography using a PhosphorImager and quantified using ImageQuant software (Molecular Dynamics, B&L systems, Zoetermeer, The Netherlands).

Statistical Analysis

Analysis of variance was performed, followed by an unpaired t-test. Differences were considered significant when $p<0.05$. Data were represented as the mean ± standard error of the mean (SEM).

Results

Clinical symptoms

Rats treated with DSS suffered weight loss compared to control animals (Fig. 1). Immediately after the beginning of DSS treatment, rats started to lose weight. Weight loss progressed during and shortly after DSS treatment. On day 10, when weight loss of DSS-treated rats was maximal, DSS-treated rats weighed 25% less than control rats. On day 11, 5 days after the end of the DSS administration, rats started to gain weight again. Loose stools, diarrhea and bloody stools were observed within 3 days after the start of the DSS treatment. Gross bleeding first occurred on day 5, and persisted till day 8. The occurrences and recovery of the different clinical symptoms in time are specified in Fig. 1.

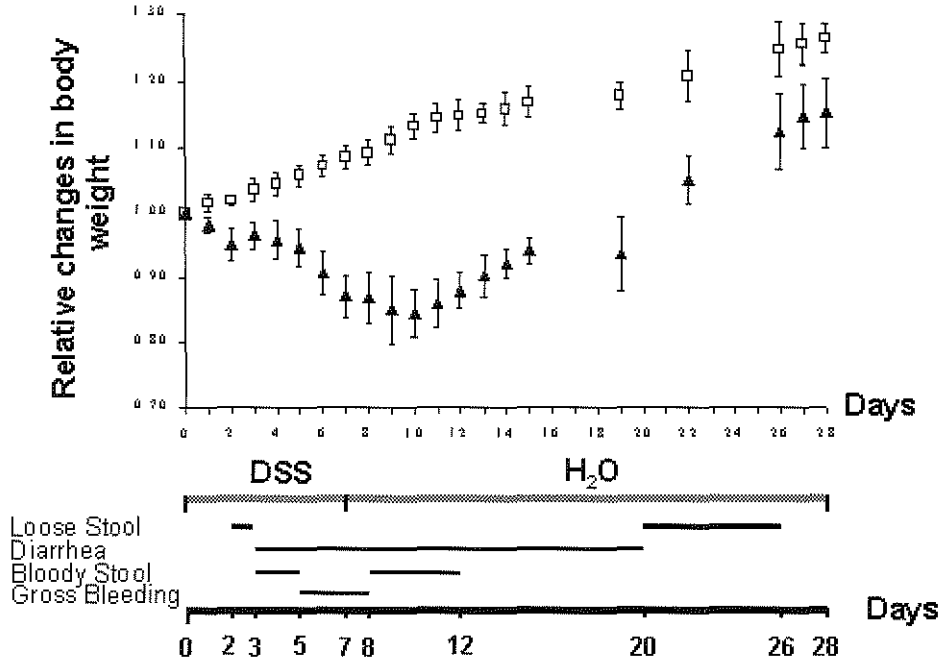

Figure 1. Effects of DSS treatment on body weight and the occurrence of clinical symptoms. Relative changes in body weight of control (□) and DSS treated (▲) rats. Error bars reflect the standard deviations of the relative changes in body weight on each day. The body weight of each individual animal was set arbitrarily at 1 on day 0 of the experiment. Clinical symptoms *i.e.* loose stool, diarrhea, bloody stool and gross bleeding are presented as a function of time. Days of DSS/water treatment are indicated by the dashed line. Note that changes in body weight coincided with changes in clinical symptoms.

Morphology

The colonic tissue showed dramatic morphological changes depending on time of treatment and localization within the colon, and was divided into 3 phases: onset of disease, active disease and regenerative phase. Onset of disease (day 2) was characterized by a slight flattening of the crypt epithelial cells (Fig 2B, *see Appendix*), and a slight increase in the number of apoptotic cells in the crypts and surface epithelium in both proximal and distal colon (Fig. 2C, *Appendix*). Moreover, in the distal colon focal crypt distortions were observed that varied from atrophy to complete loss (Fig. 2B, *Appendix*). During active disease (day 5-7) areas were seen with flattened crypt cells, crypt loss, massive inflammatory infiltrate, flattening of the surface epithelium, focal erosions, and necrotic cells in both colonic segments. The histological damage was focal in nature and most severe in the distal colon on days 5-7 (Fig. 2D, *Appendix*). Specifically, approx. 50% of the distal colonic tissue consisted of areas with crypt loss or erosions, while approx. 20% of the proximal colon was severely affected during this phase. During the regenerative phase (day 28) the epithelial morphology of the proximal colon completely recovered. In contrast, in the distal colon branched crypts and pronounced crypt elongations along side erosions, which involved less than 10% of the total surface, were still apparent (Fig. 2E, *Appendix*).

Table 1. ***Number of BrdU-positive cells in the proximal and distal colon during and after DSS treatment.***

Days of /after DSS treatment	**Proximal colon** ± SEM	**Distal colon** ± SEM
0 (control)	$15.0 \pm 0.7^{*\dagger}$	$13.6 \pm 0.03^{**}$
2	$7.6 \pm 0.5^{\ddagger}$	$5.0 \pm 0.2^{\dagger\dagger}$
5	$16.2 \pm 0.8^{\S}$	$7.2 \pm 0.7^{\ddagger\ddagger\ \S\S}$
7	19.2 ± 0.2	15.5 ± 1.5
28	$15.2 \pm 0.6^{\P}$	17.1 ± 1.4

The number of BrdU-positive cells in 6 well-oriented crypts was counted and expressed per crypt, per intestinal segment, per time point (± SEM). Significant differences were observed in the proximal as well as distal colon. Proximal colon: day 0 and days 2 ($^{*}p<0.001$) and 7($^{\dagger}p<0.01$); day 2 and days 5, 7 and 28 ($^{\ddagger}p<0.001$); day 5 and day 7 ($^{\S}p<0.05$); day 7 and day 28 ($^{\P}p<0.01$). Distal colon: day 0 and days 2 and 5 ($^{**}p<0.01$); day 2 and days 7 and 28 ($^{\dagger\dagger}p<0.001$); day 5 and day 7 ($^{\ddagger\ddagger}p<0.01$); day 5 and day 28 ($^{\S\S}p<0.001$).

Proliferation

Epithelial proliferation was studied by immunohistochemical detection and quantification of incorporated BrdU (Table 1, Fig. 3, *see Appendix*). Decreased numbers of BrdU-positive cells were seen in the crypt compartment of each colonic segment on day 2, indicating that BrdU incorporation was decreased during the first days of DSS treatment (Fig. 3B, *Appendix*). As DSS administration continued, a clear increase in BrdU-positive crypt cells was observed in proximal colon (day 7). In the distal colon increased numbers of BrdU-positive cells were only seen in elongated crypts in the proximity of ulcerations and/or areas with crypt depletion and a

flattened surface epithelium (Fig. 3C, *Appendix*). However, in the epithelium located more distantly from ulcerations the number of BrdU-positive cells was still decreased at day 5 (Table 1). In addition, due to the DSS-induced crypt loss (approx. 50% of the surface area distally and approx. 20% proximally) the overall number of BrdU-positive cells in the proximal and distal colon decreased compared to control tissue. On day 28, 21 days after ending DSS treatment, the levels of BrdU-positive crypt cells had returned to control values in the proximal colon. In the distal colon, increased numbers of BrdU-positive cells were still observed in elongated crypts adjacent to erosions or areas covered by a flattened surface epithelium (Fig. 3D, *Appendix*). The number of BrdU-positive cells in elongated crypts in the distal colon located more distantly from ulcerations was comparable to control values (Table 1).

Enterocyte-specific CA I expression

CA I is expressed by surface enterocytes of the proximal- and distal colon [13, 21, 22], and was used as marker for colonic enterocyte function. In the proximal colon, the CA I expression appeared unaltered during DSS treatment in areas with intact crypts and normal appearing surface epithelium (not shown). In the distal colon, however, some surface enterocytes were CA I negative during DSS administration (day 5 and 7) in areas with intact crypts and otherwise normally appearing surface epithelium (not shown). Moreover, in both proximal colon and distal colon, CA I expression was almost completely absent on days 5 and 7 in areas with a flattened surface epithelium and crypt loss (Fig. 4B, *see Appendix*). During the regenerative phase (day 28) the CA I expression was restored in the entire proximal colon and also in those areas of the distal colon where the epithelial morphology appeared normal (not shown). Moreover, flattened surface epithelium adjacent to ulcers was frequently CA I positive (Fig. 4C, *Appendix*).

Biochemical analysis of CA I protein levels in the proximal colon revealed a slight, but not significant, decrease in CA I protein levels in the course of DSS treatment (Fig. 5). Remarkably, during the regenerative phase (day 28) an overshoot in CA I expression was seen in this segment, with CA I levels that were significantly higher than on days 5 and 7. In the distal colon more pronounced alterations in CA I protein levels were observed. CA I expression levels decreased significantly until day 7, the end of DSS treatment. During the regenerative phase (day 28) CA I expression returned to levels that were not significant different from control values.

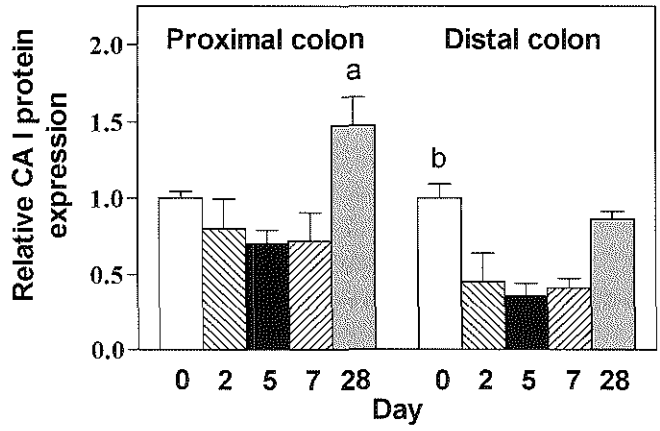

Figure 5. CA I expression levels during the different phases of the DSS-induced disease. CA I levels in each colonic segment of control and DSS-treated rats were quantified. Thereafter, the values of the control rats were averaged per segment and arbitrarily set on 1. The CA I levels in each segment of DSS-treated rats were expressed as relative values compared to control values (day 0). Finally, the mean ± standard error of the mean (SEM) was denoted. Statistical analysis was performed using analysis of variance followed by an unpaired t-test. In the proximal colon CA I levels were slightly, but not significantly, decreased during DSS treatment. In contrast on day 28, CA I levels appeared significantly increased compared to day 5 and 7 ($^{a}p<0.05$). In contrast in the distal colon CA I levels were significantly decreased on days 2, 5 and 7 ($^{b}p<0.05$).

Goblet cell-specific Muc2 and TFF3 expression

To study goblet cell function Muc2 - and TFF3 expression was studied. In controls, Muc2 was expressed by goblet cells in the proximal and distal colon from crypt base till the surface epithelium (Fig. 6A and E, *see Appendix*). In contrast, TFF3 was expressed in the upper crypts in the proximal colon and upper 2/3 of the crypts in the distal colon (Fig. 6C and H, *Appendix*). Alterations in the localization and numbers of goblet cells were seen during and after DSS treatment in both colonic segments. During the onset of disease (day 2) Muc2- and TFF3-positive goblet cells accumulated in the surface epithelium in both proximal and distal colon (not shown). As DSS treatment progressed (day 5 and 7) the accumulation of Muc2- and TFF3-positive goblet cells in the surface epithelium became more pronounced, particularly in the proximal colon (Fig. 6B and D, *Appendix*). In the distal colon, the area of TFF3 expression was extended from upper 2/3 of the crypt toward the crypt bottom in elongated crypts (Fig. 6J, *Appendix*). In areas with flattened crypts TFF3 was expressed strongly in the upper crypts and surface epithelium, and although very weakly also in the deeper crypt region (Fig. 6I, *Apendix*). Muc2 expression in the proximal and distal colon appeared unaltered, independent of crypt morphology, during active disease. Specifically, Muc2 was expressed in small goblet cells within damaged crypts and in small goblet cells in elongated crypts (Fig. 6F and G, *Appendix*). Due to the massive crypt damage, crypt loss, and loss of surface epithelium in the

distal colon (approx. 50%), the overall number of goblet cells decreased in the latter segment. During the regenerative phase (day 28) elevated numbers of Muc2- and TFF3-positive goblet cells were still seen in the surface epithelium of distal colon (Fig. 6K and L, *Appendix*), but not in the proximal colon. Especially in the distal colon, crypts were elongated and primarily contained large goblet cells.

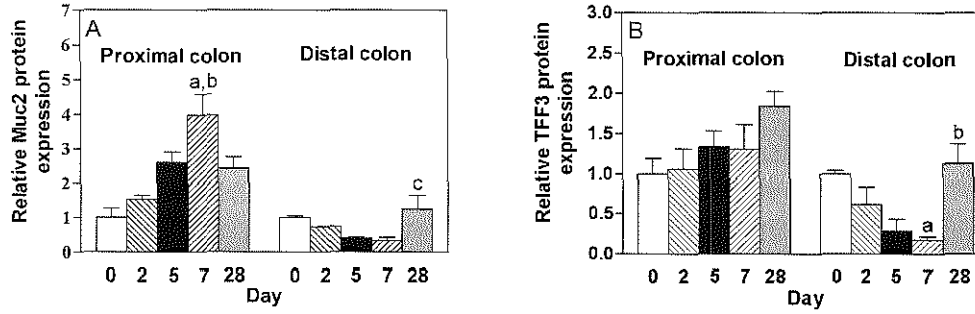

Figure 7. Muc2 (A) and TFF3 expression levels (B) during the different phases of the DSS-induced disease. Muc2 and TFF3 levels in each colonic segment of control and DSS-treated rats were quantified. Thereafter, the values of the control rats were averaged per segment and arbitrarily set on 1.The Muc2 and TFF3 levels in each segment of DSS-treated rats were expressed as relative values compared to control values (day 0). Finally, the mean ± standard error of the mean (SEM) was denoted. Statistical analysis was performed using analysis of variance followed by an unpaired t-test. In the proximal colon Muc2 expression was significantly increased on day 7 compared to day 0 ($^{a}p<0.01$) and day 2 ($^{b}p<0.05$). In the distal colon significant differences in Muc2 levels were seen between day 28 and days 5 and 7 ($^{c}p<0.05$). Significant decreased TFF3 levels were observed in the distal colon on day 7 compared to controls ($^{a}p<0.05$), and on days 5 and 7 compared to day 28 ($^{b}p<0.05$).

Biochemical analysis of Muc2 protein levels demonstrated a progressive increase in Muc2 levels in the proximal colon in the course of DSS treatment (Fig. 7A). On day 7, this increase in Muc2 levels in the proximal colon was fourfold compared to control values and was significantly different from control values and onset of disease. Thereafter, during the regenerative phase (day 28), the Muc2 levels in the proximal colon decreased but were still elevated compared to the control levels. In the distal colon, however, a trend to decreased Muc2 expression levels was observed during active disease (day 5-7), while during the regenerative phase (day 28) Muc2 levels returned to control levels. Similar to Muc2 expression levels, TFF3 levels seemed to increase in the proximal colon during and after DSS treatment (Fig. 7B). This increase in TFF3 protein levels, however, was not statistically significant. In the distal colon, TFF3 expression levels were significantly decreased during active disease (day 5-7) compared to controls. During the regenerative phase (day 28) TFF3 levels had increased again, and were comparable with control levels.

Discussion

As DSS-induced colitis is commonly used as a model for human IBD, knowledge is essential to be able to understand the mechanisms underlying the pathology of DSS-induced colitis. Therefore, we analyzed the occurrence of clinical symptoms, epithelial gene expression, proliferation, and cell death during DSS-induced colitis. In our study, DSS-induced clinical symptoms *i.e.* body weight loss, loose and bloody stools, diarrhea, and gross bleeding started within several days after the beginning of the DSS treatment, were most severe at the end of DSS-treatment, and disappeared only gradually during the recovery period. Previous studies in mice and rats confirm this pattern of occurrence and recovery of clinical symptoms [1, 5, 8, 23]. The pathological features such as crypt loss, ulcerations, and inflammatory infiltrate that appeared in our rat DSS colitis model are similar to those seen in UC [3, 24] and in DSS-treated mice [3, 5, 24]. Furthermore, DSS-induced damage in rat started and was most severe within the distal colon, and was focal in nature, and was comparable to DSS-induced colitis in mice and UC in human [3, 5, 24].

Our study is the first to describe the response of the colonic epithelium with respect to proliferation and apoptosis during the different phases of DSS-induced disease. DSS administration induced a decrease in proliferative activity and an increase in the number of apoptotic crypt cells, in the proximal colon as well as in the distal colon, during the onset of disease. These data demonstrate that DSS exerts its toxic effects on the epithelium via the relatively undifferentiated crypt cells. This is similar to humans with active UC, in which the numbers of apoptotic cells and proliferating cells in the crypt compartment are also increased [25, 26]. The increased number of apoptotic cells in the surface epithelium suggests that DSS also affects mature surface cells. However, we can not exclude the possibility that these surface cells were already damaged by DSS when they were relatively immature crypt cells. When DSS feeding was continued, the initial decrease in proliferative activity was followed by epithelial hyper-proliferation in the entire proximal colon and in the proximity of ulcerations in the distal colon. These data clearly demonstrate that the inhibiting effect of DSS on epithelial proliferation can be overruled leading to hyper-proliferation. However, the mechanism(s) and growth factor(s) responsible for this phenomenon remain to be identified.

Apart from the DSS-induced alterations in epithelial proliferation and cell death, epithelial cell functions might also be affected. Therefore, we examined the effects of DSS on enterocyte-specific CA I expression and goblet cell-specific Muc2 and TFF3 expression. The effects of DSS feeding on CA I expression levels were most pronounced in the distal colon, where it induced a significant decrease in CA I levels during onset of disease and active disease. This indicates that specific enterocyte functions were down-regulated and thus that colonic functions are impaired during DSS treatment. Immunohistochemical analysis of the distal colon revealed CA I-negative surface cells during active disease in areas with apparently normal crypts and surface epithelium. In addition, the majority of flattened surfaces epithelial cells overlying mucosa with crypt distortions were CA I-negative, in the proximal colon as

well as the distal colon. These data suggest that during transition of areas with intact crypts and surface epithelium into areas with crypt loss and flattened surface epithelium, specific enterocyte functions are down- regulated before restitution is initiated. Later in the course of the disease, during the recovery phase, the surface epithelial cells of the distal colon near ulcers were still flattened but were frequently CA I-positive. Moreover, during this disease phase CAI protein levels restored to control levels in the distal colon and were even up-regulated in the proximal colon. These data imply that in addition to epithelial proliferation, epithelial differentiation restored during the recovery phase to accelerate the recovery of colonic functions. Similar results have been reported by Fonti *et al.* who observed a reduction in CA I expression in active UC, whereas in humans with UC in remission CA I expression was restored to control levels [27]. Moreover, in rat the down-regulation of CA I expression during DSS treatment correlated with the occurrence of loose stools and diarrhea, suggesting that CA I might play a role in DSS-induced diarrhea.

Quantitative analysis of Muc2 and TFF3 demonstrated a trend toward decreased Muc2 levels and significantly decreased TFF3 levels in the distal colon. As DSS-induced crypt loss and ulcerations were most severe in the distal colon, (approx. 50% distally vs. approx. 20% proximally) the decreased Muc2 and TFF3 levels in this segment during active disease are largely due to the dramatic decrease in the overall number of goblet cells. Reduced numbers of goblet cells have also been reported in the colon of humans with active UC [28]. Additionally, MUC2 levels in the sigmoid colon have also been found to be significantly lower in active UC compared to controls and UC in remission [18, 19]. Yet, despite the DSS-induced damage a progressive increase in Muc2 levels and maintenance of TFF3 levels were observed in the proximal colon during DSS-treatment. Furthermore, immunohistochemical analysis revealed an accumulation of Muc2- and TFF3-positive goblet cells in the surface epithelium of the proximal and distal colon, suggesting selective sparing of goblet cells during DSS-induced colitis. In addition to the accumulation of goblet cells in the surface epithelium, alterations in goblet cell morphology and gene expression were observed in the crypts during active disease and the regenerative phase. Specifically, goblet cells in flattened or elongated crypts of the proximal and distal colon were small, but remained Muc2-positive. During this disease phase TFF3 expression was extended toward the crypt bottom especially in elongated crypts of the distal colon, implying an up-regulation of the epithelial repair capacity in these crypts. Finally, during the regenerative phase crypts were elongated and primarily contained large goblet cells. In conjunction, these data imply that goblet cells play a pivotal role in epithelial defense against luminal substances and organisms, and in epithelial repair via Muc2 and TFF3 synthesis, respectively.

Conclusions

DSS-induced clinical symptoms and morphological alterations in rat are comparable with clinical symptoms and morphological changes seen in DSS-induced colitis in mice and UC in

humans. The primary *in vivo* actions of DSS on the epithelium are inhibition of proliferation and the induction of apoptosis. The epithelium responded to these changes by a rapid hyper-proliferation to re-establish epithelial homeostasis and functions. Epithelial hyper-proliferation was accompanied by flattening of the surface epithelium *i.e.* restitution. Collectively, these data underline that maintenance and restoration of epithelial barrier function are of primary importance. During the recovery phase when erosions were still present, the increase in epithelial proliferation coincided with a re-establishment of enterocyte gene expression (*i.e.* CA I expression), indicating that next to epithelial barrier function, epithelial cell function plays an important role in the restoration of full colonic integrity. Goblet cells are of significant importance in the protection and repair of the intestinal surface epithelium as during DSS-colitis: 1) Muc2 and TFF3 expression in the proximal colon were up-regulated or at least maintained, 2) Muc2 and TFF3-positive goblet cells accumulated in the surface epithelium, 3) small goblet cells in the flattened colonic crypts continued to express Muc2, and 4) TFF3 expression extended to the crypt bottom.

Acknowledgements

This work was financed in part by Numico BV, Zoetermeer, The Netherlands. The authors thank Prof. Dr WS Sly and Prof. Dr DK Podolsky for kindly providing anti-rat CA I antibodies and WE9 (anti-human MUC2 antibodies), respectively.

References

1. Cooper HS, Murthy SN, Shah RS, Sedergran DJ. Clinicopathologic study of dextran sulfate sodium experimental murine colitis. Lab Invest 1993;69:238-49.

2. Greenfield SM, Punchard NA, Teare JP, Thompson RPH. The mode of action of the aminosalicylates in inflammatory bowel disease. Aliment Pharmacol Ther 1993;7:369-383.

3. Hamilton SR. Diagnosis and comparison of ulcerative colitis and Crohn's disease involving the colon. Churchill Livingstone, 1983.

4. Murthy SN, Cooper HS, Shim H, Shah RS, Ibrahim SA, Sedergran DJ. Treatment of dextran sulfate sodium-induced murine colitis by intracolonic cyclosporin. Dig Dis Sci 1993;38:1722-34.

5. Okayasu I, Hatakeyama S, Yamada M, Ohkusa T, Inagaki Y, Nakaya R. A novel method in the induction of reliable experimental acute and chronic ulcerative colitis in mice. Gastroenterology 1990;98:694-702.

6. Yamada M, Ohkusa T, Okayasu I. Occurrence of dysplasia and adenocarcinoma after experimental chronic ulcerative colitis in hamsters induced by dextran sulphate sodium. Gut 1992;33:1521-7.

7. Axelsson LG, Landstrom E, Bylund-Fellenius AC. Experimental colitis induced by dextran sulphate sodium in mice: beneficial effects of sulphasalazine and olsalazine. Aliment Pharmacol Ther 1998;12:925-34.

8. Bylund-Fellenius A-C, Landström E, Axelsson L-G, Midtvedt T. Experimental colitis induced by dextran sulphate in normal and germfree mice. Microbial Ecology in Health and Disease 1994;7:207-215.

9. Dieleman LA, Ridwan BU, Tennyson GS, Beagley KW, Bucy RP, Elson CO. Dextran sulfate sodium-induced colitis occurs in severe combined immunodeficient mice. Gastroenterology 1994;107:1643-52.

10. Ni J, Chen SF, Hollander D. Effects of dextran sulphate sodium on intestinal epithelial cells and intestinal lymphocytes. Gut 1996;39:234-41.

11. Tessner TG, Cohn SM, Schloemann S, Stenson WF. Prostaglandins prevent decreased epithelial cell proliferation associated with dextran sodium sulfate injury in mice. Gastroenterology 1998;115:874-82.

12. Charney AN, Dagher PC. Acid-base effects on colonic electrolyte transport revisited. Gastroenterology 1996;111:1358-68.

13. Fleming RE, Parkkila S, Parkkila AK, Rajaniemi H, Waheed A, Sly WS. Carbonic anhydrase IV expression in rat and human gastrointestinal tract regional, cellular, and subcellular localization. J Clin Invest 1995;96:2907-13.

14. Sowden J, Leigh S, Talbot I, Delhanty J, Edwards Y. Expression from the proximal promoter of the carbonic anhydrase 1 gene as a marker for differentiation in colon epithelia. Differentiation 1993;53:67-74.

15. Tytgat KMAJ, Bovelander FJ, Opdam FJ, Einerhand AWC, Büller HA, Dekker J. Biosynthesis of rat MUC2 in colon and its analogy with human MUC2. Biochem J 1995;309:221-9.

16. Mashimo H, Wu DC, Podolsky DK, Fishman MC. Impaired defense of intestinal mucosa in mice lacking intestinal trefoil factor. Science 1996;274:262-5.

17. Tytgat KMAJ, Klomp LW, Bovelander FJ, Opdam FJ, Van der Wurff A, Einerhand AWC, Büller HA, Strous GJ, Dekker J. Preparation of anti-mucin polypeptide antisera to study mucin biosynthesis. Anal Biochem 1995;226:331-41.

18. Tytgat KMAJ, van der Wal JW, Einerhand AWC, Büller HA, Dekker J. Quantitative analysis of MUC2 synthesis in ulcerative colitis. Biochem Biophys Res Commun 1996;224:397-405.

19. Van Klinken BJW, Van der Wal JW, Einerhand AWC, Büller HA, Dekker J. Sulphation and secretion of the predominant secretory human colonic mucin MUC2 in ulcerative colitis. Gut 1999;44:387-93.

20. Podolsky DK, Fournier DA, Lynch KE. Human colonic goblet cells. Demonstration of distinct subpopulations defined by mucin-specific monoclonal antibodies. J Clin Invest 1986;77:1263-71.

21. Bekku S, Mochizuki H, Takayama E, Shinomiya N, Fukamachi H, Ichinose M, Tadakuma T, Yamamoto T. Carbonic anhydrase I and II as a differentiation marker of human and rat colonic enterocytes. Res Exp Med (Berl) 1998;198:175-85.

22. Lonnerholm G, Midtvedt T, Schenholm M, Wistrand PJ. Carbonic anhydrase isoenzymes in the caecum and colon of normal and germ-free rats. Acta Physiol Scand 1988;132:159-66.

23. Takizawa H, Shintani N, Natsui M, Sasakawa T, Nakakubo H, Nakajima T, Asakura H. Activated immunocompetent cells in rat colitis mucosa induced by dextran sulfate sodium and not complete but partial suppression of colitis by FK506. Digestion 1995;56:259-64.

24. Riddell RH. Pathology of idiopatic inflammatory bowel diseases. In: Kirsner JB, Shorter RG, eds. Inflammatory Bowel Diseases. Philadelphia: Lea Febiger, 1988:329-350.

25. Arai N, Mitomi H, Ohtani Y, Igarashi M, Kakita A, Okayasu I. Enhanced epithelial cell turnover associated with p53 accumulation and high p21WAF1/CIP1 expression in ulcerative colitis. Mod Pathol 1999;12:604-11.

26. Iwamoto M, Koji T, Makiyama K, Kobayashi N, Nakane PK. Apoptosis of crypt epithelial cells in ulcerative colitis. J Pathol 1996;180:152-9.

27. Fonti R, Latella G, Caprilli R, Frieri G, Marcheggiano A, Sambuy Y. Carbonic anhydrase I reduction in colonic mucosa of patients with active ulcerative colitis. Dig Dis Sci 1998;43:2086-92.

28. Jacobs LR, Huber PW. Regional distribution and alterations of lectin binding to colorectal mucin in mucosal biopsies from controls and subjects with inflammatory bowel diseases. J Clin Invest 1985;75:112-8.

Chapter 4

Distinct responses of enterocytes and goblet cells in experimental colitis: *implications for ion uptake and for mucosal protection*

Published as:
Ingrid B. Renes, Melissa Verburg, Daniëlle J.P.M. Van Nispen, Hans A. Büller, Jan Dekker, and Alexandra W.C. Einerhand. Distinct responses of enterocytes and goblet cells in experimental colitis: *implications for ion uptake and for mucosal protection. Am J Physiol Gastrointest Liver Physiol* 2002, 283:G169-G179.

Summary

In the present study we aimed to investigate enterocyte- and goblet cell-specific functions during the different phases of acute colitis induced with dextran sulfate sodium (DSS). Thereto, rats were treated with DSS for 7 days, followed by a 7-day recovery period. Colonic tissue was excised on days 2 (onset of disease), 7 (active disease), and 14 (regenerative phase). Enterocyte functions were studied by the expression of carbonic anhydrases (CAs), sodium hydrogen exchangers (NHEs) and intestinal fatty acid-binding protein (i-FABP), and by alkaline phosphatase (AP) activity. The expression and secretion of the mucin Muc2 and trefoil factor family peptide 3 (TFF3) were used as parameters for goblet cell function. DSS induced a down-regulation of the CAs, NHEs, and i-FABP in some normal appearing surface enterocytes and in most of the flattened surface enterocytes during onset of - and active disease. During the regenerative phase most enterocytes expressed these genes again. Quantitative analysis revealed a significant decrease in CAs, NHEs and i-FABP expression levels during onset of - and active disease. During the regenerative phase the expression levels of the CAs restored, whereas the expression levels of the NHEs and i-FABP remained decreased. In contrast, enterocyte-specific AP activity was maintained in normal and flattened enterocytes during DSS-induced colitis. Goblet cells continued to express Muc2 and TFF3 during and after DSS treatment. Moreover, Muc2 and TFF3 expression and secretion levels were maintained or even increased during each of the DSS-induced disease phases. In conclusion: DSS-induced colitis was associated with decreased expression of CAs, NHEs, and I-FABP. The loss of these genes possibly accounts for some of the pathology seen in colitis. The maintenance or up-regulation of Muc2 and TFF3 synthesis and secretion levels implies that goblet cells at least maintain their epithelial defense and repair capacity during acute inflammation induced by DSS.

Abbreviations: AP, alkaline phosphatase; CA, carbonic anhydrase; DSS, dextran sulfate sodium; FABP, fatty acid binding protein; NHE, sodium hydrogen exchanger; UC, ulcerative colitis.

Introduction

The colonic epithelium consists of two major cell types; enterocytes and goblet cells, which play a key role in the maintenance of colonic functions. The enterocytes express specific proteins like carbonic anhydrases (CAs) and sodium hydrogen exchangers (NHEs) that are involved in colonic CO_2 excretion, intracellular pH regulation, Na^+ and Cl^- absorption, and indirectly in water transport [1]. CA I, an isoform of the CAs, is localized in the cytoplasm of the surface enterocytes [2]. CA I catalyses the reversible hydration of CO_2 providing H^+ and HCO_3^- ions to the apical Na^+/H^+ and Cl^-/HCO_3^- exchangers [1]. In contrast to CA I, the exact function of the CA isoenzyme IV still awaits characterization. CA IV protein is strategically positioned along the apical membrane of the surface enterocytes [3]. Therefore it seems likely that CA IV, similar to CA I, participates in the colonic ion and fluid transport. The apical Na^+/H^+ exchangers that are responsible for electroneutral Na^+ absorption in the colon are NHE2 and -3 [4, 5]. Both NHE isoforms are expressed by colonic surface enterocytes [6, 7]. Together with Cl^-/HCO_3^- exchangers the two NHE isoforms regulate Na^+ and Cl^- absorption. As water passively follows ion movements this process is an important factor in colonic water absorption as well. Supportive to the role of NHE3 in colonic water absorption is the fact that NHE3 deficient mice suffer from diarrhea [8].

The colonic enterocytes also express gene products that are assumed to be involved in fatty acid uptake and cellular transport of fatty acids; the fatty acid binding proteins (FABPs) [9]. In the colon two isoforms of FABPs were identified, intestinal (i-) and liver (l-) FABP. Both types of FABP are expressed by the colonic surface enterocytes [10, 11]. Interestingly, colonic enterocytes also express alkaline phosphatase (AP) which is known to detoxify endotoxin, and thus plays a significant role in the innate defense of the colonic mucosa [12].

Goblet cells, the second major cell type in the colonic epithelium, express the secretory mucin Muc2 [13], which is the structural component of the mucus layer. Muc2 protein is expressed by crypt and surface goblet cells in the proximal as well as distal colon. After synthesis Muc2 is secreted into the lumen and forms a gel-like mucus layer. This mucus layer serves as a barrier to protect the epithelium from mechanical stress, noxious agents, viruses and other pathogens [14, 15]. Goblet cells are also known to synthesize and secrete trefoil factor family peptide 3 (TFF3), a bioactive peptide which is involved in epithelial repair [16]. In the proximal colon TFF3 protein is expressed by goblet cells in the upper one third of the crypts and in surface epithelium, whereas in the distal colon TFF3 protein is observed in goblet cells located in the upper two thirds of the crypts and in the surface epithelium. As TFF3 acts as a motogen, *i.e.* promotes cell migration without promoting cell division, it stimulates epithelial restitution and thus epithelial repair [17].

In healthy colon, the above-described enterocyte and goblet cell-specific functions are tightly regulated. Yet during inflammatory diseases like ulcerative colitis (UC) and in experimental colitis, colonic enterocyte and goblet cell functions are altered. For example, in humans with active UC CA I protein levels and total CA activity were significantly reduced [18].

Furthermore, in UC aberrations in Na^+ and Cl^- absorption and secretion were observed, suggesting alterations in the expression levels or activity of electrolyte exchangers [19-21]. In experimental colitis a disruption in colonic electrolyte transport was reported [22]. Also, goblet cell-specific Muc2 expression was significantly reduced in humans with active UC [23]. In these studies the colonic epithelium was investigated during chronic inflammation, nevertheless information on enterocyte and goblet cell functioning during acute inflammation is limited.

In the present study we investigated cell type-specific gene expression, as a measure of enterocyte and goblet cell function, in the proximal and distal colon during different phases of acute colitis induced with dextran sulfate sodium (DSS). Enterocyte-specific functions were studied by the analysis of CA I and IV, NHE2 and -3, i-FABP, and AP expression. Muc2 and TFF3 expression was analyzed to study goblet cell-specific functions. In conjunction these data were used to determine the functioning of enterocytes and goblet cells during DSS-induced acute colitis.

Materials & Methods

Animals

Eight weeks-old, specified pathogen free, male Wistar rats (Broekman, Utrecht, The Netherlands) were housed at constant temperature and humidity on a 12-h light-dark cycle. One week prior to and during the experiment the rats were housed individually. The rats had free access to a standard pelleted diet (Hope Farms, Woerden, The Netherlands) and sterilized tap water (controls) or sterilized tap water supplemented with DSS. All the experiments were performed with the approval of the Animal Studies Ethics Committee of our institution.

Experimental Design

Rats were given 7% DSS (37-40 kD, TdB Consultansy, Uppsala, Sweden) in their drinking water for 7 days, followed by a 7-day recovery period during which DSS was omitted from the drinking water. Fresh DSS solutions were prepared daily. On day 0 (control), day 2 (onset of disease), day 7 (active colitis), and day 14 (regenerative phase), five animals per time point were sacrificed. Segments of the proximal and distal colon were dissected and prepared for light microscopy or snap frozen in liquid nitrogen and stored in -70°C till RNA and protein isolation. Additionally, to study Muc2 and TFF3 secretion two tissue explants (10 mm^3) of the proximal colon and 3 explants of the distal colon were cultured in RPMI medium (Gibco-BRL, Gaithersburg MD, USA) for 4.5 h. Thereafter, the tissue as well as the culture medium was collected and homogenized in, or culture medium was mixed with, a Tris buffer containing 1% (wt/vol.) SDS and protease inhibitors as described previously [23, 24].

Immunohistochemistry

Five μm thick sections were cut and prepared for immunohistochemistry as described previously [25]. Briefly, sections were incubated overnight with one of the following enterocyte-

specific antibodies: anti-mouse CA I (1:16000, kindly provided by Prof. W.S. Sly), anti-rat CA IV (1:16000) [3], anti-rat NHE2 (1:1500) [7], anti-rat NHE3 (1:1500) [6], anti-rat i-FABP (1:4000) [26]; and the goblet cell-specific antibodies: WE9 (1:300) [27] to detect Muc2 and anti-rat TFF3 (1:6000, Prof. Dr D.K. Podolsky). Immunoreaction was detected using the Vectastain ABC Elite Kit (Vector Laboratories, Burlingame, England), and staining was developed using 3,3'-diaminobenzidine.

Histochemistry

Enterocyte-specific AP activity was assessed on colonic tissue sections using an one-step assay. Thereto deparaffinazed and rehydrated tissue sections were incubated with a Tris-buffer (pH 9.5) containing 50 µl 4-nitroblue tetrazolium chloride (NBT) (Vector Laboratories) and 37.5 µl 5-bromo-4-chloro-3-indolyl-phosphate (BCIP) (Vector Laboratories) according to the manufacturer's protocol. The color reaction was performed for 1 h in the dark and was stopped with distilled water and mounted with aquamount® improved (Gurr, Brunschwig, Amsterdam, The Netherlands).

In Situ Hybridization

Non-radioactive *in situ* hybridizations were performed according to the method described previously with slight modifications [28]. Briefly, sections were deparaffinized, hydrated and incubated in the following solutions: 0.2 M HCl, distilled water, 0.1% (wt/vol.) pepsin (Sigma, St. Louis, USA) in 0.01 M HCl, 0.2% (wt/vol.) glycine in phosphate buffered saline (PBS), PBS, 4% (wt/vol.) paraformaldehyde in PBS, PBS and finally in 2 X SSC. Until hybridization, sections were stored in a solution of 50 % (vol./vol.) formamide in 2 X SSC at 37°C. For hybridization, cell type-specific probes were diluted in hybridization solution (50% (vol./vol.) deionized formamide, 10% (wt/vol.) dextran sulfate, 2 X SSC, 1 X Denhardt's solution, 1 µg/ml tRNA, 250 µg/ml herring sperm DNA to a concentration of 100 ng/ml, incubated at 68°C for 15 min and layered onto the sections. Sections were hybridized overnight at 55°C in a humid chamber. Post-hybridization washes were performed at 45°C using the following steps: 50% (vol./vol.) formamide in 2 X SSC, 50% (vol./vol.) formamide in 1 X SSC and 0.1 X SSC. A 15 min incubation with RNase T1 (2 U/ml in 1 mM EDTA in 2 X SSC) at 37°C was followed by washes of 0.1 X SSC at 45°C and 2 X SSC at room temperature. The digoxigenin-labeled hybrids were detected by incubation with anti-digoxigenin (Fab, 1:2000) conjugated to alkaline phosphatase for 2.5 h at room temperature. Thereafter, sections were washed in 0.025% (vol./vol.) Tween 20® (Merck, Darmstadt, Germany) in Tris buffered saline pH 7.5. For staining, sections were layered with detection buffer pH 9.5 (0.1 M Tris, 0.1 M NaCl, 0.05 M $MgCl_2$) containing 0.33 mg/ml NBT, 0.16 mg/ml BCIP, 8 % polyvinylalcohol (Mw 31000-50000, Aldrich Chemical Milwaukee, WI, USA) and 1 mM levamisol (Sigma). The color reaction was performed overnight in the dark and was stopped when the desired intensity of the resulting blue precipitate was reached. Finally, sections were washed in 10 mM Tris containing 1 mM EDTA pH 9.5, distilled water and mounted with aquamount® improved (Gurr). As control for aspecific binding of probes or for aspecific signal (*i.e.*

endogenous AP activity), the cell type-specific probes were replaced by sense-strand RNA or omitted from the hybridization solution, respectively. No color reaction was seen on sections incubated with these types of control hybridization solution.

Probe preparation for in situ hybridization

Digoxigenin-11-UTP labeled RNA probes were prepared according to the manufacturer's protocol (Boehringer Mannheim GmbH, Mannheim, Germany) using T3, T7 or SP6 RNA polymerase. The following enterocyte-specific probes were used: A 890 bp XhoI/BamHI fragment of mouse CA I cDNA clone ligated in pBluescript KS [29], a 690 bp XbaI/EcoRI fragment of rat CA IV cDNA clone ligated in pGEM4 [30]. As goblet cell-specific probes a 200 bp EcoRI/NotI fragment based on the 1.1 kb fragment of rat Muc2 as described previously [25], and a 438 bp EcoRI fragment of rat TFF3 ligated in pBluescript KS were used [31]. Probes longer than 700 bp were hydrolyzed.

Protein dot blots

The expression of enterocyte and goblet cell-specific markers was detected and quantified as described previously [24]. Briefly, small tissue pieces (10 mm^3) of the proximal (n=2 per animal) and distal colon (n=3 per animal) were homogenized, protein concentration was measured, and 0.5 µg protein of each homogenate was dot-blotted on nitrocellulose (Nitran; Schleier & Schuell, Dassell, Germany). Thereafter, the blots were blocked for 1 h with blocking buffer containing 50 mM Tris, pH 7.8, 5% (wt/vol.) non-fat dry milk powder (Lyempf, Kampen, The Netherlands), 2 mM $CaCl_2$, 0.05% (vol./vol.) Nonidet P40® (BDH, Brunschwig Chemie, Amsterdam, The Netherlands), and 0.01% (vol./vol.) antifoam (Sigma). The blots were incubated 18 h with anti-CA I, anti-CA IV, anti-i-FABP, anti-TFF3, or the Muc2 specific antibody WE9 (see *immunohistochemistry* for antibody references). After washing in blocking buffer, the blot was incubated with ^{125}I-labeled protein A (Amersham, Bucks, United Kingdom, specific activity 33.8 mCi/mg) for 2 h. Binding of ^{125}I-labeled protein A to the marker specific antibodies was detected using a PhosphorImager. The elicited signal was quantified and the expression of the cell type-specific markers was expressed per µg protein of the tissue. Average expression levels of the cell type-specific markers were calculated per segment per rat, followed by calculation of the mean expression of the cell type-specific markers (± SEM) for each of the disease phases studied.

The specificity of each of the antibodies used in this study was determined, under the same conditions, by Western blot. To determine Muc2 and TFF3 secretion levels, homogenates and their corresponding media were dot-blotted and treated as described above for the expression of the enterocyte- and goblet cell markers. The percentage of Muc2 and TFF3 secretion was calculated as the amount of Muc2 or TFF3 in the medium divided by the sum of the amount of Muc2 or TFF3 in tissue and in the medium.

Northern dot blots

Total RNA was isolated from proximal and distal colonic segments using Trizol® (Gibco-BRL) following the manufacturer's protocol. The integrity of the RNA was assessed by analysis of the 28S and 18S ribosomal RNAs after electrophoresis and staining with ethidium bromide. Subsequently, 1 μg of total RNA from each segment was dot-blotted on Hybond-N^+ (Amersham). The blot was hybridized to ^{32}P-labeled cell type-specific cDNA probes. Hybridization of the probe to the cell type-specific mRNAs was detected and quantified using a PhosphorImager. Thereafter, the blot was stripped and re-probed with a 1.4 kb GAPDH cDNA as probe [25]. Hybridized signals of each cell type-specific marker were corrected for glyceraldehyde-3-phosphate dehydrogenase (GAPDH) mRNA to correct for the amount of loading. In addition to the enterocyte- and goblet cell-specific probes that were used for the *in situ* hybridization studies, a 736 bp XbaI/EcoRI fragment of rat NHE2 cDNA clone ligated in pGEM-7Z (provided by Dr C. M. Bookstein), a 359 bp EcoRI/HindIII fragment of rat NHE3 cDNA clone ligated in pGEM-4Z (provided by Dr C.M. Bookstein), and a 564 bp fragment of rat i-FABP cDNA clone ligated in pBR322 [32] were also used as enterocyte-specific markers. Average mRNA levels of the cell type-specific markers were calculated per segment per rat followed by calculation of the mean mRNA expression levels of the markers (± SEM) for each of the disease phases studied.

When using the above described probes under the same conditions by Northern blot a specific band for each of the probes was obtained.

Statistical Analysis

To compare two groups an unpaired t-test was used and to compare 3 or more groups, analysis of variance was performed followed by an unpaired t-test. Differences were considered significant when $p<0.05$. Data were represented as the mean ± standard error of the mean (SEM).

Results

Localization of enterocyte-specific markers

Cell type-specific markers were detected *in situ* at the mRNA and/or at the protein level by means of *in situ* hybridization and immunohistochemistry, respectively. CA I, and i-FABP expression levels strongly decrease from mid to distal colon [3, 10], thus slight differences in sampling position of the distal colonic segments might influence the expression levels of CA I and i-FABP. Therefore, CA I and i-FABP were only used as markers for enterocyte functioning in the proximal colon. CA IV, NHE2, and NHE3 were used as enterocyte markers in both proximal and distal colon.

The mRNA of the enterocyte-specific marker CA I, that is normally expressed in the upper half of the crypts in the proximal colon (Fig. 1A, *see Appendix*), remained expressed

during the onset of disease (not shown). During active disease CA I mRNA expression was still detected at low levels in areas with a normal appearing morphology (Fig. 1B, *Appendix*), but not in areas with crypt damage and a flattened surface epithelium (not shown). During the regenerative phase CA I mRNA expression pattern was comparable to controls (Fig. 1C, *Appendix*). Similarly, CA I protein, which is normally expressed by the surface epithelial cells [2], was absent in the flattened epithelial enterocytes during the active phase of the disease, but reappeared during the regenerative phase (not shown).

The mRNA and protein of CA IV is expressed by surface enterocytes in the proximal and distal colon (Fig. 1D and G, *Appendix*). During and after DSS treatment CA IV mRNA expression was seen in the normal appearing surface epithelium as well as in the flattened surface epithelium of the proximal and distal colon (*e.g.* Fig. 1E and F, *Appendix*). Focussing on CA IV protein, we observed that the flattened surface enterocytes were CA IV-negative during active disease in the proximal (not shown) as well as distal colon (Fig. 1H, *Appendix*). During the regenerative phase CA IV protein expression was seen in surface epithelium with a normal appearing morphology, and also in some of the flattened surface cells (Fig. 1I, *Appendix*).

The expression pattern of sodium hydrogen exchangers NHE2 and -3 was analyzed by immunohistochemistry. Both NHE2 and -3 were expressed in the apical membrane of the surface enterocytes in the proximal and distal colon of controls (Fig. 1J, NHE2, *Appendix*). During DSS treatment NHE2 and -3 protein were decreased or absent in many surface enterocytes with a normal appearing morphology in the proximal and distal colon (not shown). Additionally most of the flattened surface enterocytes were also NHE2 and -3 protein negative (Fig. 1K, NHE2, *Appendix*). During the regenerative phase NHE2 and -3 protein was expressed by all the enterocytes with a normal appearing morphology (not shown), and by some of the flattened surface enterocytes (Fig. 1L, NHE2, *Appendix*).

Intestinal FABP was expressed in the surface epithelium of the proximal colon (Fig. 1M, *Appendix*). During the onset of disease and during active disease the colonic surface epithelium became i-FABP-negative (Fig. 1N, *Appendix*). During the regenerative phase most surface enterocytes were i-FABP-positive again (Fig. 1O, *Appendix*).

The *in situ* AP activity was observed in the brush border of the surface enterocytes in both colonic segments (Fig. 1P-R, proximal colon, *Appendix*). During and after DSS treatment, AP activity remained present in the surface epithelium (Fig. 1Q and R, *Appendix*), even in the flattened surface enterocytes during active disease and during the regenerative phase. Moreover, during active disease AP activity seemed to be increased (Fig. 1Q, *Appendix*).

Quantitation of enterocyte-specific mRNA and protein expression

The mRNA - and/or protein expression of the enterocyte-specific markers CA I, CA IV, NHE2, NHE3, and i-FABP was detected and quantified by means of mRNA - and/or protein dot blotting. We observed a significant decrease in CA I mRNA levels in the proximal colon during active disease (Fig. 2A). Subsequently, during the regenerative phase CA I mRNA

levels normalized again. Similarly, at the protein level CA I expression in the proximal colon was significantly decreased during active disease and increased again during the regenerative phase (Fig. 3A). Unlike the mRNA levels, CA I protein levels remained significantly lower than the control levels during the latter phase.

The mRNA levels of the other CA isoform, CA IV, were only slightly and not significantly decreased in the proximal colon, and were unaltered in the distal colon during DSS-induced disease (Fig. 2). However, CA IV protein levels were decreased during active disease in both proximal and distal colon (Fig. 3). During the regenerative phase CA IV protein levels increased again in both colonic segments. Despite the increase in CA IV protein levels in the proximal and distal colon during the regenerative phase, the protein levels remained lower than control levels.

The mRNA levels of the sodium hydrogen exchanger NHE2 were strongly decreased in the proximal and distal colon during each disease phase (Fig. 2A and B). Similar to NHE2 mRNA levels, NHE3 mRNA levels significantly decreased in the proximal colon during each phase of disease. Furthermore, in the distal colon NHE3 mRNA levels were decreased during active disease and the regenerative phase. The amount of protein in the excised colonic tissue was limited, therefore NHE2 and -3 levels in the tissue samples were not determined.

Focussing on i-FABP, we observed a significant down-regulation of i-FABP mRNA and protein levels in the proximal colon during each phase of disease (Fig. 2A and 3A).

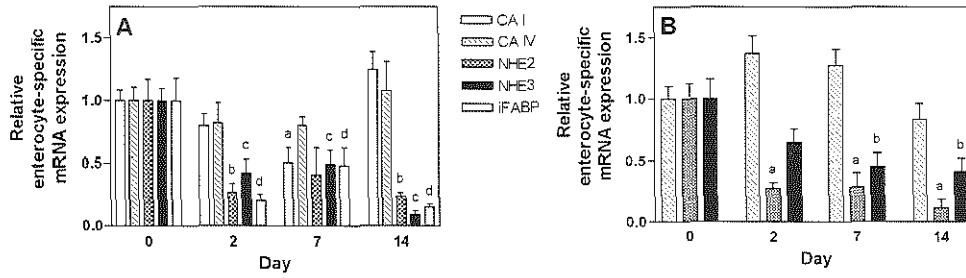

Figure 2. Enterocyte-specific mRNA expression levels in the proximal (A) and distal colon (B) during DSS-induced colitis. Expression levels of the specific genes were quantified and averaged per segment in control and DSS-treated rats. Expressed values (± SEM) are given relative to control values, which were arbitrarily set on 1. CA I, white bars; CA IV, hatched bars; NHE2, blocked bars; NHE3, black bars; i-FABP, grey bars. In the proximal colon significant differences were seen in: CA I expression between day 7 and days 0 and 14 (a, $p<0.05$); NHE2 expression between day 0 and days 2 and 14 (b, $p<0.05$); NHE3 expression between day 0 and days 2, 7, and 14 (c, $p<0.05$); and in i-FABP expression between day 0 and days 2, 7, and 14 (d, $p<0.05$). In the distal colon significant differences were observed in: NHE2 expression between day 0 and days 2, 7, and 14 (a, $p<0.001$); and in NHE3 expression between day 0 and days 7 and 14 (b, $p<0.05$).

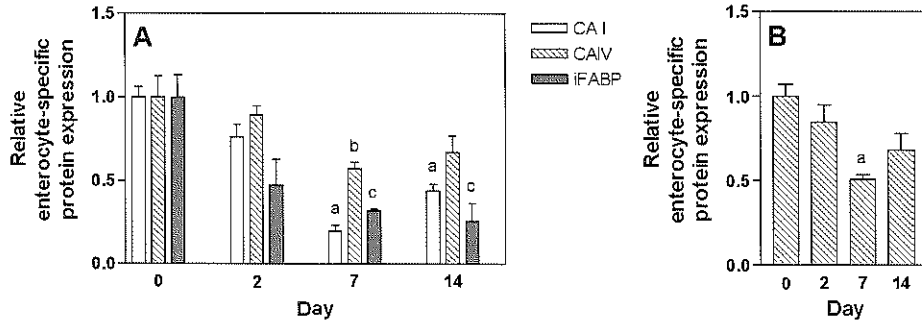

Figure 3. Enterocyte-specific protein levels in the proximal (A) and distal colon (B) during DSS-induced colitis. Expression levels of the specific genes were quantified and averaged per segment in control and DSS-treated rats. Expressed values (± SEM) are given relative to control values, which were arbitrarily set on 1. CA I, white bars; CA IV, hatched bars; i-FABP, grey bars. In the proximal colon the following significant differences were observed: CA I expression between day 0 and days 7 and 14 (a, $p<0.001$); CA IV expression between day 0 and 7 (b, $p<0.05$); and i-FABP between day 0 and days 7 and 14 (c, $p<0.05$). In the distal colon significant differences were seen in CA IV expression between day 7 and days 0 and 2 (a, $p<0.05$).

Localization of goblet cell-specific markers

Recently, we demonstrated that DSS induced crypt loss, ulcerations and concomitant goblet cell loss in the proximal and distal colon [33]. In the present study, we focussed on the areas in which the goblet cells remained. In rat control the mRNA and protein of the mucin Muc2 are expressed by all goblet cells in the proximal and distal colon (Fig. 4A and D, *see Appendix*). During each of the DSS-induced disease phases Muc2 mRNA and protein expression by goblet cells was observed in areas with elongated crypts, as well as in areas with flattened crypt and surface cells. Especially in the distal colon the elongated crypts mainly contained Muc2 mRNA and protein-positive goblet cells during active disease and the regenerative phase (Fig. 4B, C, and H, *Appendix*). The mRNA and protein of TFF3 is expressed by goblet cells in the upper half and upper two thirds of the crypts and surface epithelium in the proximal colon and distal colon, respectively (Fig. 4E, distal colon, *Appendix*). During disease, in both the proximal and distal colon, TFF3 mRNA and protein expression extended from surface epithelium toward the lower crypt region, in areas with elongated crypts and in areas with flattened crypts. In the distal colon, TFF3 mRNA and protein expression was even observed at the crypt bottom during these disease phases, especially in elongated crypts (Fig. 4F and G, *Appendix*).

Noteworthy, goblet cells positive for Muc2- and TFF3 mRNA and protein accumulated in the surface epithelium in the proximal and distal colon during each of the DSS-induced disease phases (Fig. 4D and H, Muc2 protein expression in the distal colon, *Appendix*).

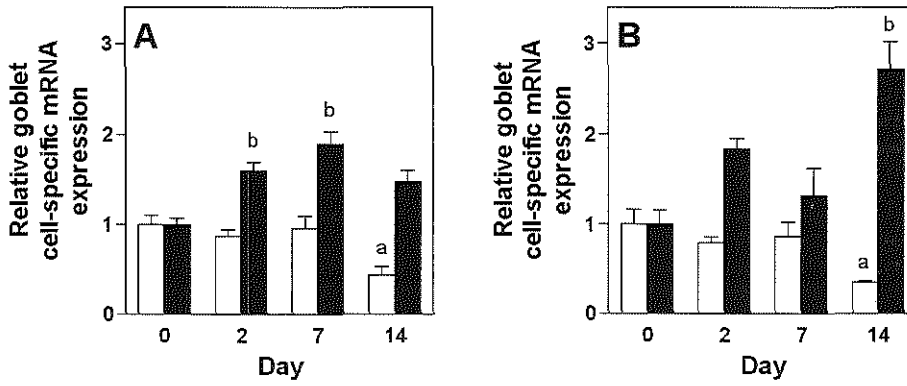

Figure 5. Goblet cell-specific mRNA expression levels in the proximal (A) and distal colon (B) during DSS-induced colitis. Expression levels of the specific genes were quantified and averaged per segment in control and DSS-treated rats. Expressed values (± SEM) are given relative to control values, which were arbitrarily set on 1. Muc2, white bars; TFF3, black bars. In the proximal colon significant differences were observed in: Muc2 expression on day 14 compared to days 0 and 7 (a, $p<0.05$); and in TFF3 expression on day 0 compared to days 2 and 7 (b, $p<0.01$). In the distal colon significant differences were seen in: Muc2 expression on day 0 compared to day 14 (a, $p<0.05$); and in TFF3 expression on day 14 compared to days 0 and 7 (b, $p<0.01$).

Quantitation of goblet cell-specific mRNA and protein expression

The expression of the goblet cell-specific markers Muc2 and TFF3 was determined and quantified at the mRNA and protein level by protein and RNA dot blots, respectively. The Muc2 mRNA expression appeared largely unaltered in the proximal and distal colon during the onset of disease and active disease compared to controls (Fig. 5A and B). In contrast, during the regenerative phase Muc2 mRNA levels significantly decreased in both colonic segments. Muc2 protein levels showed a slight but not significant increase in the proximal colon during onset of disease and during active disease (Fig. 6A). During the regenerative phase Muc2 protein levels normalized in the latter segment. In contrast, in the distal colon Muc2 protein levels were unaltered during onset of disease and active disease, but significantly increased during the regenerative phase (Fig. 6B).

Remarkable alterations in TFF3 expression levels were observed at the mRNA as well as protein levels (Figs 5 and 6). In the proximal colon TFF3 mRNA was significantly increased during the onset of disease and active disease (Fig. 5A). During the regenerative phase TFF3 mRNA levels in the proximal colon decreased and were comparable to control levels. TFF3 mRNA expression in the distal colon seemed to be slightly, but not significantly, increased during the onset of disease and active disease (Fig. 5B). Moreover, within the latter colonic segment a strong and significant increase in TFF3 mRNA expression was observed during the

regenerative phase. TFF3 protein levels in the proximal colon were maintained during eachdisease phase (Fig. 6A). In the distal colon no alteration in TFF3 protein levels were seen during onset of disease and active disease (Fig. 6B). During the regenerative phase, however, TFF3 protein levels were significantly increased in the latter segment.

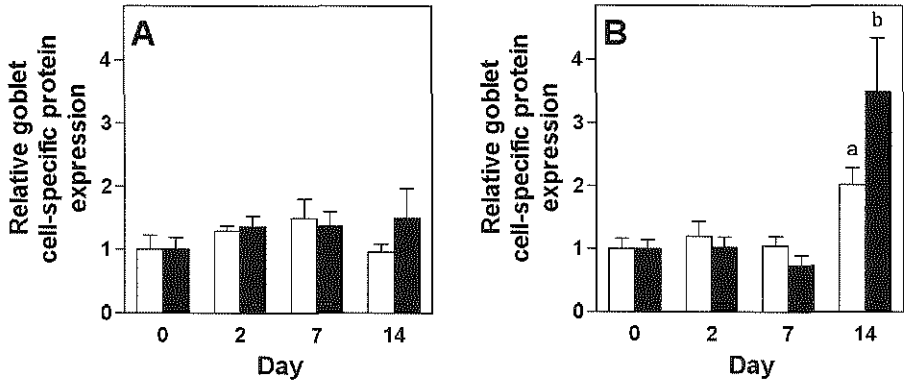

Figure 6. Goblet cell-specific protein expression levels in the proximal (A) and distal colon (B) during DSS-induced colitis. Expression levels of the specific genes were quantified and averaged per segment in control and DSS-treated rats. Expressed values (± SEM) are given relative to control values, which were arbitrarily set on 1. Muc2, white bars; TFF3, black bars. In the proximal colon no significant differences were observed. In the distal colon significant differences were seen in: Muc2 expression on day 14 compared to days 0 and 7 (a, $p<0.05$); and in TFF3 expression on day 14 compared to days 0, 2, and 7 (b, $p<0.01$).

Secretion of Muc2 and TFF3

The percentage of Muc2 secretion was calculated as the amount of Muc2 in the medium divided by the sum of the amount of Muc2 in tissue and in the medium. TFF3 secretion levels were calculated in a similar way as the Muc2 secretion levels. In both proximal and distal colon Muc2 secretion levels were maintained during each phase of disease (Fig. 7A). In contrast to the unaltered Muc2 secretion levels, TFF3 secretion levels progressively increased during disease in both colonic segments (Fig. 7B). In the proximal colon, a 3-fold increase in TFF3 secretion levelwas seen during active disease and the regenerative phase. Moreover, in the distal colon the up-regulation of TFF3 secretion was 4-fold during active disease and the regenerative phase.

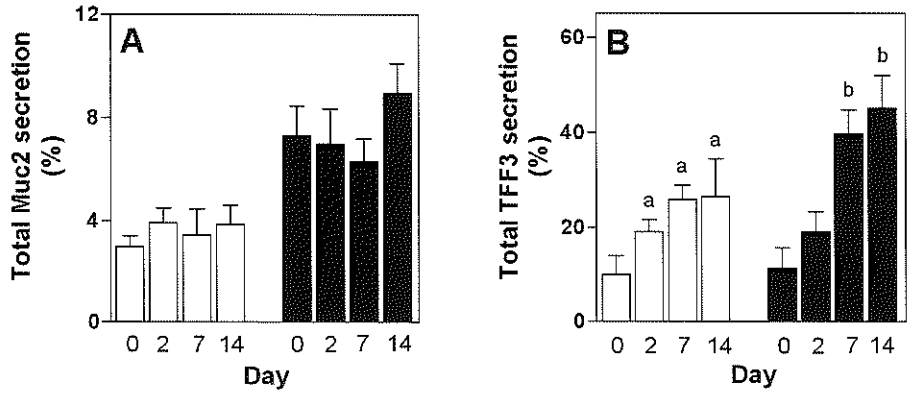

Figure 7. Muc2 and TFF3 secretion during DSS-induced colitis. Percentage of Muc2 secretion (A) and TFF3 secretion (B) in the proximal (white bars) and distal colon (black bars) at day 0 (controls), day 2, day 7, and day 14. Mean total Muc2 and TFF3 secretion (± SEM) is presented. In the proximal colon significant differences were observed in TFF3 secretion on day 0 compared to days 2, 7, and 14 (a, $p<0.05$). In the distal colon significant differences were observed in TFF3 secretion on day 0 compared to days 7 and 14 (b, $p<0.01$).

Discussion

In the present study, we investigated enterocyte and goblet cell-specific functions during DSS-induced colitis by measuring cell-type specific gene expression. The *in situ* detection of the enterocyte-specific gene products revealed a down-regulation of CA I mRNA and protein, CA IV protein, NHE2 and -3 protein, and i-FABP protein in some of the normal appearing enterocytes and in most of the flattened surface enterocytes during DSS treatment. In contrast, the enterocyte-specific AP-activity is maintained or even up-regulated during DSS-colitis, in both normal appearing enterocytes and flattened enterocytes. These data demonstrate that distinct enterocyte specific genes are down-regulated during the process of epithelial restitution, whereas others are maintained or even up-regulated. The down-regulation of the CAs, NHEs, and i-FABP may indicate loss of enterocyte function, and it may contribute to the pathology seen in DSS-induced colitis. Additionally, as AP activity is known to play a critical role in the innate defense of the intestinal mucosa [12, 34], these data suggest that epithelial defense is maintained or even increased during DSS-induced colitis.

Quantitative analysis revealed remarkable alterations in the enterocyte-specific CA I and CA IV expression during DSS-colitis. Specifically, CA I mRNA and protein levels were reduced during active disease in the proximal colon. During the regenerative phase both CA I mRNA and protein were normalized again. In contrast, CA IV expression was only down-regulated at the protein level, but not at the mRNA level during active disease in the proximal

and distal colon. In both colonic segments CA IV protein levels increased again during the regenerative phase. These findings suggest that DSS effects on CA I expression were mediated via effects on transcript abundance, whereas effects on CA IV were mediated at the post-transcriptional level. Furthermore, the alterations in CA I mRNA and protein levels during DSS-induced acute colitis are in line with alterations observed in humans with UC. Namely, in patients with active UC both CA I mRNA and protein were significantly down-regulated, whereas in UC in remission these levels increased again [18]. Thus, although DSS-induced colitis is a relatively acute model, whereas UC in patients is chronic, similar alterations in CA I expression levels seem to occur. Unfortunately, data on CA IV expression levels in humans or other experimental colitis models are currently lacking. Nevertheless, what are the consequences of CAs down-regulation during inflammation? Speculating, as CA I catalyses the formation of H^+ and HCO_3^- ions [1, 3], down-regulation of CA I would lead to reduced levels of H^+ and HCO_3^- levels and thus indirectly to a reduction in the activity of the apical Na^+/H^+ and Cl^-/HCO_3^- exchangers. This in turn may lead to reduced NaCl and water absorption. In other words, down-regulation of CA I protein levels might contribute to the diarrhea, which is observed during DSS-induced colitis [35, 36]. Furthermore as CA IV is likely to participate in the colonic ion and fluid transport as well, the down-regulation of CA IV during DSS treatment might also contribute to the induction and/or perpetuation of the DSS-induced diarrhea.

The sodium hydrogen exchangers NHE2 and NHE3 were down-regulated at the mRNA and protein level during DSS-induced colitis in the proximal and distal colon, suggesting that DSS affects these genes at the mRNA level. Previous studies demonstrate that aldosterone, glucocorticoids, and IFN-γ down-regulate NHE2 and NHE3 at mRNA, protein, and activity level in rat colon [37-39]. It is very likely that the DSS-induced down-regulation in NHE2 and –3 mRNA and protein leads to decreased activity levels of both exchangers. This in turn suggests that DSS-induced diarrhea *i.e.* reduced water absorption might partly be caused by a down-regulation of the sodium exchangers. Currently it remains unclear whether the damage induced by DSS is responsible for the decrease in these CAs and/or sodium hydrogen exchangers, or that the epithelium actively down-regulates the expression of these specific genes to initiate watery diarrhea, in order to expel pathogens and noxious agents like DSS from the intestinal lumen.

Focussing on i-FABP we observed a down-regulation of i-FABP mRNA and protein levels in the proximal colon during DSS-induced disease suggesting that, similar to NHE2 and -3, DSS affected i-FABP expression at the mRNA level. More generally, these results suggest that in addition to electrolyte and water absorption, uptake and/or cellular transport of fatty acids were also diminished during DSS-colitis.

In situ hybridization and immunohistochemical studies demonstrated that, despite the DSS-induced changes in epithelial morphology, *i.e.* crypt and surface cell flattening and crypt elongation, goblet cells continued to express Muc2 and TFF3 mRNA and protein. These findings demonstrate that goblet cells maintain their capacity to express Muc2 and TFF3 during the process of restitution, *i.e.* flattening of epithelial cells. During active disease and the

regenerative phase TFF3 mRNA and protein expression was extended toward the crypt bottom. Additionally, elongated crypts mainly contained goblet cells positive for Muc2 and TFF3 mRNA and protein. Similarly, goblet cells positive for Muc2 and TFF3 mRNA and protein accumulated in the surface epithelium during each disease phase. Recently, we demonstrated that DSS treatment induced loss of crypt and surface epithelium and concomitant goblet cell loss [33]. These data suggest that the DSS-induced loss of crypts and surface epithelium and the ensuing loss of goblet cells in some areas is, at least partly, compensated by an increase in the number of goblet cells in elongated crypts and surface epithelium in other areas. Taken together these data emphasize that goblet cells, and particularly Muc2 and TFF3 are of critical importance to maintain epithelial protection and to stimulate epithelial repair during acute inflammation and regeneration, respectively.

Quantitative analysis of goblet cell-specific Muc2 expression revealed pronounced changes in mRNA and protein levels in the proximal and distal colon during DSS-induced colitis. Specifically, both Muc2 mRNA and protein levels were maintained or even up-regulated during the onset and active disease in both colonic segments. During the regenerative phase Muc2 mRNA levels decreased in both colonic segments, whereas Muc2 protein levels were comparable to controls or even up-regulated. Additionally, Muc2 secretion levels appeared to be maintained during each of the DSS-induced disease phases in both colonic segments. The down-regulation of Muc2 mRNA in conjunction with the retained or even increased Muc2 protein levels during the regenerative phase suggest an increased translation efficacy and/or an altered mRNA/protein stability. More importantly, the maintained or increased Muc2 protein levels in conjunction with the retained Muc2 secretion levels suggest that the thickness of the mucus layer is at least maintained or even increased, offering optimal protection to the colonic epithelium during DSS-induced colitis.

TFF3 mRNA and protein levels were maintained or even increased during each DSS-induced disease phase in the proximal as well as distal colon. As alterations in TFF3 protein levels were similar to alterations in TFF3 mRNA levels, we conclude that DSS effects on TFF3 expression levels are mediated primarily via transcript abundance. Besides the maintained or up-regulated TFF3 protein levels during DSS-colitis, TFF3 secretion levels appeared to increase progressively, indicating that the luminal TFF3 content is increased during each phase of DSS-induced colitis. Presently, information on TFF3 protein expression and secretion in other colitis models is lacking. Yet, TFF3 deficient mice had impaired mucosal healing and manifested poor epithelial regeneration after DSS treatment [16]. Rectal instillation of TFF3 was able to prevent the marked ulceration that occurred after DSS treatment in these TFF3 deficient mice. Further, in an *in vitro* model of epithelial restitution addition of TFF3 to wounded monolayers of confluent IEC-6 cells stimulated epithelial migration [40]. In concert, these findings suggest that TFF3 plays a pivotal role in epithelial repair during acute inflammation and that the epithelial repair capacity is enhanced in this acute model of colitis.

In summary, DSS induced a down-regulation of CA I, CA IV, NHE2 and NHE3, and i-FABP gene expression during active colitis. Down-regulation of these genes may account for

some of the pathology seen during DSS-induced colitis. Furthermore, enterocyte-specific AP activity was maintained or even up-regulated in normal appearing and flattened surface cells during active disease, supporting an important role for enterocytes in the innate defense of the mucosa during acute colitis. DSS-induced diarrhea may be largely attributed to down-regulation of the CAs and NHEs. In contrast to enterocyte-specific gene expression, goblet cells continued to express Muc2 and TFF3 during DSS-colitis. Moreover, Muc2 and TFF3-positive goblet cells accumulated in the surface epithelium and TFF3 expression extended from surface epithelium to crypt bottom. Collectively, these data imply that goblet cells play a pivotal role in epithelial defense against luminal substances and pathogens via Muc2 synthesis and secretion, and in epithelial repair via TFF3 synthesis and secretion.

Acknowledgements

This work was partly financed by Numico BV, Zoetermeer, The Netherlands. We thank the following scientists for kindly providing the antibodies or cDNAs used in this study: Prof. Dr W.S. Sly for anti-mouse CA I and anti-rat CA IV antibodies; Dr R.E. Fleming for mouse CA I and rat CA IV cDNAs; Dr C.M. Bookstein for anti-rat NHE2 and anti-rat NHE3 antibodies, and rat NHE2 and -3 cDNAs; Prof. Dr J.I. Gordon for anti-rat intestinal-FABP antibodies and cDNAs; Prof. Dr D.K. Podolsky for WE9, anti-rat TFF3 antibodies, and rat TFF3 cDNA.

References

1. Charney AN, Dagher PC. Acid-base effects on colonic electrolyte transport revisited. Gastroenterology 1996;111:1358-68.

2. Sowden J, Leigh S, Talbot I, Delhanty J, Edwards Y. Expression from the proximal promoter of the carbonic anhydrase 1 gene as a marker for differentiation in colon epithelia. Differentiation 1993;53:67-74.

3. Fleming RE, Parkkila S, Parkkila AK, Rajaniemi H, Waheed A, Sly WS. Carbonic anhydrase IV expression in rat and human gastrointestinal tract regional, cellular, and subcellular localization. J Clin Invest 1995;96:2907-13.

4. Musch MW, Bookstein C, Xie Y, Sellin JH, Chang EB. SCFA increase intestinal Na absorption by induction of NHE3 in rat colon and human intestinal C2/bbe cells. Am J Physiol Gastrointest Liver Physiol 2001;280:G687-93.

5. Cho JH, Musch MW, Bookstein CM, McSwine RL, Rabenau K, Chang EB. Aldosterone stimulates intestinal Na+ absorption in rats by increasing NHE3 expression of the proximal colon. Am J Physiol 1998;274:C586-94.

6. Bookstein C, DePaoli AM, Xie Y, Niu P, Musch MW, Rao MC, Chang EB. Na+/H+ exchangers, NHE-1 and NHE-3, of rat intestine. Expression and localization. J Clin Invest 1994;93:106-13.

7. Bookstein C, Xie Y, Rabenau K, Musch MW, McSwine RL, Rao MC, Chang EB. Tissue distribution of Na+/H+ exchanger isoforms NHE2 and NHE4 in rat intestine and kidney. Am J Physiol 1997;273:C1496-505.

8. Schultheis PJ, Clarke LL, Meneton P, Miller ML, Soleimani M, Gawenis LR, Riddle TM, Duffy JJ, Doetschman T, Wang T, Giebisch G, Aronson PS, Lorenz JN, Shull GE. Renal and intestinal absorptive defects in mice lacking the NHE3 Na+/H+ exchanger. Nat Genet 1998;19:282-5.

9. Alpers DH, Bass NM, Engle MJ, DeSchryver-Kecskemeti K. Intestinal fatty acid binding protein may favor differential apical fatty acid binding in the intestine. Biochim Biophys Acta 2000;1483:352-62.

10. Simon TC, Roberts LJ, Gordon JI. A 20-nucleotide element in the intestinal fatty acid binding protein gene modulates its cell lineage-specific, differentiation-dependent, and cephalocaudal patterns of expression in transgenic mice. Proc Natl Acad Sci U S A 1995;92:8685-9.

11. Simon TC, Cho A, Tso P, Gordon JI. Suppressor and activator functions mediated by a repeated heptad sequence in the liver fatty acid-binding protein gene (Fabpl). Effects on renal, small intestinal, and colonic epithelial cell gene expression in transgenic mice. J Biol Chem 1997;272:10652-63.

12. Poelstra K, Bakker WW, Klok PA, Kamps JA, Hardonk MJ, Meijer DK. Dephosphorylation of endotoxin by alkaline phosphatase in vivo. Am J Pathol 1997;151:1163-9.

13. Tytgat KMAJ, Bovelander FJ, Opdam FJ, Einerhand AWC, Büller HA, Dekker J. Biosynthesis of rat MUC2 in colon and its analogy with human MUC2. Biochem J 1995;309:221-9.

14. Forstner JF, Forstner GG. Gastrointestinal mucus. In: LR J, ed. Physiology of the Gastrointestinal Tract. Volume 2. 3 rd ed. New York: Raven, 1994:1255-1283.

15. Van Klinken BJW, Dekker J, Büller HA, Einerhand AWC. Mucin gene structure and expression: protection vs. adhesion. Am J Physiol 1995;269:G613-27.

16. Mashimo H, Wu DC, Podolsky DK, Fishman MC. Impaired defense of intestinal mucosa in mice lacking intestinal trefoil factor. Science 1996;274:262-5.

17. Wong WM, Poulsom R, Wright NA. Trefoil peptides. Gut 1999;44:890-5.

18. Fonti R, Latella G, Caprilli R, Frieri G, Marcheggiano A, Sambuy Y. Carbonic anhydrase I reduction in colonic mucosa of patients with active ulcerative colitis. Dig Dis Sci 1998;43:2086-92.

19. Ejderhamn J, Finkel Y, Strandvik B. Na,K-ATPase activity in rectal mucosa of children with ulcerative colitis and Crohn's disease. Scand J Gastroenterol 1989;24:1121-5.

20. Hawker PC, McKay JS, Turnberg LA. Electrolyte transport across colonic mucosa from patients with inflammatory bowel disease. Gastroenterology 1980;79:508-11.

21. Rachmilewitz D, Karmeli F, Sharon P. Decreased colonic Na-K-ATPase activity in active ulcerative colitis. Isr J Med Sci 1984;20:681-4.

22. Bell CJ, Gall DG, Wallace JL. Disruption of colonic electrolyte transport in experimental colitis. Am J Physiol 1995;268:G622-30.

23. Tytgat KMAJ, van der Wal JW, Einerhand AWC, Büller HA, Dekker J. Quantitative analysis of MUC2 synthesis in ulcerative colitis. Biochem Biophys Res Commun 1996;224:397-405.

24. Dekker J, Van Klinken BJW, Büller HA, Einerhand AWC. Quantitation of biosynthesis and secretion of mucin using metabolic labeling. Methods Mol Biol 2000;125:65-73.

25. Verburg M, Renes IB, Meijer HP, Taminiau JA, Büller HA, Einerhand AWC, Dekker J. Selective sparing of goblet cells and paneth cells in the intestine of methotrexate-treated rats. Am J Physiol Gastrointest Liver Physiol 2000;279:G1037-47.

26. Cohn SM, Simon TC, Roth KA, Birkenmeier EH, Gordon JI. Use of transgenic mice to map cis-acting elements in the intestinal fatty acid binding protein gene (Fabpi) that control its cell lineage- specific and regional patterns of expression along the duodenal-colonic and crypt-villus axes of the gut epithelium. J Cell Biol 1992;119:27-44.

27. Tytgat KMAJ, Klomp LW, Bovelander FJ, Opdam FJ, Van der Wurff A, Einerhand AWC, Büller HA, Strous GJ, Dekker J. Preparation of anti-mucin polypeptide antisera to study mucin biosynthesis. Anal Biochem 1995;226:331-41.

28. Lindenbergh-Kortleve DJ, Rosato RR, van Neck JW, Nauta J, van Kleffens M, Groffen C, Zwarthoff EC, Drop SL. Gene expression of the insulin-like growth factor system during mouse kidney development. Mol Cell Endocrinol 1997;132:81-91.

29. Fraser PJ, Curtis PJ. Molecular evolution of the carbonic anhydrase genes: calculation of divergence time for mouse carbonic anhydrase I and II. J Mol Evol 1986;23:294-9.

30. Fleming RE, Crouch EC, Ruzicka CA, Sly WS. Pulmonary carbonic anhydrase IV: developmental regulation and cell- specific expression in the capillary endothelium. Am J Physiol 1993;265:L627-35.

31. Suemori S, Lynch-Devaney K, Podolsky DK. Identification and characterization of rat intestinal trefoil factor: tissue- and cell-specific member of the trefoil protein family. Proc Natl Acad Sci U S A 1991;88:11017-21.

32. Lowe JB, Sacchettini JC, Laposata M, McQuillan JJ, Gordon JI. Expression of rat intestinal fatty acid-binding protein in Escherichia coli. Purification and comparison of ligand binding characteristics with that of Escherichia coli-derived rat liver fatty acid-binding protein. J Biol Chem 1987;262:5931-7.

33. Renes IB, Boshuizen JA, Van Nispen DJPM, Bulsing NP, Büller HA, Dekker J, Einerhand AWC. Alterations in Muc2 biosynthesis and secretion during dextran sulfate sodium-induced colitis. Am J Physiol Gastrointest Liver Physiol;in press.

34. Poelstra K, Bakker WW, Klok PA, Hardonk MJ, Meijer DK. A physiologic function for alkaline phosphatase: endotoxin detoxification. Lab Invest 1997;76:319-27.

35. Cooper HS, Murthy SN, Shah RS, Sedergran DJ. Clinicopathologic study of dextran sulfate sodium experimental murine colitis. Lab Invest 1993;69:238-49.

36. Okayasu I, Hatakeyama S, Yamada M, Ohkusa T, Inagaki Y, Nakaya R. A novel method in the induction of reliable experimental acute and chronic ulcerative colitis in mice. Gastroenterology 1990;98:694-702.

37. Cho JH, Musch MW, DePaoli AM, Bookstein CM, Xie Y, Burant CF, Rao MC, Chang EB. Glucocorticoids regulate Na+/H+ exchange expression and activity in region- and tissue-specific manner. Am J Physiol 1994;267:C796-803.

38. Rocha F, Musch MW, Lishanskiy L, Bookstein C, Sugi K, Xie Y, Chang EB. IFN-gamma downregulates expression of Na(+)/H(+) exchangers NHE2 and NHE3 in rat intestine and human Caco-2/bbe cells. Am J Physiol Cell Physiol 2001;280:C1224-32.

39. Yun CH, Gurubhagavatula S, Levine SA, Montgomery JL, Brant SR, Cohen ME, Cragoe EJ, Jr., Pouyssegur J, Tse CM, Donowitz M. Glucocorticoid stimulation of ileal Na+ absorptive cell brush border Na+/H+ exchange and association with an increase in message for NHE-3, an epithelial Na+/H+ exchanger isoform. J Biol Chem 1993;268:206-11.

40. Dignass A, Lynch-Devaney K, Kindon H, Thim L, Podolsky DK. Trefoil peptides promote epithelial migration through a transforming growth factor beta-independent pathway. J Clin Invest 1994;94:376-83.

Chapter 5

Alterations in Muc2 biosynthesis and secretion during dextran sulphate sodium-induced colitis

Published as:
Ingrid B. Renes, Jos A. Boshuizen, Daniëlle J.P.M. Van Nispen, Nathalie P. Bulsing, Hans A. Büller, Jan Dekker, and Alexandra W.C. Einerhand.
Alterations in Muc2 biosynthesis and secretion during dextran sulfate sodium-induced colitis. *Am J of Physiol Gastrointest Liver Physiol* 2002, 282:G382-G389.

Summary

To gain insight in Muc2 synthesis and secretion during dextran sodium sulfate (DSS)-induced colitis, rats were treated with DSS for 7 days. Colonic segments were excised on days 0 (control), 2 (onset of disease), 7 (active disease) and 14 (regenerative phase) for histological evaluation. Explants were metabolically labeled with [^{35}S]amino acids or [^{35}S]sulfate followed by chase-incubation. Homogenates were analyzed by SDS-PAGE and ^{35}S-labeled Muc2 was quantified. Also total Muc2 protein and mRNA were quantified. DSS-induced crypt loss, ulcerations and concomitant goblet cell loss were most pronounced in the distal colon. Muc2 precursor synthesis increased progressively in the proximal colon, but was unaltered in the distal colon during onset and active disease. During the regenerative phase Muc2 precursor synthesis levels normalized in the proximal colon, but increased in the distal colon. Total Muc2 levels paralleled the changes seen in Muc2 precursor synthesis levels. During each disease phase total Muc2 secretion was unaltered in the proximal and distal colon. [^{35}S]sulfate incorporation into Muc2 only decreased in the proximal colon during active disease and the regenerative phase, while secretion of [^{35}S]sulfate-labeled Muc2 increased. During the regenerative phase Muc2 mRNA levels were down-regulated in both colonic segments. In conclusion: DSS-induced loss of goblet cells was accompanied by an increase or maintenance of Muc2 precursor synthesis, total Muc2 levels, and Muc2 secretion. In the proximal colon Muc2 becomes undersulfated, while sulfated Muc2 was preferentially secreted. Collectively, these data suggest specific adaptations of the mucus layer to maintain the protective capacities during DSS-induced colitis.

Abbreviations: DSS, dextran sulfate sodium; TCA, trichloroacetic acid; UC, ulcerative colitis.

Introduction

The colonic epithelium is covered by a mucus layer, which protects the epithelium against mechanical stress, luminal substances and pathogens [1, 2]. The mucin Muc2, which is synthesized by the goblet cells, appears to be the predominant secretory mucin in healthy colon of human, rat and mouse [3-5]. As mucins are the structural components of the mucus layer [1, 2], changes in mucin quantity, secretion and structure could lead to diminished protection of the colonic epithelium. Indeed, in humans with ulcerative colitis (UC) changes in the number of goblet cells, thickness of the mucus layer, and Muc2 synthesis, secretion and sulfation were reported. Specifically, goblet cells contain less mucin and are reduced in number in active UC [6, 7]. The mucus layer in UC patients is thinner than in controls [8]. Mucin sialylation appears to be increased in patients with inactive UC [9]. MUC2 precursor synthesis and total Muc2 levels in active UC are significantly decreased compared to controls and UC in remission [10]. Moreover, because less MUC2 is synthesized in active UC, MUC2 secretion is decreased in this stage of the disease [11]. Further, sulfation of MUC2 appeared to be decreased in the rectum and sigmoid colon of patients with UC [11, 12].

To gain insight into the mechanisms underlying the pathology of colitis, several experimental colitis models are currently used as model for human inflammatory bowel disease. One thoroughly described colitis model regarding clinical symptoms, histopathological changes and the application of therapeutic drugs, is the dextran sulfate sodium (DSS)-induced colitis model [13-17]. The DSS-induced colitis model gives the opportunity to study the dynamic disease process in different regions of the colon from the onset of disease to complete remission. In humans such a study is not possible, especially because the disease is usually diagnosed during advanced stages. Besides the DSS-model can be used to develop new therapeutic strategies. Previous studies demonstrated that DSS is directly cytotoxic to the colonic epithelium, inducing crypt damage, crypt loss and massive erosions [13, 14, 18], leading to an overall decrease in the number of goblet cells. Analogous to UC, the DSS-induced goblet cell loss might also have consequences for the thickness and constitution of the mucus layer and specifically for Muc2 synthesis and secretion. Therefore it is of relevance to analyze Muc2 synthesis both quantitatively and qualitatively in the DSS-induced colitis model.

In this study we investigated changes in numbers of goblet cells, Muc2 precursor synthesis, total Muc2, Muc2 secretion and sulfation in a rat DSS-induced colitis model. These aspects were studied in the proximal as well as distal colon from onset of disease to the regenerative phase of disease. Collectively these data were used to establish how the mucin production in the colonic epithelium adapted to the damage induced during DSS-colitis.

Methods

Animals

Eight weeks-old, specified pathogen free, male Wistar rats (Broekman, Utrecht, The Netherlands) were housed at constant temperature and humidity on a 12-h light-dark cycle. One week prior to and during the experiment the rats were housed individually. The rats had free access to a standard pelleted diet (Hope Farms, Woerden, The Netherlands) and sterilized tap water (controls) or sterilized tap water supplemented with DSS. All the experiments were performed with the approval of the Animal Studies Ethics Committee of our university.

Experimental Design

Rats were given 7% DSS (37-40 kD, TdB Consultansy, Uppsala, Sweden) in their drinking water for 7 days, followed by a 7-day recovery period during which DSS was omitted from the drinking water. Fresh DSS solutions were prepared daily. On day 0 (control), 2, 7, and 14, five animals per timepoint were sacrificed. Segments of the proximal colon and distal colon were dissected and prepared for light microscopy or snap frozen in liquid nitrogen and stored in -70 °C till RNA isolation. In addition, tissue explants (10 mm^3) of each colonic segment were metabolically labeled, as described below, to study mucin biosynthesis.

Histology and immunohistochemistry

Colonic segments were fixed in 4% (w/v) paraformaldehyde immediately after excision, embedded and prepared for light microscopy. Sections were stained with hematoxylin and eosin (HE) to study DSS-induced crypt loss and ulcerations. The area of crypt loss and ulcerations was measured using a micrometer in 3 tissue sections per segment and the area involved was expressed as the percentage of the total mucosal surface area. The score of crypt loss and ulceration was averaged per segment per animal. Thereafter, the mean score per segment per timepoint (± SEM) was calculated.

Five µm thick sections were cut and prepared for immunohistochemistry as described previously [19]. To identify goblet cells, sections were incubated with a 1:500 dilution of a Muc2 specific monoclonal antibody (WE9) which recognizes the non-*O*-glycosylated unique termini of Muc2 [20]. Immunoreaction was detected using the Vectastain ABC Elite Kit (Vector Laboratories, Burlingame, England) and staining was developed using 3,3'-diaminobenzidine. Finally, sections were counterstained with hematoxylin.

Metabolic Labeling of Tissue

Metabolic labeling of colonic tissue *in vitro* was performed as described earlier [10, 11, 21, 22]. Briefly, Muc2 biosynthesis was studied by metabolic labeling with ^{35}S-labeled amino acids ([^{35}S]-methionine/cysteine, Tran-^{35}S-label, ICN, Zoetermeer, The Netherlands), to label polypeptides, or with [^{35}S]sulfate (ICN) to label mature mucins. Two tissue explants (10 mm^3) of the proximal colon and 3 explants of the distal colon were cultured and pulse-labeled with either Tran-^{35}S-label or [^{35}S]sulfate for 30 min, using 100 µCi of each label per 100 µl

medium per tissue explant. In case of pulse labeling with [^{35}S]sulfate, the pulse labeling was followed by a chase incubation of 4 h in the absence of radiolabeled sulfate. Thereafter, the tissue as well as the culture medium was collected. After the respective pulse or pulse-chase experiments, explants were homogenized in, or culture medium was mixed with, a Tris buffer containing 1% SDS and protease inhibitors.

Measurement of protein synthesis

Protein concentration of each homogenate was measured using a BCA protein assay reagent kit (Pierce, Rockford, IL). Total incorporation of radioactivity in proteins was determined after trichloroacetic acid (TCA, Merck, Darmstadt, Germany) precipitation by autoradiography using a PhosphorImager, as described previously [10]. The protein synthesis within the tissue was calculated as the amount of incorporated radioactivity ([^{35}S]amino acids) in the TCA precipitate divided by the total protein content of the homogenate. Average protein synthesis of the explants (given as a.u./µg of tissue) was calculated per segment per rat, followed by calculation of the mean protein synthesis (± SEM) per segment for each phase of disease.

Quantitation of radiolabeled Muc2

An aliquot of each [^{35}S]amino acid-labeled and [^{35}S]sulfate-labeled homogenate was analyzed on reducing SDS-PAGE (3% stacking and 4% running gel) as described [21]. To visualize and quantify mucin-bands, the gels were fixed with 10% methanol/10% acetic acid, PAS-stained and analyzed by fluorography and autoradiography using a PhosphorImager. For reference to very high molecular weight molecules, metabolically labeled, unreduced rat gastric mucin precursors were used (molecular weight of monomer and dimer, 300 kDa and 600 kDa, respectively [23]. To determine the Muc2 precursor biosynthesis, the amount of [^{35}S]amino acid-labeled Muc2 in the tissue was divided by the amount of incorporated radioactivity ([^{35}S]amino acids) in the TCA-precipitate. Sulfate incorporation into Muc2 was determined as the sum of [^{35}S]sulfate-labeled Muc2 in tissue and media expressed relative to [^{35}S]amino acids-labeled Muc2 in tissue as determined in separate duplicate/triplicate explants. For each segment, the [^{35}S]sulfate incorporation into Muc2 was corrected for differences in protein contents between the individual explants. The percentage of [^{35}S]sulfate-labeled secreted Muc2 was calculated as the amount of [^{35}S]sulfate-labeled Muc2 in the medium divided by the sum of the amount of [^{35}S]sulfate-labeled Muc2 in the tissue and in the medium. This was multiplied by 100 to give the percentage of [^{35}S]sulfate-labeled secreted Muc2. For the Muc2 precursor synthesis, sulfate incorporation into Muc2 and secretion of [^{35}S]sulfate-labeled Muc2 average values were calculated per segment per rat, followed by mean values (± SEM) for each of the disease phases studied.

Quantitation of total Muc2 and total Muc2 secretion

Quantitation of total Muc2 and total Muc2 secretion was described previously [21]. In order to analyze the concentrations of total Muc2 and total Muc2 secretion, each [^{35}S]amino acid-labeled homogenate, [^{35}S]sulfate-labeled homogenate and medium was dot-blotted on

nitrocellulose (Nitran; Schleier & Schuell, Dassell, Germany). Briefly, the blots were blocked for 1 h with blocking buffer containing 50 mM Tris-HCl, pH 7.8, 5% (wt/vol) non-fat dry milk powder (Lyempf, Kampen, The Netherlands), 2 mM $CaCl_2$, 0.05% Nonidet P40 (BDH), and 0.01% antifoam (Sigma). The blots were incubated 18 h with the Muc2 specific antibody WE9 or anti-rat colonic mucin (RCM) [4, 20]. After washing in blocking buffer, the blot was incubated with ^{125}I-labeled protein A (Amersham, Bucks, United Kingdom, specific activity 33.8 mCi/mg) for 2 h. The blot was covered by two sheets of 3MM Whatman filter paper, to eliminate background radiation of ^{35}S-label, and binding of ^{125}I-labeled protein A to the Muc2 specific antibodies was detected using a PhosphorImager. The elicited signal was quantified and total Muc2 was expressed per μg protein of the tissue to determine total Muc2 levels. The percentage of total Muc2 secretion was calculated as the amount of Muc2 in the medium divided by the sum of the amount of Muc2 in tissue and in the medium. This was multiplied by 100 to give the percentage of total Muc2 secretion. Averages of total Muc2 and total Muc2 secretion were calculated per segment per rat, followed by calculation of the mean total Muc2 secretion (± SEM) for each of the disease phases studied.

Quantitation of Muc2 mRNA

Total RNA was isolated from proximal and distal colon using Trizol® following the manufacturers protocol (Gibco-BRL, Gaithersburg MD, USA). The integrity of the RNA was assessed by analysis of the 28S and 18S ribosomal RNAs after electrophoresis and staining with ethidium bromide. Subsequently, 1 μg of total RNA from each segment was dot-blotted on Hybond-N^+ (Amersham). The blot was hybridized to a ^{32}P-labeled rat Muc2 cDNA probe, as described [19]. Hybridization of the probe to Muc2 mRNA was detected and quantified using a PhosphorImager. Hybridized signals were corrected for glyceraldehyde-3-phosphate dehydrogenase (GAPDH) mRNA to correct for the amount of loading by using 1.4 kb GAPDH cDNA as a probe [19]. Average Muc2 mRNA levels were calculated per segment per rat, followed by calculation of the mean Muc2 mRNA expression levels (± SEM) for each of the disease phases studied.

Statistical Analysis

To compare two groups an unpaired t-test was used and to compare 3 or more groups, analysis of variance was performed followed by an unpaired t-test. Differences were considered significant when $p<0.05$. Data were represented as the mean ± standard error of the mean (SEM).

Results

Evaluation of DSS-induced damage

DSS-treated rats were assigned, according to time of DSS treatment, to the following groups: onset of disease (day 2), active disease (day 7), regenerative phase of disease (day 14) and a

control group (no DSS). Representative immunohistochemical stainings of MUC2 in the distal colon of each group are given in figure 1 (*see Appendix)*. Additionally, crypt loss and ulcerations were scored and the mucosal area involved was expressed as the percentage of the total mucosal surface area (Table 1). The first signs of DSS-induced damage consisted of crypt loss (6.3%) appearing in the distal colon during the onset of disease (Fig. 1B, *Appendix*). During active disease crypt loss and ulcerations were observed in the proximal colon and distal colon (Fig. 1C, *Appendix*). The damage was most pronounced in the distal colon where it involved 40.1% of the total mucosal surface versus 12.5% of the proximal colon. During the regenerative phase, crypt loss and ulcerations were still observed in the proximal colon (6.6%) and distal colon (20.6%) (Fig. 1D, *Appendix*).

Table 1. Crypt loss and ulcerations in the proximal and distal colon during different phases of DSS-induced colitis and in controls.

Day of DSS Treatment (disease phase)	Proximal colon: crypt loss/ulceration (± SEM)	Distal colon: crypt loss/ulceration (± SEM)
0 (control)	0 (± 0.0)	0 (± 0.0)
2 (onset of disease)	0.0 (± 0.0)*	6.3 (± 2.1)
7 (active disease)	12.5 (± 4.0)*†	40.1 (± 4.9)**
14 (regenerative phase)	6.6 (± 2.4)*	20.6 (± 3.5)††‡

The mean score of crypt loss and ulcerations per segment per day (±SEM) are expressed. Statistically significant differences were seen between proximal and distal colon during days 2, 7, and 14 ($^{*}p<0.02$). In the proximal colon significant differences were seen between day 0 and 7, and day 2 and 7 ($^{\dagger}p<0.01$). Significant differences in the distal colon were observed between day 0 and 7, and day 2 and day 7 ($^{**}p<0.001$); day 0 and 14, day 7 and 14 ($^{\dagger\dagger}p<0.01$); day 2 and day 14 ($^{\ddagger}p<0.05$).

Total protein synthesis

In the proximal colon, total protein synthesis progressively increased during onset and active disease (Fig. 2). During the latter disease phase, total protein synthesis was significantly increased compared to the other groups. In the distal colon total protein synthesis levels were slightly, but not significantly, increased during onset and active disease.

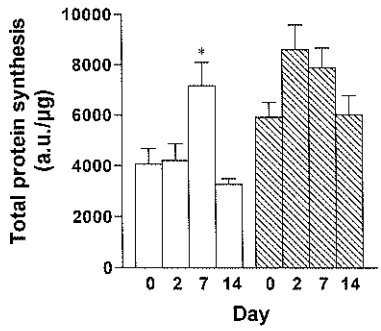

Figure 2. Total protein synthesis of proximal (open bars) and distal (hatched bars) colonic explants of control and DSS-treated rats. Mean protein synthesis (± SEM) was calculated per segment for each disease phase; day 0, control; day 2, onset of disease; day 7, active disease; day 14, regenerative phase. Statistical significant differences were seen in the proximal colon between day 7 and the other groups ($^{*}p<0.05$).

Identification and quantitation of Muc2 precursor synthesis

We previously demonstrated that Muc2 is the major colonic mucin in rat [4]. It is synthesized as a precursor protein with an apparent molecular mass of about 600 kDa, after pulse-labeling with [^{35}S]amino acids followed by immunoprecipitations [4]. This 600 kDa band can only be metabolically labeled with amino acids, can not be stained by PAS, and can not be metabolically labeled with [^{35}S]sulfate. In the present study, we could easily identify the Muc2 precursor band, according to the biochemical criteria as described above, in tissue homogenates after pulse labeling with [^{35}S]amino acids for 30 min (Fig. 3A). After identification, the specific radioactivity present in the Muc2 precursor band was quantified and the Muc2 precursor synthesis was calculated. Muc2 precursor synthesis was significantly higher in the proximal colon compared to distal colon during each phase of the disease (Fig. 3). In the proximal colon Muc2 precursor increased in the course of DSS treatment. In active disease the increase was two-fold, and significantly different from control levels. During the regenerative phase, Muc2 precursor synthesis decreased, but still tended to be elevated compared to control levels. In the distal colon, Muc2 precursor synthesis was maintained during the onset of disease and active disease. During the regenerative phase, however, Muc2 precursor synthesis increased significantly compared to controls and the previous phases of disease.

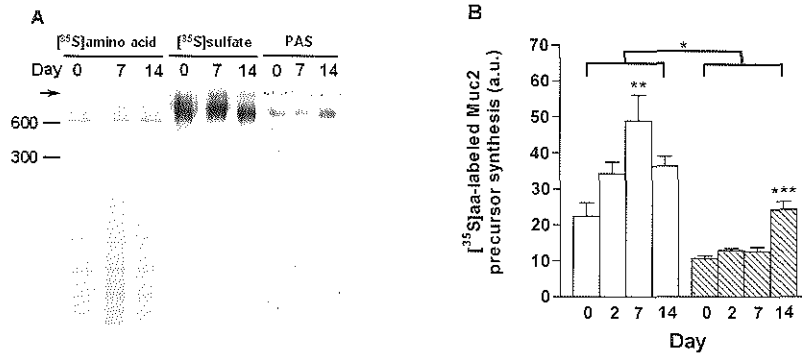

Figure 3. Identification of precursor and mature MUC2 (panel A) and quantification of Muc2 precursor synthesis (panel B). Shown are representative examples of proximal colonic tissue explants of day 0 (control), day 7 (active disease), and day 14 (regenerative phase) metabolically labeled with [^{35}S]amino acids, [^{35}S]sulfate, or stained with PAS (panel A). Arrow indicates the border between the running and stacking gel. For reference to very high molecular weight molecules, metabolically labeled, unreduced rat gastric mucin precursors are indicated on the left (molecular weight of monomer and dimer, 300 kDa and 600 kDa, respectively) [23]. Note that precursor MUC2 has a molecular mass of 600 kDa, cannot be metabolically labeled with [^{35}S]sulfate, and cannot be stained with PAS. Mature MUC2 has an apparent molecular mass of 650 kDa and is PAS stainable. After identification, the specific radioactivity present in the Muc2 precursor band was quantified and the Muc2 precursor synthesis was calculated. Mean precursor synthesis (± SEM) in the proximal colon (open bars) and distal colon (hatched bars) for each group is given; day 0, control; day 2, onset of disease; day 7, active disease; day 14, regenerative phase. Significant differences were seen between the proximal and distal colon in each group ($^{*}p<0.02$); within the proximal colon between day 7 and day 0 ($^{**}p<0.01$); within the distal colon between day 14 and each of the other groups ($^{***}p<0.001$).

Quantitation of total Muc2

The regenerative phase excluded, total Muc2 in each group was slightly higher in the proximal colon than in the distal colon (Fig. 4). Although not statistically significant, total Muc2 levels in the proximal colon increased during the onset of disease and active disease, but normalized during the regenerative phase. In contrast, in the distal colon total Muc2 was unaltered during onset of disease and active disease, but significantly increased during the regenerative phase. Comparison of total Muc2 levels determined with either WE9 or anti-RCM revealed similar expression patterns during the different phases of disease (not shown).

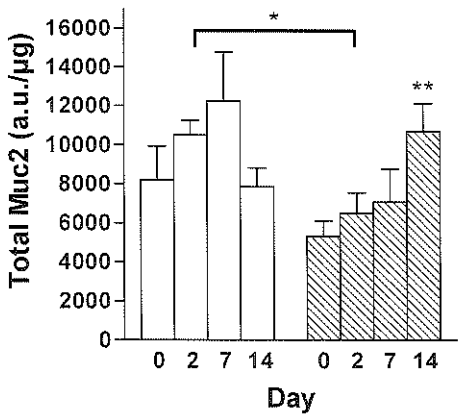

Figure 4. Total Muc2 levels in the proximal colon (open bars) and distal colon (hatched bars) during and after DSS treatment. Mean total Muc2 levels (± SEM) are given for each group; day 0, control; day 2, onset of disease; day 7, active disease; day 14, regenerative phase. Statistically significant differences were seen between the proximal colon and distal colon on day 2 ($^{*}p<0.02$) and within the distal colon between day 14 and day 0 ($^{**}p<0.05$).

Quantitation of total Muc2 secretion

Total Muc2 secretion in the proximal colon was significantly lower in controls and during the regenerative phase than in the distal colon (Fig. 5). Compared to controls, total Muc2 secretion in the proximal and distal colon was unchanged during each disease phase. Comparison of total Muc2 secretion levels determined with either WE9 or anti-RCM revealed similar expression patterns during the different phases of disease (not shown).

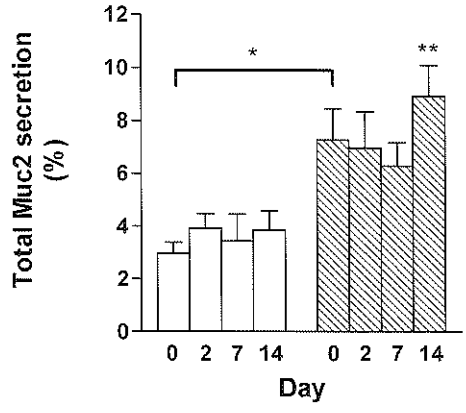

Figure 5. Secretion of total Muc2 in proximal (open bars) and distal colon (hatched bars) during and after DSS treatment. Mean total Muc2 secretion (± SEM) is presented for each of the disease phases studied; day 0, control; day 2, onset of disease; day 7, active disease; day 14, regenerative phase. Statistically significant differences were seen between the proximal and distal colon on day 0 ($^{*}p=0.0112$), and on day 14 ($^{**}p=0.046$).

Identification of mature Muc2 and quantitation of [^{35}S]sulfate incorporation into Muc2

By performing pulse-chase experiments with [^{35}S]sulfate followed by immunoprecipitations, our laboratory previously demonstrated that mature rat Muc2, with an apparent molecular mass of 650 kDa on SDS-PAGE, was detectable after 30 min pulse labeling and 4 h chase incubation in tissue and medium [4]. The "650 kDa" band was PAS-stainable and, after Western blotting, was recognized by anti-Muc2 antibodies [4]. In the present study, mature Muc2 could also be easily identified by PAS-staining on SDS-PAGE. After pulse labeling with [^{35}S]sulfate, 4 h chase incubation and homogenization, [^{35}S]sulfate-labeled mature Muc2 was detected on SDS-PAGE at an identical position (about 650 kDa) as the PAS-stained band (Fig. 3A). After identification and quantitation the amount of [^{35}S]sulfate incorporation into Muc2 was determined.

Comparing proximal with distal colon, the amount of [^{35}S]sulfate incorporation into Muc2 was significantly lower in the proximal colon in each group investigated (Fig. 6). In the proximal colon, [^{35}S]sulfate-incorporation into Muc2 was significantly reduced in each disease phase compared to controls. In the distal colon no significant alterations in sulfate incorporation were observed between any of the disease phases and the control group.

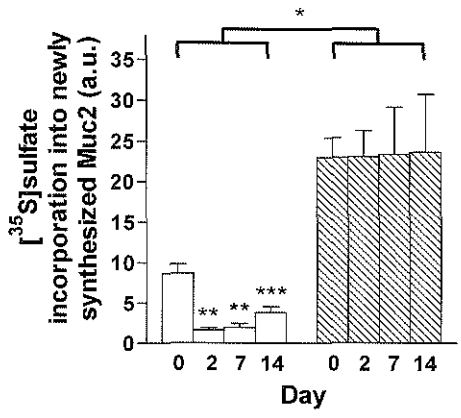

Figure 6. [^{35}S]sulfate incorporation into Muc2 in proximal colon (open bars) and distal colon (hatched bars) during and after DSS treatment. Mean [^{35}S]sulfate incorporation into Muc2 (± SEM) for each group is given; day 0, control; day 2, onset of disease; day 7, active disease; day 14, regenerative phase. [^{35}S]sulfate incorporation into Muc2 in the distal colon was significantly higher in each group than in the proximal colon ($^{*}p<0.02$). In the proximal colon [^{35}S]sulfate incorporation into Muc2 decreased in each disease group compared to controls: days 2 and 7 versus day 0 ($^{**}p<0.001$); day 14 versus day 0 ($^{***}p<0.01$).

Quantitation of [^{35}S]sulfate-labeled Muc2 secretion

Analysis of [^{35}S]sulfate-labeled Muc2 secretion revealed differences between the proximal and distal colon (Fig. 7). Specifically, in the proximal colon the amount of secreted [^{35}S]sulfate-labeled Muc2 was increased in active disease and the regenerative phase. In contrast, in the distal colon [^{35}S]sulfate-labeled Muc2 secretion appeared unaltered during the various disease phases. Comparing proximal colon with distal colon revealed that the secretion of [^{35}S]sulfate-labeled Muc2 in the distal colon was much higher in each group.

Quantitation of Muc2 mRNA

Muc2 mRNA levels in the proximal colon were significantly higher than in the distal colon in controls and each disease phase (Fig. 8). Both in proximal colon as well as distal colon Muc2

mRNA levels were maintained during the onset of disease and active disease. In contrast, in the regenerative phase Muc2 mRNA levels were significantly decreased compared to control values in both colonic segments.

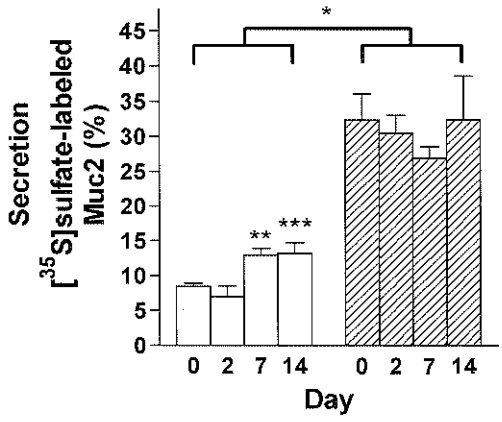

Figure 7. Secretion of [^{35}S]sulfate-labeled Muc2 in proximal (open bars) and distal colon (hatched bars) during and after DSS treatment. Mean [^{35}S]sulfate-labeled Muc2 secretion (± SEM) for each group is given; day 0, control; day 2, onset of disease; day 7, active disease; day 14, regenerative phase. [^{35}S]sulfate-labeled Muc2 secretion in the distal colon was significantly higher in each group than in the proximal colon ($^{*}p<0.01$). Within the proximal colon significantly increased [^{35}S]sulfate-labeled Muc2 secretion was observed during day 7 versus day 2 ($^{**}p<0.05$) and day 14 versus days 0 and 2 ($^{***}p<0.05$).

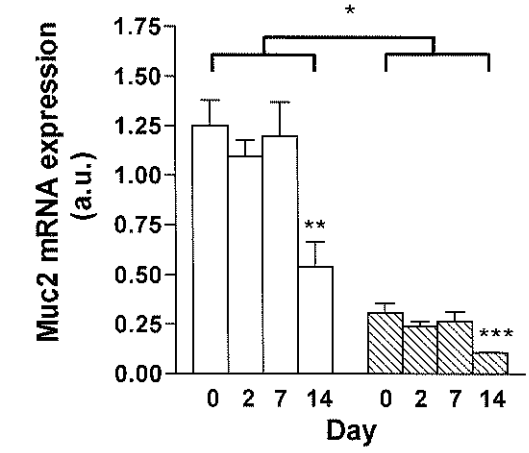

Figure 8. Muc2 mRNA in the proximal (open bars) and distal colon (hatched bars) during and after DSS treatment. Mean Muc2 mRNA expression levels (± SEM) are given for each of the disease phases studied; day 0, control; day 2, onset of disease; day 7, active disease; day 14, regenerative phase. Significant differences in Muc2 mRNA levels were seen between the proximal colon and distal colon in each group ($^{*}p<0.01$). Significant decreased Muc2 mRNA levels were seen during day 14 versus days 0 and 7 ($^{**}p<0.05$) in the proximal colon and during day 14 versus day 0 ($^{***}p<0.05$) in the distal colon.

Discussion

In the present study, we investigated changes in numbers of goblet cells, Muc2 biosynthesis, secretion, and sulfation in the proximal and distal colon of DSS-treated rats. Morphological analysis revealed that the DSS-induced damage, *i.e.* crypt loss and ulcerations started, and was most pronounced, in the distal colon, analogous to DSS-induced damage in mice and UC in human [24-26]. Moreover, as a consequence of the DSS-induced damage the overall number of

goblet cells decreased in the proximal colon and distal colon. Similarly, reduced numbers of goblet cells were also reported in the colon of humans with active UC [6].

Total protein synthesis of the explants was significantly increased during active disease in the proximal colon. This increase can be, at least partly, attributed to the two-fold increase in Muc2 precursor synthesis in this colonic segment. No differences were seen between controls, onset of disease and the regenerative phase. Although not significantly, protein synthesis of the distal colon seemed to be increased as well during onset of disease and active disease. As during these phases Muc2 precursor synthesis was unaltered, synthesis of other proteins must be increased.

Detailed analysis of the Muc2 precursor synthesis demonstrated a progressive increase in Muc2 precursor synthesis in the proximal colon during the onset of disease and active disease, followed by normalization of Muc2 precursor synthesis levels during the regenerative phase. In the distal colon Muc2 precursor synthesis was maintained during the onset of disease and active disease, but increased significantly during the regenerative phase. Although the differences were less pronounced, also the alterations in total Muc2 protein were similar to alterations seen in Muc2 precursor synthesis. Moreover, total Muc2 secretion was maintained during each disease phase studied. These data in conjunction demonstrate that in rat the DSS-induced damage and thus loss of goblet cells is accompanied by an increase, or at least a maintenance, of Muc2 precursor biosynthesis, total Muc2 levels, and total Muc2 secretion. This implies an increase in Muc2 synthesis per goblet cell, and more importantly these data suggest that the thickness of the mucus layer is at least maintained or even increased, offering optimal protection to the colonic epithelium during the different phases of the disease. Yet, these data are in contrast with changes as seen in humans with active UC. Namely, in humans MUC2 precursor synthesis and total MUC2 levels were significantly decreased in active UC compared to controls and UC in remission [10, 11]. In part, these differences might be explained by the difference in type of colitis between DSS-induced colitis in rat and UC in human. The DSS-induced colitis is a relatively acute model, while UC in patients is chronic.

Sulfate is incorporated in the last steps of mucin-biosynthesis [27]. Changes in sulfate incorporation into Muc2 and the secretion of sulfate-labeled Muc2 could reflect changes in the structure of Muc2, and indicate qualitative changes in the mucus layer. Therefore, we performed metabolic labeling studies with [^{35}S]sulfate in the course of DSS-induced disease. In the proximal colon, [^{35}S]sulfate incorporation was decreased, while [^{35}S]sulfate-labeled Muc2 secretion was increased, during active disease and the regenerative phase. Thus, in the proximal colon [^{35}S]sulfate-labeled Muc2 was preferentially secreted during active colitis and the regenerative phase. As a result of the decreased incorporation of sulfate into Muc2, in combination with the preferential secretion of sulfated Muc2, the sulfate content of the secreted Muc2 in the proximal colon may be normal during active disease. Previously, Van Klinken *et al.* reported similar results for the distal colon in humans with active UC [11]. In the distal colon of rats, however, no alterations in [^{35}S]sulfate incorporation into Muc2 and [^{35}S]sulfate-labeled Muc2 secretion were observed in active disease or any other disease

phase. Comparing the proximal colon with the distal colon, [^{35}S]sulfate incorporation into Muc2 and secretion of [^{35}S]sulfate-labeled Muc2 was significantly lower in the proximal colon in controls and during each disease phase studied. Previously, we demonstrated that degree of Muc2 sulfation is increased from proximal to distal colon in rat healthy colon [4]. As sulfate is thought to confer resistance to enzymatic degradation of the mucus layer [28], Muc2 synthesized in the proximal colon may be more sensitive to enzymatic degradation than Muc2 produced in the distal colon. Therefore, the higher Muc2 precursor synthesis levels and higher total Muc2 levels in the proximal colon might constitute a mechanism within the proximal colon to compensate for the increased sensitivity of Muc2 to enzymatic degradation.

In the distal colon, where Muc2 precursor synthesis and total Muc2 levels were lower and the [^{35}S]sulfate incorporation into Muc2 and the secretion of [^{35}S]sulfate-labeled Muc2 were both higher compared to proximal colon, the high sulfate content confers optimal resistance to enzymatic degradation. On the other hand, a high sulfate content could also be disadvantageous, because more sulfate residues would be available to sulfate-reducing bacteria, which produce sulfides that are highly toxic to the colonic mucosa. In the colon of UC patients these bacteria are indeed overrepresented [29]. If in DSS-treated rats sulfate-reducing bacteria would be overrepresented during DSS treatment, then the higher degree of sulfation in the distal colon might be one of the reasons why the distal colon is more severely damaged by DSS than the proximal colon. However, to assess the effects of alterations in Muc2 sulfation in relation to enzymatic degradation and sulfate-reducing bacteria during DSS-induced colitis, further studies are necessary.

Focussing on Muc2 mRNA, a significant down-regulation of Muc2 mRNA levels were observed in proximal and distal colon during the regenerative phase. Taking into account that the Muc2 precursor synthesis and total Muc2 levels in both colonic segments were maintained or increased during the regenerative phase, these data indicate that the Muc2 translation efficiency was increased during the latter disease phase. Once more, these data emphasize the importance of Muc2 production and the mucus layer in protecting the colonic surface epithelium.

In summary, DSS induced a decrease in the number of goblet cells in proximal and distal colon. This is accompanied by the maintenance, or even an increase, of 1) Muc2 precursor biosynthesis, 2) total Muc2 levels, and 3) total Muc2 secretion. These quantitative data suggest a maintained, or even elevated, barrier function of the mucus layer during DSS-induced disease. During active disease and the regenerative phase Muc2 becomes undersulfated in the proximal colon, while sulfated Muc2 is preferentially secreted. However, due to the decreased incorporation of sulfate into Muc2, the sulfate content of luminal Muc2 will likely be unaltered. As Muc2 mRNA decreased and total Muc2 levels were maintained or elevated during the regenerative phase, Muc2 translation efficiency is specifically increased during this phase. Collectively, these data emphasize the importance of the protective mucus layer, and suggest enhanced protective capacities through the mucus layer during the different phases of DSS-induced colitis.

Acknowledgments

The authors thank Prof. DK. Podolsky for kindly providing the anti-Muc2 antibody WE9.

References

1. Forstner JF, Forstner GG. Gastrointestinal mucus. In: LR J, ed. Physiology of the Gastrointestinal Tract. Volume 2. 3 rd ed. New York: Raven, 1994:1255-1283.

2. Van Klinken BJW, Dekker J, Büller HA, Einerhand AWC. Mucin gene structure and expression: protection vs. adhesion. Am J Physiol 1995;269:G613-27.

3. Tytgat KMAJ, Büller HA, Opdam FJ, Kim YS, Einerhand AWC, Dekker J. Biosynthesis of human colonic mucin: Muc2 is the prominent secretory mucin. Gastroenterology 1994;107:1352-63.

4. Tytgat KMAJ, Bovelander FJ, Opdam FJ, Einerhand AWC, Büller HA, Dekker J. Biosynthesis of rat MUC2 in colon and its analogy with human MUC2. Biochem J 1995;309:221-9.

5. Van Klinken BJW, Einerhand AWC, Duits LA, Makkink MK, Tytgat KMAJ, Renes IB, Verburg M, Büller HA, Dekker J. Gastrointestinal expression and partial cDNA cloning of murine Muc2. Am J Physiol 1999;276:G115-24.

6. Jacobs LR, Huber PW. Regional distribution and alterations of lectin binding to colorectal mucin in mucosal biopsies from controls and subjects with inflammatory bowel diseases. J Clin Invest 1985;75:112-8.

7. McCormick DA, Horton LW, Mee AS. Mucin depletion in inflammatory bowel disease. J Clin Pathol 1990;43:143-6.

8. Pullan RD, Thomas GA, Rhodes M, Newcombe RG, Williams GT, Allen A, Rhodes J. Thickness of adherent mucus gel on colonic mucosa in humans and its relevance to colitis. Gut 1994;35:353-9.

9. Parker N, Tsai HH, Ryder SD, Raouf AH, Rhodes JM. Increased rate of sialylation of colonic mucin by cultured ulcerative colitis mucosal explants. Digestion 1995;56:52-6.

10. Tytgat KMAJ, van der Wal JW, Einerhand AWC, Büller HA, Dekker J. Quantitative analysis of MUC2 synthesis in ulcerative colitis. Biochem Biophys Res Commun 1996;224:397-405.

11. Van Klinken BJW, Van der Wal JW, Einerhand AWC, Büller HA, Dekker J. Sulphation and secretion of the predominant secretory human colonic mucin MUC2 in ulcerative colitis. Gut 1999;44:387-93.

12. Raouf AH, Tsai HH, Parker N, Hoffman J, Walker RJ, Rhodes JM. Sulphation of colonic and rectal mucin in inflammatory bowel disease: reduced sulphation of rectal mucus in ulcerative colitis [see comments]. Clin Sci (Colch) 1992;83:623-6.

13. Cooper HS, Murthy SN, Shah RS, Sedergran DJ. Clinicopathologic study of dextran sulfate sodium experimental murine colitis. Lab Invest 1993;69:238-49.

14. Murthy SN, Cooper HS, Shim H, Shah RS, Ibrahim SA, Sedergran DJ. Treatment of dextran sulfate sodium-induced murine colitis by intracolonic cyclosporin. Dig Dis Sci 1993;38:1722-34.

15. Bjorck S, Jennische E, Dahlstrom A, Ahlman H. Influence of topical rectal application of drugs on dextran sulfate- induced colitis in rats. Dig Dis Sci 1997;42:824-32.

16. Axelsson L-G, Ahlstedt S. Actions of sulphasalazine and analogues in animal models of experimental colitis. Inflammopharmacology 1993;2:219-232.

17. Axelsson LG, Landstrom E, Bylund-Fellenius AC. Experimental colitis induced by dextran sulphate sodium in mice: beneficial effects of sulphasalazine and olsalazine. Aliment Pharmacol Ther 1998;12:925-34.

18. Ni J, Chen SF, Hollander D. Effects of dextran sulphate sodium on intestinal epithelial cells and intestinal lymphocytes. Gut 1996;39:234-41.

19. Verburg M, Renes IB, Meijer HP, Taminiau JA, Büller HA, Einerhand AWC, Dekker J. Selective sparing of goblet cells and paneth cells in the intestine of methotrexate-treated rats. Am J Physiol Gastrointest Liver Physiol 2000;279:G1037-47.

20. Tytgat KMAJ, Klomp LW, Bovelander FJ, Opdam FJ, Van der Wurff A, Einerhand AWC, Büller HA, Strous GJ, Dekker J. Preparation of anti-mucin polypeptide antisera to study mucin biosynthesis. Anal Biochem 1995;226:331-41.

21. Dekker J, Van Klinken BJW, Büller HA, Einerhand AWC. Quantitation of biosynthesis and secretion of mucin using metabolic labeling. Methods Mol Biol 2000;125:65-73.

22. Van Klinken BJW, Büller HA, Einerhand AWC, Dekker J. Identification of mucins using metabolic labeling, immunoprecipitation, and gel electrophoresis. Methods Mol Biol 2000;125:239-47.

23. Dekker J, Strous GJ. Covalent oligomerization of rat gastric mucin occurs in the rough endoplasmic reticulum, is N-glycosylation-dependent, and precedes initial O-glycosylation. J Biol Chem 1990;265:18116-22.

24. Hamilton SR. Diagnosis and comparison of ulcerative colitis and Crohn's disease involving the colon. In: Norris HT, ed. Pathology of the colon, small intestine, and anus. New York: Churchill Livingstone, 1983:77-107.

25. Okayasu I, Hatakeyama S, Yamada M, Ohkusa T, Inagaki Y, Nakaya R. A novel method in the induction of reliable experimental acute and chronic ulcerative colitis in mice. Gastroenterology 1990;98:694-702.

26. Riddell RH. Pathology of idiopatic inflammatory bowel diseases. In: Shorter RG, ed. Inflammatory Bowel Diseases. Philadelphia: Lea Febiger, 1988:329-350.

27. Strous GJ, Dekker J. Mucin-type glycoproteins. Crit Rev Biochem Mol Biol 1992;27:57-92.

28. Nieuw Amerongen AV, Bolscher JG, Bloemena E, Veerman EC. Sulfomucins in the human body. Biol Chem 1998;379:1-18.

29. Roediger WE, Moore J, Babidge W. Colonic sulfide in pathogenesis and treatment of ulcerative colitis. Dig Dis Sci 1997;42:1571-9.

Chapter 6

Enterocyte -, goblet cell -, and Paneth cell-specific responses after treatment with the cytostatic drug methotrexate

Ingrid B. Renes, Melissa Verburg, Sacha Ferdinandusse, Nathalie P. Bulsing, Hans A. Büller, Jan Dekker, and Alexandra W.C. Einerhand.

Summary

The small intestinal epithelium proliferates rapidly and is therefore very sensitive to treatment with the cytostatic drug methotrexate (MTX). In the present study, we aimed to gain more insight in epithelial proliferation, apoptosis and cell type-specific gene expression in a rat MTX-model. Small intestinal segments were excised on various days after a single dose of MTX. Epithelial proliferation and apoptosis were assessed by detection of incorporated BrdU and cleaved caspase-3, respectively. Epithelial functions were determined histochemically by the expression of cell type specific gene-products at mRNA and protein level. After MTX treatment, BrdU incorporation was diminished in the duodenum from day 1-3, in the jejunum at days 2 and 3, and in the ileum only at day 2. Increased levels of cleaved caspase-3-positive cells were observed at 6.5 h, day 1 and 2 after MTX treatment in each small intestinal segment. The enterocyte markers, sucrase-isomaltase, sodium-glucose co-transporter 1, glucose transporters 2 and -5, and intestinal- and liver fatty acid binding protein were down-regulated at days 3 and 4 after MTX at both mRNA and protein level in each small intestinal segment. In contrast, enterocyte-specific alkaline phosphatase (AP) activity was maintained after MTX. Moreover, after MTX goblet cells maintained their capacity to synthesize the mucin Muc2 and trefoil family factor 3 (TFF3). Lysozyme expression by Paneth cells was also maintained after MTX treatment. In conclusion: the effects of MTX on epithelial proliferation indicated that the sensitivity of the epithelium toward MTX decreases from duodenum toward the ileum. MTX-induced enterocyte malfunctioning with respect to degradation and uptake/transport of nutrients. Enterocytes and Paneth cells actively contribute to the epithelial defense after MTX treatment by maintaining AP activity and lysozyme expression, respectively. Maintenance of Muc2 and TFF3 expression by goblet cells after treatment with MTX underlines the importance of goblet cells in epithelial protection and repair.

Abbreviations: FAE, follicle-associated epithelium, Glut2 and -5, glucose transporter 2 and -5; i- and l-FABP, intestinal- and liver fatty acid binding protein; SGLT1, sodium glucose transporter 1; SI, sucrase-isomaltase; TFF3, trefoil factor 3.

Introduction

The cytostatic drug methotrexate (MTX) is a folate antagonist, which inhibits a key enzyme in the thymidylate cycle, dihydrofolate reductase (DHFR) [1, 2]. The formation of thymidylate is a key step in the synthesis of DNA. Thus in rapidly dividing cells like tumor cells, bone marrow cells, and small intestinal epithelial cells, the inhibition of thymidylate biosynthesis by MTX, leads to a decrease in thymidine triphosphate pools, a decrease in DNA synthesis, and eventually cell death. Additionally, MTX, its metabolites, and the folate byproducts (dihydrofolate and 10-formyldihydrofolate), which are formed by the inhibition of DHFR, not only inhibit DNA synthesis, but can also inhibit de novo purine synthesis [1, 2]. Thus in tumor tissue as well as in normal tissue MTX treatment can lead to the inhibition of DNA, RNA synthesis, and thereby to inhibition of protein synthesis.

The small intestinal epithelium proliferates rapidly and is therefore very sensitive to MTX treatment. The effects of methotrexate (MTX) on the small intestinal epithelium of human and rat are well described [3-6]. MTX is known to induce loss of crypts, crypt and villus atrophy, and flattening of crypt - and villus cells [3-7]. This damage occurs as a consequence of the MTX-induced inhibition of epithelial proliferation and induction of epithelial apoptosis in the crypt compartment. Additionally, during MTX-induced damage in rat small intestine sucrase-isomaltase (SI) and lactase enzyme activities were significantly decreased [5]. Further, treatment of rats with sub-lethal doses of MTX induced Paneth cell hyperplasia [8]. Yet, besides these data, information on enterocyte, goblet cell, and Paneth cell specific gene expression is lacking.

In the present study, we aimed to assess epithelial proliferation, apoptosis and cell type-specific gene expression after MTX treatment. As enterocytes are specialized in the degradation, uptake and transport of nutrients the following markers were used to analyze enterocyte function: sucrase-isomaltase (SI), sodium glucose co-transporter 1 (SGLT1), glucose/fructose transporters 2 and -5 (Glut2 and -5), and liver- and intestinal fatty acid binding protein (i- and l-FABP). Goblet cell function was analyzed by the expression of the mucin Muc2, which is the structural component of the protective mucus layer [9], and trefoil family factor 3 (TFF3), a bioactive peptide that is implied in epithelial protection and repair [10, 11]. Paneth cells were analyzed by the expression of the anti-bacterial enzyme lysozyme. In addition, clinical symptoms like body weight loss, reduced food intake, loose stools, and diarrhea were evaluated after MTX administration. We aimed to gain more insight in epithelial functions in general and in enterocyte, goblet cell, and Paneth cell functions in particular.

Methods

Animals

Eight weeks-old, specified pathogen free, male Wistar rats (Broekman, Utrecht, The Netherlands) were housed individually at constant temperature and humidity on a 12-h light-dark cycle. The rats had free access to a standard pelleted diet (Hope Farms, Woerden, The Netherlands) and water. All the experiments were performed with the approval of the Animal Studies Ethics Committee of our institution.

Experimental Design

A dosage of 30 mg/kg MTX (Ledertreaxate SP Forte, Cyanamid Benelux, Etten-Leur, The Netherlands) was injected intravenously under light anesthesia. Control animals were treated with equivalent volumes of 0.9% (wt/vol.) NaCl solution. To study epithelial proliferation, 50 mg BrdU/kg body weight (Sigma, St. Louis, USA) was injected intraperitoneally 1 h before decapitation. On 6.5 h, days 1, 2, 3, and 4 after MTX four animals per time point were sacrificed. One control animal per time point was sacrificed at 6.5 h after MTX and on days 1, 2 and 4. Segments of the duodenum, jejunum and ileum were dissected, immediately fixed in 4% (wt/vol.) paraformaldehyde in phosphate buffered saline (PBS) and prepared for light microscopy. Body weight, food intake, loose stools, and diarrhea were scored daily during the experiment.

Histology

Sections of 5 μm thickness were routinely stained with alcian blue-nuclear fast red (BDH, Brunschwig Chemie, Amsterdam, The Netherlands) to study goblet cells and morphological alterations like crypt - and villus atrophy.

Immunohistochemistry

Five μm thick paraffin sections were cut and deparaffinized through a graded series of xylol-ethanol. To visualize BrdU incorporation, sections were incubated with 2 M HCl for 1.5 h, washed in borate buffer (0.1 M $Na_2B_4O_7$, pH 8.5), incubated in 0.1% (w/v) pepsin in 0.01 M HCl for 10 min at 37°C, and rinsed in PBS. Endogenous peroxidase activity was inactivated by 1.5% (v/v) hydrogen peroxide in PBS for 30 min, followed by a 30 min incubation with TENG-T (10 mM Tris-HCl, 5 mM EDTA, 150 mM NaCl, 0.25% (w/v) gelatin, 0.05% (w/v) Tween-20) to reduce non-specific binding. This was followed by overnight incubation with a 1:500 dilution of mouse anti-BrdU (Boehringer Mannheim, Mannheim, Germany). Then, the sections were incubated for 1 h with biotinylated horse anti-mouse IgG (diluted 1:2000, Vector Laboratories, England) followed by 1 h incubation with ABC/PO complex (Vectastain Elite Kit, Vector Laboratories) diluted 1:400. Binding was visualized after incubation in 0.5 mg/ml 3,3'-diaminobenzidine (DAB), 0.02%

(v/v) H_2O_2 in 30 mM imidazole, 1 mM EDTA (pH 7.0). Finally, sections were counterstained with hematoxylin, dehydrated and mounted. Apoptotic cells and the expression of the cell type-specific markers were demonstrated according to the above described protocol with omission of the HCl incubation, washing with borate buffer, and pepsin treatment. Anti-cleaved caspase-3 (1:100, Cell Signaling Technologies, Beverly, MA, USA) was used to identify apoptotic cells, anti-rat SI (1:6000, [12]), anti-rabbit SGLT1 (1:1000,[13]), anti-rat Glut2 (1:6000, Biodesign, Campro Scientific, Veenendaal, The Netherlands), anti-rat Glut5 (1:2500, [14]), anti-rat i-FABP (1:4000,[15]), and anti-rat l-FABP (1:6000, [16]) were used to determine enterocyte-specific protein expression. As marker for goblet-cell specific protein expression a Muc2 specific antibody (WE9: 1:300, [17]) and anti-rat TFF3 (1:6000, D.K. Podolsky) were used. Anti-lysozyme (1:25, Dako, Glostrup, Denmark) was used to detect Paneth cell-specific protein expression. To stain SGLT1, Glut2 and Glut5, and apoptotic cells, sections were boiled in 0.01 M citrate buffer at pH 6.0 for 10 min prior to incubation with the respective primary antibodies.

To study differences in epithelial proliferation and apoptosis, 6 well-oriented crypts were chosen per intestinal segment per animal. The crypts were located at the lateral side of the intestine. The number of BrdU- and caspase-3-positive cells in the crypts was counted and expressed per crypt, per intestinal segment, per time point. The number of cleaved caspase-3-positive cells was counted and expressed as follows: 0, 0-1 positive cell per 6 crypts; 1, 2-5 positive cells per 6 crypts; 2, >5 positive cells per 6 crypts. This scoring method was used because the variance in the number of caspase-3-positive cells between crypts per time point was relatively large. To determine the number of BrdU-positive cells in the crypts of each intestinal region, sections were judged twice by two independent observers, who were unaware of the experimental conditions.

In Situ Hybridization

Non-radioactive *in situ* hybridizations were performed according to the method described previously with slight modifications [18]. Briefly, sections were deparaffinized, hydrated and incubated in the following solutions: 0.2 M HCl, distilled water, 0.1% (w/v) pepsin in 0.01 M HCl, 0.2% (w/v) glycine in PBS, PBS, 4% (wt/v) paraformaldehyde in PBS, PBS and finally in 2 X SSC (0.03 M Na_3-citrate in 0.3 M NaCl). Until hybridization, sections were stored in a solution of 50% (v/v) formamide in 2 X SSC at 37°C. For hybridization, cell type-specific probes were diluted in hybridization solution (50% (v/v) deionized formamide, 10% (wt/v) dextran sulfate, 2 X SSC, 1 X Denhardt's solution, 1 µg/ml tRNA, 250 µg/ml herring sperm DNA) to a concentration of 100 ng/ml, incubated at 68°C for 15 min and layered onto the sections. Sections were hybridized overnight at 55°C in a humid chamber. Post-hybridization washes were performed at 45°C using the following steps: 50% (v/v) formamide in 2 X SSC, 50% (v/v) formamide in 1 X SSC and 0.1 X SSC. A 15 min incubation with RNase T1 (2 U/ml in 1 mM EDTA in 2 X SSC) at

37 °C was followed by washes of 0.1 X SSC at 45°C and 2 X SSC at room temperature. The digoxigenin-labeled hybrids were detected by incubation with anti-digoxigenin (Fab, 1:2000) conjugated to alkaline phosphatase for 2.5 h at room temperature. Thereafter, sections were washed in 0.025% (v/v) Tween in Tris-buffered saline pH 7.5. For staining, sections were layered with detection buffer (0.1 M Tris-HCl, 0.1 M NaCl, 0.05 M $MgCl_2$ pH 9.5) containing 0.33 mg/ml 4-nitroblue tetrazolium chloride, 0.16 mg/ml 5-bromo-4-chloro-3-indolyl-phosphate, 8% (v/v) polyvinylalcohol (Mw 31000-50000, Aldrich Chemical Milwaukee, WI, USA) and 1 mM levamisol (Sigma). The color reaction was performed overnight in the dark and was stopped when the desired intensity of the resulting blue precipitate was reached. Finally, sections were washed in 10 mM Tris-HCl containing 1 mM EDTA, distilled water and mounted with Aquamount improved ® (Gurr, Brunschwig, Amsterdam, The Netherlands).

Probe preparation for in situ hybridization

Digoxigenin-11-UTP-labeled RNA probes were prepared according to the manufacturer's prescription (Boehringer Mannheim GmbH, Biochemica, Mannheim, Germany) using T3, T7 or SP6 RNA polymerase. The following enterocyte-specific probes were used: A 827 bp fragment of rat SI cDNA clone ligated in pBluescript KS [19], a 1 kb NcoI fragment based on the 2.4 kb fragment of rat SGLT1 cDNA clone ligated in pBluescript II SK [20], and a 350 bp fragment of rat l-FABP cDNA clone ligated in pBluescript [21]. As Goblet cell-specific probes a 200 bp EcoRI/NotI fragment based on the 1.1 kb fragment of rat Muc2 as described previously [7], and a 438 bp EcoRI fragment of rat TFF3 ligated in pBluescript KS were used [22]. A 990 bp fragment of rat lysozyme cDNA ligated in pBluescript KS^+/L8 was used as marker for Paneth cell specific mRNA expression [23]. To determine epithelial RNA synthesis a 260 bp EcoR1/HindIII fragment ligated in pBluescript was used [24]. Transcripts longer than 450 bp were hydrolized in 80 mM $NaHCO_3$ and 120 mM Na_2CO_3, pH 10.2 to obtain probes of various lengths ≤ 450 bp [25].

Statistical Analysis

To detect significant differences in epithelial proliferation within an intestinal region and between intestinal regions, analysis of variance was performed followed by an unpaired t-test. Differences were considered significant when $p<0.05$. Data were represented as the mean ± standard error of the mean (SEM).

Results

Clinical symptoms and morphological changes

MTX treatment resulted in body weight loss and reduced food intake. The loss of body weight became apparent at day 1 after MTX injection and lasted till day 4, the last day of the experiment. Concomitant with the initial decrease in body weight was the reduced food intake, which was observed till day 3. Loose stools and mild diarrhea were seen from day 2 till day 4, the end of the experiment.

Histological evaluation revealed that MTX-induced damage to the small intestinal epithelium is characterized by crypt atrophy, villus atrophy, and flattening of crypt and villus cells (Fig. 1, *see Appendix*). Crypt atrophy was most pronounced on day 2 and villus atrophy on days 3-4 after MTX treatment (Fig. 1B and C, *Appendix*). Flattening of crypt and villus cells was most prominent on days 3-4 after treatment (Fig. 1C, *Appendix*). Generally MTX-induced damage decreased from duodenum toward the ileum (not shown).

Epithelial Proliferation

Epithelial proliferation was studied by immunohistochemical detection and quantitation of metabolically incorporated BrdU. In controls, the number of BrdU-positive cells decreased significantly from duodenal - toward the ileal crypts (Figs. 2). At 6.5 h after MTX treatment no significant changes in the number of BrdU-positive cells were observed in any intestinal segment compared to controls. Major differences in the number of BrdU-positive cells in the crypts of eachintestinal segment were observed on days 1-4 following MTX treatment. In the duodenum, significantly decreased levels of BrdU-positive cells were observed on days 1-3, and returned to control levels thereafter. In contrast, in the jejunal crypts decreased numbers of BrdU-positive cells were seen only on days 2 and 3. On day 4 the number of BrdU-positive cells in the jejunal crypts was slightly, but not significantly elevated compared to controls. Similar to the jejunum, the number of BrdU-positive cells in the ileal crypts was significantly decreased only on day 2 (Figs. 2 and 3B, *see Appendix for Fig. 3*), comparable to control levels on day 3, and even significantly increased on day 4 (Figs 2 and 3C, *Appendix*).

Epithelial apoptosis

To detect apoptotic cells we used an antibody specific for the cleaved form of caspase-3. Caspase-3 is one of the key executioners of apoptosis [26]. Activation of caspase-3 requires proteolytic cleavage of its inactive zymogen into activated p17 and p12 subunits. The antibody used in this study detects only the large fragment of activated caspase-3, whereas it does not recognize full length caspase-3 or other caspases.

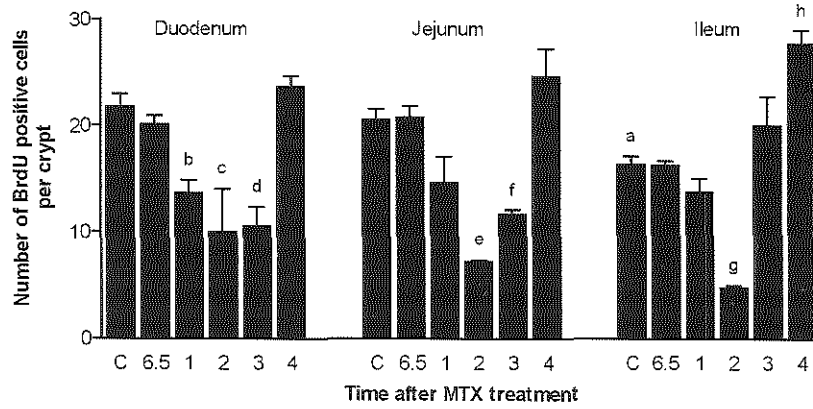

Figure 2. Epithelial proliferation in the duodenum, jejunum and ileum of control and MTX-treated rats. Proliferation was studied by immunohistochemical detection of incorporated BrdU at 6.5 h and days 1, 2, 3, and 4 after MTX. Average numbers of BrdU-positive cells in the crypts were calculated per intestinal region, per rat. Subsequently, mean BrdU-positive cell numbers (±SEM) were calculated. In control ileum proliferation was significantly lower than in duodenum and jejunum (a, $p<0.05$). In the duodenum proliferation was decreased on day 1 compared to controls and day 4 (b, $p<0.05$), on day 2 compared to controls, 6.5 h, and day 4 (c, $p<0.05$), and on day 3 compared to controls, 6.5 h, and day 4 (d, $p<0.01$). In crypts of the jejunum a significant decrease in proliferation was seen on day 2 compared to controls, 6.5 h, day 1 and day 4 (e, $p<0.05$), and on day 3 compared to controls and 6.5 h and day 4 (f, $p<0.05$). In the ileum proliferation was significantly decreased on day 2 compared to controls, 6.5 h, day 1, day 3 and day 4 (g, $p<0.05$). Within the ileum a significant increase in proliferation was seen on day 4 compared to all other groups (h, $p<0.05$).

At each time point investigated, the scores of cleaved caspase-3-positive cells were similar for the duodenum, jejunum, and ileum. MTX treatment resulted in an increase in the score of cleaved caspase-3-positive cells at 6.5 h (score of 2) and at day 1 (score of 1) in the crypts of the duodenum, jejunum, and ileum (Fig. 4B, jejunum at 6.5 h, *see Appendix*). On day 2, the score of cleaved caspase-3-positive cells decreased in the crypts of each intestinal region compared to 6.5 h and 1 day after MTX treatment, but was still elevated compared to controls (Fig. 4C, jejunum, *Appendix*). The number of cleaved caspase-3-positive cells in each intestinal region was comparable with control values on days 3 and 4 (not shown). No differences in the number or position of cleaved caspase-3-positive cells were seen between the duodenum, jejunum, or ileum, at each time point investigated. Further, there was no inter-animal variance in the score of caspase-3-positive cells at each time point investigated.

Enterocyte-specific gene expression

Enterocyte-specific mRNA expression was studied by *in situ* hybridization using rat SI -, rat SGLT1 -, and rat l-FABP specific probes. SI -, SGLT1 -, and l-FABP mRNA was normally expressed in duodenal, jejunal, and ileal villus enterocytes (Figs 5A and I, SGLT1 and l-FABP, respectively, *see Appendix*). At 6.5 h and at days 1 and 2 after MTX treatment no alterations in the enterocyte-specific mRNA expression patterns were seen in any of the intestinal segments (not shown). However, on days 3 and 4 we observed dramatic alterations in enterocyte-specific mRNA expression patterns in each intestinal segment. Specifically, in each intestinal segment SI -, SGLT1 -, and l-FABP mRNA expression was decreased on day 3 (not shown). On day 4, SI - and SGLT1 mRNA expression was even completely absent (Fig. 5B, SGLT1, *Appendix*). Similar to SI - and SGLT1 mRNA, l-FABP mRNA was decreased on days 3 and 4 after MTX treatment (Fig. 5I, l-FABP, *Appendix*). In contrast, the house keeping gene ß-actin remained expressed in the crypt and villus enterocytes of each intestinal region after MTX-treatment, indicating that the enterocytes were still metabolically active (Fig 5M, day 4, *Appendix*).

Enterocyte-specific protein expression was studied immunohistochemically using antibodies against SI, SGLT1, Glut2 and -5, and i- and l-FABP. SI -, SGLT1 - and Glut5 protein expression was normally confined to the brush border of villus enterocytes of each intestinal segment (Fig. 5C and E, SI and Glut 5, respectively, *Appendix*). Glut2 protein was expressed at the basolateral membrane of villus enterocytes in control duodenum, jejunum and ileum (Fig. 5G, *Appendix*). In contrast to the membrane-bound expression patterns of the markers described above, i- and l-FABP proteins were normally found in the cytosol of duodenal, jejunal and ileal villus enterocytes (Fig. 5K, l-FABP, *Appendix*). Similar to the mRNA expression patterns, no alterations in enterocyte-specific protein expression patterns were observed on 6.5 h and days 1 and 2 after MTX treatment (not shown). On day 3 each of the enterocyte-specific protein markers seemed decreased in the villus epithelium of each intestinal segment (not shown). On day 4, the villus enterocytes were even negative for SI -, SGLT1 -, Glut2 and Glut5 protein (Fig. 5D, SI; 5E, Glut5; 5G, Glut2, *Appendix*). Additionally, many villus enterocytes were negative for i-FABP as well as l-FABP (Fig. 5L, l-FABP, *Appendix*).

In contrast to the down-regulation of the above-described enterocyte-specific genes, enterocyte specific-AP activity was maintained on each day after MTX treatment (Fig. 6, see *Appendix*).

Goblet cell- and Paneth cell-specific gene expression

Goblet cell-specific gene expression patterns were studied using rat Muc2 - and rat TFF3 specific cRNA probes and antibodies. In controls, Muc2 - and TFF3 mRNA and protein were expressed by goblet cells in crypts and villi of the duodenum, jejunum and ileum (Fig. 7A and D, Muc2 and TFF3, respectively, *see Appendix*). After MTX treatment, Muc2 - and TFF3 protein expression

was maintained, even at day 4. Although goblet cells continued to express Muc2 - and TFF3 protein after MTX, the distribution pattern of goblet cells along the crypt-villus axis changed. Specifically, goblet cells, although flattened, remained present in the crypts on day 2 after MTX treatment (Fig 7B and E, Muc2 and TFF3, respectively, *Appendix*), but accumulated both in crypts and at villus tips on day 4 (Fig. 7 C and F, Muc2 and TFF3, respectively, *Appendix*).

Lysozyme was used as marker for Paneth cell-specific cell function. In controls lysozyme mRNA and protein was expressed in Paneth cells at the crypt base of the duodenum, jejunum and ileum (Fig 8A and C, mRNA and protein, respectively. *For figure see Appendix*). At days 2 and 3, the number of Paneth cells appeared increased and lysozyme mRNA seemed up-regulated (Fig. 8B and D, mRNA and protein on day 2, *Appendix*).

Discussion

In the present study we first characterized the rat MTX model with respect to clinical symptoms and morphological alterations within the small intestine. Subsequently, we analyzed the effects of MTX on epithelial proliferation and apoptosis, and enterocyte-, goblet cell-, and Paneth cell-specific gene expression in the duodenum, jejunum, and ileum. By studying these parameters in conjunction we aimed to gain more insight into epithelial functions in general and enterocyte, goblet cell, and Paneth cell functions in particular.

MTX-treatment resulted in body weight loss, loose stools, and mild diarrhea. Body weight loss after MTX treatment was caused both by reduced food-intake and dehydration. The latter occurred as a consequence of the MTX-induced loose stools and diarrhea. Additionally, morphological analysis demonstrated that MTX induced crypt loss and crypt - and villus atrophy, which is accompanied by flattening of crypt and villus cells in the small intestinal epithelium. Similar clinical symptoms and morphological alterations were reported in the small intestine of rat, mice and cancer patients treated with cytostatic drugs [3-5, 7, 27].

As MTX primarily affects cell proliferation and apoptosis, epithelial proliferation and apoptosis were studied. In health, epithelial proliferation decreased from duodenum toward the ileum. After MTX treatment epithelial proliferation was decreased from days 1-3 in the duodenum, days 1 and 2 in the jejunum, but only at day 2 in the ileum. These data demonstrate that the sensitivity of the epithelium toward MTX decreases from duodenum toward the ileum, which is in line with the knowledge that the sensitivity of tissues toward cytostatic agents depends primarily on the proliferation rate, *i.e.* high proliferation rate leads to high sensitivity. This is in line with a parallel study in which we demonstrated that the MTX-induced inhibition of epithelial proliferation in the normal small intestine was least affected in the ileum [7]. Moreover, in both, the

present and the parallel study a sort of 'over-compensation' is seen in the ileal epithelium, wherein epithelial hyper-proliferation is already seen at day 4 after MTX.

Analysis of MTX-induced apoptosis revealed increased apoptotic cell numbers in the crypts of each intestinal segment at 6.5 h and at days 1 and 2 after MTX. In contrast to the proliferation rates, no differences were seen in the number of MTX-induced apoptotic cells between the various intestinal regions. However, within each intestinal segment the variance in the number of caspase-3-positive cells between crypts per time point was large, therefore we can not exclude that there are small differences in the number of apoptotic cells between the duodenum, jejunum, and ileum. In conjunction, these data suggest that MTX-induced epithelial damage can be accounted for, at least partly, by the effects of MTX on epithelial proliferation and apoptosis.

Focussing on the enterocytes, a down-regulation of SI, SGLT1, Glut2 and -5, and i- and l-FABP was observed in the flattened villus enterocytes in duodenum, jejunum, and ileum after MTX treatment. Yet, these flattened enterocytes remained their capacity to express ß-actin mRNA demonstrating that they were still metabolically active and that MTX treatment did not inhibit purine synthesis completely. This implies that enterocytes might specifically down-regulate certain genes, possibly to reduce their metabolic need. Moreover, recent data from our laboratory clearly demonstrate that the down-regulation of certain enterocyte-specific genes by MTX are gene specific, *i.e.* the genes are not down-regulated to the same extent and/or at the same time after MTX-treatment [28].

Previously, it was shown that MTX decreased putrescine levels in the small intestine [29]. As putrescine appears to be an important source of energy for the small intestinal epithelium under normal conditions and under stress conditions [30], it could very well be that after MTX treatment energy sources are reduced in the small intestine. In this light, down-regulation of certain enterocyte-specific genes is necessary to retain enough energy for the enterocytes to survive and to play a role in epithelial restitution and defense. This hypothesis is further supported by the fact that enterocyte-specific AP activity, which is known to detoxify endotoxins [31, 32], was maintained in the small intestine after MTX treatment. More generally, the down-regulation of SI, SGLT1, Glut2 and -5, and i- and l-FABP suggests enterocyte malfunctioning with respect to the degradation, absorption and transport of sugars and fatty acids. Tanaka *et al.* reported similar results for enterocyte-specific SI and SGLT1 expression in the normal small intestinal epithelium of rats treated with 5-fluorouracil [33].

The goblet cells of each intestinal segment investigated maintained their capacity to produce Muc2 and TFF3 mRNA and protein after MTX treatment. In a parallel study we showed that Muc2 and TFF3 mRNA levels were maintained at days 1 and 2 after MTX, but decreased at days 3 and 4 [7]. This decrease is, at least partly, caused by a decrease in the total number of goblet cells after MTX, as demonstrated in the same study. Despite the reduction in number, the goblet cells appeared to maintain their capacity to synthesize Muc2 and TFF3. These data suggest an

important role for goblet cells in the defense and repair of the small intestinal mucosa after MTX. Interestingly, several days after MTX injection goblet cells accumulated at the villus tips. These data are in line with a previous study in which we demonstrate that the goblet cells that accumulated at villus tips after MTX were selectively spared from apoptosis [7].

Paneth cell-specific lysozyme expression was at least maintained in response to MTX treatment in the duodenum, jejunum, and ileum. Quantitation of lysozyme mRNA levels, as described in a parallel study by our laboratory, showed a strong up-regulation of lysozyme mRNA during the first two days after MTX treatment [7]. In addition, Paneth cell hyperplasia in rat small intestine after sub-lethal doses of MTX was described previously [8]. As lysozyme displays anti-bacterial activities, these data suggest that Paneth cells actively contribute to the protection of the small intestinal mucosa after MTX treatment.

In summary, the MTX-induced clinical symptoms and morphological alterations are similar to the clinical symptoms and morphological alterations seen in mice and humans after cytostatic drug treatment. MTX treatment inhibited epithelial proliferation and induced increased epithelial apoptosis. The sensitivity of the epithelium toward MTX decreased from duodenum to ileum. MTX treatment resulted in a down-regulation of enterocyte-specific genes that are involved in the degradation, absorption and transport of sugars and fatty acids, suggesting enterocyte malfunctioning with respect to the up-take and transport of nutrients. Enterocytes and Paneth cells actively contribute to the epithelial defense after MTX treatment by maintaining AP activity and lysozyme expression, respectively. Maintenance of Muc2 and TFF3 expression by goblet cells and the accumulation of goblet cells at the villus tips after MTX underlines the importance of goblet cells in epithelial protection and repair. Collectively, these data suggest that the epithelial nutrient uptake and transport capacities are down-regulated by MTX treatment whereas epithelial protection, repair and defense mechanisms are at least maintained or may even be up-regulated during damage.

Acknowledgements

We thank the following scientists for kindly providing the antibodies or cDNAs used in this study: Dr K. Y. Yeh for anti-rat SI antibodies, Dr P. G. Traber for rat SI cDNA; Dr B. Hirayama for anti-rabbit SGLT1 antibodies; Dr C. Burant for rat SGLT1 cDNA; Dr D. R. Yver for anti-rat Glut5 antibodies; Prof. Dr J. I. Gordon for anti-rat intestinal- and liver FABP antibodies, and rat intestinal - and liver FABP cDNAs; Dr D. K. Podolsky for WE9 (anti-human MUC2 antibodies), anti-rat TFF3 antibodies, and rat TFF3 cDNA; Dr J. H. Power for lysozyme cDNA.

References

1. Allegra JA. Antifolates. In: Chabner BA, Collins JM, eds. Cancer chemotherapy: Principles and Practice. Philadelphia: Lippincott, 1990:110-153.

2. Kamen BA, Cole PD, Bertino JR. Chemotherapeutic Agents: Folate Antagonists. In: Bast Jr. RC, Kufe DW, Pollock RE, Weichselbaum RR, Holland JF, Frei E, eds. Cancer Medicine. 4 ed. Hamilton: B. C. Decker INc., 1997:907-22.

3. Altmann GG. Changes in the mucosa of the small intestine following methotrexate administration or abdominal x-irradiation. Am J Anat 1974;140:263-79.

4. Pinkerton CR, Cameron CH, Sloan JM, Glasgow JF, Gwevava NJ. Jejunal crypt cell abnormalities associated with methotrexate treatment in children with acute lymphoblastic leukaemia. J Clin Pathol 1982;35:1272-7.

5. Taminiau JAJM, Gall DG, Hamilton JR. Response of the rat small-intestine epithelium to methotrexate. Gut 1980;21:486-92.

6. Trier JS. Morphological alterations induced by methotrexate in the mucosa of human proximal intestine. Gastroenterology 1962:295-305.

7. Verburg M, Renes IB, Meijer HP, Taminiau JA, Büller HA, Einerhand AWC, Dekker J. Selective sparing of goblet cells and paneth cells in the intestine of methotrexate-treated rats. Am J Physiol Gastrointest Liver Physiol 2000;279:G1037-47.

8. Jeynes BJ, Altmann GG. Light and scanning electron microscopic observations of the effects of sublethal doses of methotrexate on the rat small intestine. Anat Rec 1978;191:1-17.

9. Van Klinken BJW, Dekker J, Büller HA, Einerhand AWC. Mucin gene structure and expression: protection vs. adhesion. Am J Physiol 1995;269:G613-27.

10. Dignass A, Lynch-Devaney K, Kindon H, Thim L, Podolsky DK. Trefoil peptides promote epithelial migration through a transforming growth factor beta-independent pathway. J Clin Invest 1994;94:376-83.

11. Mashimo H, Wu DC, Podolsky DK, Fishman MC. Impaired defense of intestinal mucosa in mice lacking intestinal trefoil factor. Science 1996;274:262-5.

12. Yeh KY, Yeh M, Holt PR. Thyroxine and cortisone cooperate to modulate postnatal intestinal enzyme differentiation in the rat. Am J Physiol 1991;260:G371-8.

13. Hirayama BA, Lostao MP, Panayotova-Heiermann M, Loo DD, Turk E, Wright EM. Kinetic and specificity differences between rat, human, and rabbit Na+- glucose cotransporters (SGLT-1). Am J Physiol 1996;270:G919-26.

14. Payne J, Maher F, Simpson I, Mattice L, Davies P. Glucose transporter Glut 5 expression in microglial cells. Glia 1997;21:327-31.

15. Cohn SM, Simon TC, Roth KA, Birkenmeier EH, Gordon JI. Use of transgenic mice to map cis-acting elements in the intestinal fatty acid binding protein gene (Fabpi) that control its cell lineage-specific and regional patterns of expression along the duodenal-colonic and crypt-villus axes of the gut epithelium. J Cell Biol 1992;119:27-44.

16. Sweetser DA, Hauft SM, Hoppe PC, Birkenmeier EH, Gordon JI. Transgenic mice containing intestinal fatty acid-binding protein-human growth hormone fusion genes exhibit correct regional and cell-specific expression of the reporter gene in their small intestine. Proc Natl Acad Sci U S A 1988;85:9611-5.

17. Tytgat KMAJ, Bovelander FJ, Opdam FJ, Einerhand AWC, Büller HA, Dekker J. Biosynthesis of rat MUC2 in colon and its analogy with human MUC2. Biochem J 1995;309:221-9.

18. Lindenbergh-Kortleve DJ, Rosato RR, van Neck JW, Nauta J, van Kleffens M, Groffen C, Zwarthoff EC, Drop SL. Gene expression of the insulin-like growth factor system during mouse kidney development. Mol Cell Endocrinol 1997;132:81-91.

19. Traber PG. Regulation of sucrase-isomaltase gene expression along the crypt-villus axis of rat small intestine. Biochem Biophys Res Commun 1990;173:765-73.

20. You G, Lee WS, Barros EJ, Kanai Y, Huo TL, Khawaja S, Wells RG, Nigam SK, Hediger MA. Molecular characteristics of Na(+)-coupled glucose transporters in adult and embryonic rat kidney. J Biol Chem 1995;270:29365-71.

21. Simon TC, Roth KA, Gordon JI. Use of transgenic mice to map cis-acting elements in the liver fatty acid-binding protein gene (Fabpl) that regulate its cell lineage- specific, differentiation-dependent, and spatial patterns of expression in the gut epithelium and in the liver acinus. J Biol Chem 1993;268:18345-58.

22. Suemori S, Lynch-Devaney K, Podolsky DK. Identification and characterization of rat intestinal trefoil factor: tissue- and cell-specific member of the trefoil protein family. Proc Natl Acad Sci U S A 1991;88:11017-21.

23. Yogalingam G, Doyle IR, Power JH. Expression and distribution of surfactant proteins and lysozyme after prolonged hyperpnea. Am J Physiol 1996;270:L320-30.

24. Krasinski SD, Estrada G, Yeh KY, Yeh M, Traber PG, Rings EH, Büller HA, Verhave M, Montgomery RK, Grand RJ. Transcriptional regulation of intestinal hydrolase biosynthesis during postnatal development in rats. Am J Physiol 1994;267:G584-94.

25. Cox KH, DeLeon DV, Angerer LM, Angerer RC. Detection of mRNAs in sea urchin embryos by in situ hybridization using asymmetric RNA probes. Dev Biol 1984;101:485-502.

26. Nicholson DW, Ali A, Thornberry NA, Vaillancourt JP, Ding CK, Gallant M, Gareau Y, Griffin PR, Labelle M, Lazebnik YA, et al. Identification and inhibition of the ICE/CED-3 protease necessary for mammalian apoptosis. Nature 1995;376:37-43.

27. Nagai Y, Horie T, Awazu S. Vitamin A, a useful biochemical modulator capable of preventing intestinal damage during methotrexate treatment. Pharmacol Toxicol 1993;73:69-74.

28. Verburg M, Renes IB, Van Nispen DJPM, Ferdinandusse S, Jorritsma M, Büller HA, Einerhand AWC, Dekker J. Specific responses in rat small intestinal gene expression and protein levels during cytostatic drug-induced damage and regeneration. Journal of Histochemistry and Cytochemistry;in press.

29. Watanabe S, Sato S, Nagase S, Shimosato K, Ohkuma S. Effects of methotrexate and cyclophosphamide on polyamine levels in various tissues of rats. J Drug Target 1999;7:197-205.

30. Bardocz S, Grant G, Brown DS, Pusztai A. Putrescine as a source of instant energy in the small intestine of the rat. Gut 1998;42:24-8.

31. Poelstra K, Bakker WW, Klok PA, Kamps JA, Hardonk MJ, Meijer DK. Dephosphorylation of endotoxin by alkaline phosphatase in vivo. Am J Pathol 1997;151:1163-9.

32. Poelstra K, Bakker WW, Klok PA, Hardonk MJ, Meijer DK. A physiologic function for alkaline phosphatase: endotoxin detoxification. Lab Invest 1997;76:319-27.

33. Tanaka H, Miyamoto KI, Morita K, Haga H, Segawa H, Shiraga T, Fujioka A, Kouda T, Taketani Y, Hisano S, Fukui Y, Kitagawa K, Takeda E. Regulation of the PepT1 peptide transporter in the rat small intestine in response to 5-fluorouracil-induced injury. Gastroenterology 1998;114:714-23.

Chapter 7

Protection of Peyer's patch-associated crypt and villus epithelium against methotrexate-induced damage is based on its distinct regulation of proliferation

Published as:
Ingrid B. Renes, Melissa Verburg, Nathalie P. Bulsing, Sacha Ferdinandusse, Hans A. Büller, Jan Dekker, and Alexandra W.C. Einerhand. Protection of the Peyer's patch-associated crypt and villus epithelium against methotrexate-induced damage is based on its distinct regulation of proliferation. Journal of Pathology 2002, 198:60-68.

Summary

The crypt and villus epithelium associated with Peyer's patches (PPs) was largely spared from methotrexate (MTX)-induced damage compared to the epithelium located more distantly from PPs, *i.e.* the non-patch (NP) epithelium. To assess the mechanism(s) preventing damage to the PP epithelium after MTX treatment, epithelial proliferation, apoptosis and cell functions were studied in a rat-MTX model. Small intestinal segments containing PPs were excised after MTX-treatment. Epithelial proliferation and apoptosis were assessed by detection of incorporated BrdU and cleaved caspase-3, respectively. Epithelial functions were determined by the expression of cell type specific gene-products at mRNA and protein level. Before and after MTX treatment, the number of BrdU-positive cells was higher in PP crypts than in NP crypts. BrdU incorporation was diminished in NP crypts, while in PP crypts incorporation was hardly affected. In PP and NP crypts, similar and increased levels of cleaved caspase-3-positive cells were observed after MTX. The enterocyte markers, sucrase-isomaltase, sodium-glucose cotransporter 1, glucose transporters 2 and -5, and intestinal- and liver fatty acid binding protein were down-regulated after MTX in NP epithelium, but not in PP epithelium. In contrast, expression of the goblet cell markers, Muc2 and trefoil factor 3, and the Paneth cell marker lysozyme was maintained after MTX in both PP and NP epithelium. In conclusion: As MTX-induced apoptosis was similar in PP versus NP crypts, the protection of the PP epithelium seems to be based on differences in regulation of epithelial proliferation. Enterocyte functioning in the PP epithelium was unaffected by MTX treatment. Goblet and Paneth cell functioning was maintained in NP and PP epithelium.

Abbreviations: FAE, follicle-associated epithelium, Glut2 and -5, glucose transporter 2 and -5; i- and l-FABP, intestinal- and liver fatty acid binding protein; NP, non-patch; PP, Peyer's patch; SGLT1, sodium glucose transporter 1; SI, sucrase-isomaltase; TFF3, trefoil factor 3.

Introduction

The small intestinal epithelium proliferates rapidly and is therefore very sensitive to cytostatic drug treatment. Cytostatic drugs primarily inhibit DNA synthesis thereby deranging epithelial homeostasis leading to impaired intestinal epithelial functions [1]. Among the cytostatic agents, the effects of methotrexate (MTX) on the small intestinal epithelium of human and rat are well described [1-4]. MTX is known to induce loss of crypts, crypt and villus atrophy, and flattening of crypt - and villus cells [1-5]. This damage occurs as a consequence of the MTX-induced inhibition of epithelial proliferation and induction of epithelial apoptosis. Recently, we demonstrated that MTX also induced a down-regulation of enterocyte-specific gene expression leading to enterocyte malfunctioning with regard to the degradation and absorption of nutrients [5]. In contrast, goblet cell - and Paneth cell gene expression were maintained after MTX treatment, suggesting that both goblet cells and Paneth cells were selectively spared.

In the small intestinal mucosa lymphoid nodules, also known as Peyer's patches (PP), are located at the anti-mesenteric side of the intestine. The PPs consist of immunocompetent cells covered partly by follicle-associated epithelium and partly by the normal intestinal (crypt/villus) epithelium. Intriguingly, we recently observed that the epithelial morphology up to 2-3 crypt-villus units adjacent to and overlying the PP remained relatively intact after MTX-treatment when compared to the 'non-patch' (NP) epithelium [6]. Yet, the mechanisms involved in the protection of the PP epithelium were unidentified.

In the present study, we aimed to assess the mechanism(s) responsible for the protection of the PP epithelium from morphological damage after MTX treatment. Secondly, as the morphology of the PP epithelium was relatively but not completely unaffected after MTX treatment, we studied epithelial cell functions of the PP epithelial cells after MTX treatment. Therefore, special attention was paid to epithelial proliferation, apoptosis and cell type-specific gene expression. As enterocytes are specialised in the degradation, uptake and transport of nutrients the following markers were used to analyse enterocyte function: sucrase-isomaltase (SI), sodium glucose transporter 1 (SGLT1), glucose/fructose transporters 2 and -5 (Glut2 and -5), and liver- and intestinal fatty acid binding protein (i- and l-FABP). Goblet cell function was analysed by the expression of the mucin Muc2, which is the structural component of the protective mucus layer [7], and trefoil factor 3 (TFF3), a bioactive peptide that is implied in epithelial protection and repair [8, 9]. Paneth cells were analysed by the expression of the anti-bacterial enzyme lysozyme. By studying these parameters in conjunction we aimed to get insight in PP epithelial protection, to be able to develop therapies to prevent intestinal damage occurring as a side effect in cytostatic drug treatment.

Methods

Animals

Eight weeks-old, specified pathogen free, male Wistar rats (Broekman, Utrecht, The Netherlands) were housed individually at constant temperature and humidity on a 12-h light-dark cycle. The rats had free access to a standard pelleted diet (Hope Farms, Woerden, The Netherlands) and water. All the experiments were performed with the approval of the Animal Studies Ethics Committee of our institution.

Experimental Design

A dosage of 30 mg/kg MTX (Ledertreaxate SP Forte, Cyanamid Benelux, Etten-Leur, The Netherlands) was injected intravenously under light anaesthesia. Control animals were treated with equivalent volumes of 0.9% NaCl solution. To study epithelial proliferation, 50 mg BrdU/kg body weight (Sigma, St. Louis, USA) was injected intraperitoneally 1 h before decapitation. On 6.5 h, days 1, 2, 3, and 4 after MTX four animals per timepoint were sacrificed. One control animal per timepoint was sacrificed at 6.5 h after MTX and on days 1, 2 and 4. Segments of the duodenum, jejunum and ileum containing PPs were dissected, immediately fixed in 4% paraformaldehyde in phosphate buffered saline (PBS) and prepared for light microscopy.

Histology

Sections of 5 μm thickness were routinely stained with alcian blue-nuclear fast red (BDH, Brunschwig Chemie, Amsterdam, The Netherlands) to study goblet cells and morphological alterations like crypt - and villus atrophy.

Immunohistochemistry

Five μm thick paraffin sections were cut and deparaffinized through a graded series of xylol-ethanol. To visualize BrdU incorporation, sections were incubated with 2 M HCl for 1.5 h, washed in borate buffer (0.1 M $Na_2B_4O_7$, pH 8.5), incubated in 0.1% (w/v) pepsin in 0.01 M HCl for 10 min at 37°C, and rinsed in PBS. Endogenous peroxidase activity was inactivated by 1.5% (v/v) hydrogen peroxide in PBS for 30 min, followed by a 30 min incubation with TENG-T (10 mM Tris-HCl, 5 mM EDTA, 150 mM NaCl, 0.25% (w/v) gelatin, 0.05% (w/v) Tween-20) to reduce non-specific binding. This was followed by overnight incubation with a 1:500 dilution of mouse anti-BrdU (Boehringer Mannheim, Mannheim, Germany). Then, the sections were incubated for 1 h with biotinylated horse anti-mouse IgG (diluted 1:2000, Vector Laboratories, England) followed by 1 h incubation with ABC/PO complex (Vectastain Elite Kit, Vector Laboratories) diluted 1:400. Binding was visualised after incubation in 0.5 mg/ml 3,3'-diaminobenzidine (DAB), 0.02% (v/v) H_2O_2 in 30 mM imidazole, 1 mM EDTA (pH 7.0). Finally, sections were counterstained with haematoxylin, dehydrated and mounted. Apoptotic cells and the expression of the cell type-specific markers were demonstrated according to the above described protocol with omission of the HCl incubation, washing with borate buffer, and

pepsin treatment. Anti-cleaved caspase-3 (1:100, Cell Signaling Technologies, Beverly, MA, USA) was used to identify apoptotic cells, anti-rat SI (1:6000, [10]), anti-rabbit SGLT1 (1:1000, [11]), anti-rat Glut2 (1:6000, Biodesign, Campro Scientific, Veenendaal, The Netherlands), anti-rat Glut5 (1:2500, [12]), anti-rat i-FABP (1:4000, [13]), and anti-rat l-FABP (1:6000, [14]) were used to determine enterocyte-specific protein expression. As marker for goblet-cell specific protein expression a Muc2 specific antibody (WE9: 1:300, [15]) and anti-rat TFF3 (1:6000) were used. Anti-lysozyme (1:25, Dako, Glostrup, Denmark) was used to detect Paneth cell-specific protein expression. To stain SGLT1, Glut2 and Glut5, and apoptotic cells, sections were boiled in 0.01 M citrate buffer at pH 6.0 for 10 min prior to incubation with the respective primary antibodies.

To study differences in epithelial proliferation and apoptosis between the PP - and NP epithelium, 6 well-oriented PP - and NP crypts were chosen per intestinal segment per animal. The 6 PP crypts were located adjacent to (3 crypts at each side of the PP) or overlying a PP and the NP crypts were located at the lateral side of the intestine. The number of BrdU-positive cells in the crypts was counted and expressed per crypt, per intestinal segment, per time point. The number of cleaved caspase-3-positive cells was counted and expressed as follows: 0, 0-1 positive cell per 6 crypts; 1, 2-5 positive cells per 6 crypts; 2, >5 positive cells per 6 crypts. This scoring method was used because the variance in the number of caspase-3-positive cells between crypts per time point was relatively large. To determine the number of BrdU- and caspase-3-positive cells in PP - and NP crypts in each intestinal region, sections were judged twice by two independent observers, who were unaware of the experimental conditions.

In Situ Hybridisation

Non-radioactive *in situ* hybridizations were performed according to the method described previously with slight modifications [16]. Briefly, sections were deparaffinized, hydrated and incubated in the following solutions: 0.2 M HCl, distilled water, 0.1% (w/v) pepsin in 0.01 M HCl, 0.2% (w/v) glycine in PBS, PBS, 4% paraformaldehyde in PBS, PBS and finally in 2 X SSC (0.03 M Na_3-citrate in 0.3 M NaCl). Until hybridisation, sections were stored in a solution of 50% (v/v) formamide in 2 X SSC at 37°C. For hybridisation, cell type-specific probes were diluted in hybridisation solution (50% (v/v) deionized formamide, 10% (w/v) dextran sulfate, 2 X SSC, 1 X Denhardt's solution, 1 µg/ml tRNA, 250 µg/ml herring sperm DNA) to a concentration of 100 ng/ml, incubated at 68°C for 15 min and layered onto the sections. Sections were hybridised overnight at 55°C in a humid chamber. Post-hybridisation washes were performed at 45°C using the following steps: 50% (v/v) formamide in 2 X SSC, 50% (v/v) formamide in 1 X SSC and 0.1 X SSC. A 15 min incubation with RNase T1 (2 U/ml in 1 mM EDTA in 2 X SSC) at 37 °C was followed by washes of 0.1 X SSC at 45°C and 2 X SSC at room temperature. The digoxigenin-labeled hybrids were detected by incubation with anti-digoxigenin (Fab, 1:2000) conjugated to alkaline phosphatase for 2.5 h at room temperature. Thereafter, sections were washed in 0.025% (v/v) Tween in Tris-buffered saline pH 7.5. For staining, sections were layered with detection buffer (0.1 M Tris-HCl, 0.1 M NaCl, 0.05 M $MgCl_2$ pH 9.5) containing 0.33 mg/ml 4-nitroblue tetrazolium chloride, 0.16 mg/ml 5-bromo-4-chloro-3-indolyl-phosphate, 8% (v/v) polyvinylalcohol (Mw 31000-50000, Aldrich Chemical

Milwaukee, WI, USA) and 1 mM levamisol (Sigma). The color reaction was performed overnight in the dark and was stopped when the desired intensity of the resulting blue precipitate was reached. Finally, sections were washed in 10 mM Tris-HCl containing 1 mM EDTA, distilled water and mounted with Aquamount improved (Gurr, Brunschwig, Amsterdam, The Netherlands).

Probe preparation for in situ hybridisation

Digoxigenin-11-UTP-labeled RNA probes were prepared according to the manufacturer's prescription (Boehringer Mannheim GmbH, Biochemica, Mannheim, Germany) using T3, T7 or SP6 RNA polymerase. The following enterocyte-specific probes were used: A 827 bp fragment of rat SI cDNA clone ligated in pBluescript KS [17], a 1 kb NcoI fragment based on the 2.4 kb fragment of rat SGLT1 cDNA clone ligated in pBluescript II SK [18], and a 350 bp fragment of rat I-FABP cDNA clone ligated in pBluescript [19]. As Goblet cell-specific probes a 200 bp EcoRI/NotI fragment based on the 1.1 kb fragment of rat Muc2 as described previously [5], and a 438 bp EcoRI fragment of rat TFF3 ligated in pBluescript KS were used [20]. A 990 bp fragment of rat lysozyme cDNA ligated in pBluescript KS^+/L8 was used as marker for Paneth cell specific mRNA expression [21]. Transcripts longer than 450 bp were hydrolised in 80 mM $NaHCO_3$ and 120 mM Na_2CO_3, pH 10.2 to obtain probes of various lengths $\leq$ 450 bp [22].

Statistical Analysis

To detect significant differences in epithelial proliferation between the PP - and NP epithelium within an intestinal region and between intestinal regions, analysis of variance was performed followed by an unpaired t-test. Differences were considered significant when $p<0.05$. Data were represented as the mean $\pm$ standard error of the mean (SEM).

Results

Histological Evaluation

MTX-induced damage to the 'normal' small intestinal epithelium, *i.e.* 'non-patch' (NP) epithelium, is characterised by villus atrophy, and flattening of crypt and villus cells [3, 5]. In the present study, we observed similar changes in the NP epithelium of the duodenum, jejunum and ileum after MTX treatment (Fig. 1C, jejunum, *see Appendix*). However, focussing on the epithelium near a PP (*i.e.* 2-3 crypt-villus units adjacent to and lining the PP) in each small intestinal segment, we observed that MTX-induced damage was much less pronounced (fig. 1D, jejunum, *Appendix*).

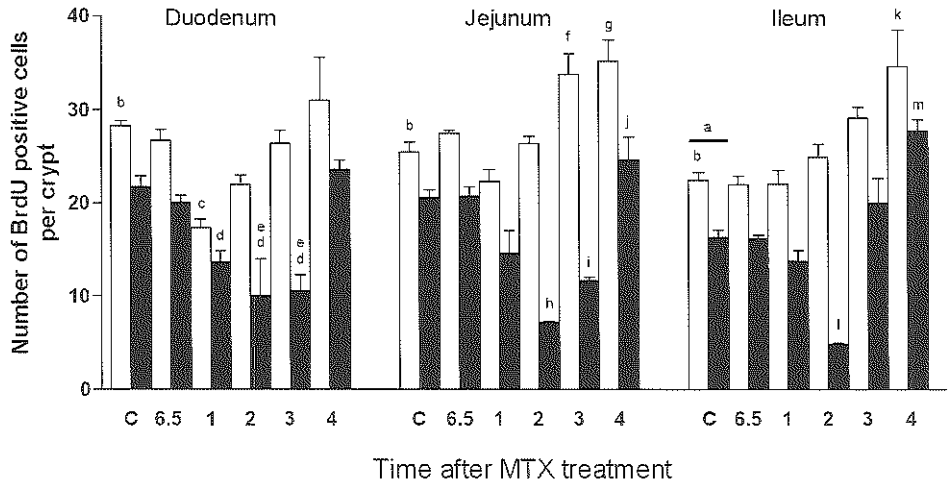

Figure 2. Epithelial proliferation in the duodenum, jejunum and ileum of control and MTX-treated rats. Proliferation was studied by immunohistochemical detection of incorporated BrdU at 6.5 h and days 1, 2, 3, and 4 after MTX. Average numbers of BrdU-positive cells in both the Peyer's patch (PP) crypts (white bars) and 'non-patch' (NP) crypts (black bars) were calculated per intestinal region, per rat. Subsequently, mean BrdU-positive cell numbers (±SEM) were calculated for PP - and NP crypts. In control ileum proliferation in PP - and NP crypts was significantly lower than in duodenum and jejunum (a, $p<0.05$). In each intestinal region of controls, proliferation in the PP crypts was significantly higher than in the NP crypts (b, $p<0.015$). In the PP crypts of the duodenum proliferation was significantly decreased on day 1 compared to controls and day 4 (c, $p<0.05$). In contrast, in the NP crypts of the duodenum proliferation was decreased on days 1-3 compared to controls and day 4 (d, $p<0.05$) and on days 2 and 3 compared to 6.5 h (e, $p<0.05$). In the jejunum, proliferation in PP crypts was significantly increased on day 3 compared to controls and day 1 (f, $p<0.05$) and on day 4 compared to controls, 6.5 h, and days 1 and 2 (g, $p<0.05$). In the NP crypts of the jejunum a significant decrease in proliferation was seen on day 2 compared to controls, 6.5 h, and days 1 and 4 (h, $p<0.05$), and on day 3 compared to controls and 6.5 h (i, $p<0.05$). On day 4, a significant increase in proliferation in NP crypts was seen compared to days 1-3 (j, $p< 0.01$). In the PP crypts of the ileum proliferation was significantly increased on day 4 compared to controls, 6.5 h, and days 1 and 2 (k, $p<0.05$). In the NP crypts of the ileum proliferation was significantly decreased on day 2 compared to controls, 6.5 h, days 1, 3 and 4 (l, $p<0.05$), and significantly increased on day 4 compared to all other groups (m, $p<0.05$).

Epithelial Proliferation

Epithelial proliferation was studied by immunohistochemical detection and quantitation of metabolically incorporated BrdU. In controls, the number of BrdU-positive cells in PP crypts was significantly higher than in NP crypts in each intestinal segment (Fig. 2). In addition, the number of BrdU-positive cells in control intestine decreased significantly from duodenum toward the ileum in both the PP - and NP crypts. At 6.5 h after MTX treatment no changes in the number of BrdU-positive cells were observed in any intestinal segment in the NP and PP

crypts compared to controls. However, major differences in the number of BrdU-positive cells in each intestinal segment, in both PP and NP crypts, were observed on days 1-4 following MTX treatment. In the duodenum, significantly decreased levels of BrdU-positive cells were seen only on day 1 in the PP crypts, whereas decreased levels were observed on days 1-3 in the NP crypts. In addition, in the PP crypts of the duodenum the number of BrdU-positive cells were comparable with control levels on days 2 and 3, and were slightly increased on day 4 although not significantly. In the jejunum, no alterations in the number of BrdU-positive cells were seen in the PP crypts on days 1 and 2. However, on days 3 and 4 the levels of BrdU-positive cells were significantly increased in the PP crypts compared to controls. In contrast, in the NP crypts of this segment decreased numbers of BrdU-positive cells were seen on days 2 and 3. On day 4 the number of BrdU-positive cells in the NP crypts was comparable to controls. Similar to the jejunum, the number of BrdU-positive cells in the ileal PP crypts was unaltered on days 1 and 2, and significantly increased on days 3 and 4. On the other hand, in the NP crypts the number of BrdU-positive cells was significantly decreased on day 2, comparable with control levels on day 3, and significantly increased on day 4.

Epithelial apoptosis

To detect apoptotic cells we used an antibody specific for the cleaved form of caspase-3. Caspase-3 is one of the key executioners of apoptosis [23]. Activation of caspase-3 requires proteolytic cleavage of its inactive zymogen into activated p17 and p12 subunits. The antibody used in this study detects only the large fragment of activated caspase-3, whereas it does not recognise full length caspase-3 or other caspases.

Table 1. Scoring of caspase-3-positive cells in PP- and NP crypts in the duodenum of control and MTX-treated rats.

Time after MTX treatment	NP crypts	PP crypts
6.5 h	2	2
Day 1	2	2
Day 2	1	1
Day 3	0	0
Day 4	0	0
control	0	0

The number of cleaved caspase-3 positive cells were counted in the Peyer's patch (PP) epithelium and the non-patch (NP) epithelium of the duodenum, jejunum, and ileumand were expressed as follows: 0, 0-1 positive cell per 6 crypts; 1, 1-5 positive cells per 6 crypts; 2, >5 positive cells per 6 crypts. No differences were observed in the scores between duodenum, jejunum, and ileum. Therefore, only the scores of the duodenum are given.

At each time point investigated, the scores of cleaved caspase-3-positive cells were similar for the duodenum, jejunum, and ileum. Therefore, only the scores for the duodenum are given in table 1. MTX treatment resulted in an increase in the score of cleaved caspase-3-positive cells at 6.5 h and at day 1 in both NP - and PP crypts (Table 1 and Fig. 3B, *see*

Appendix). On day 2, the score of cleaved caspase-3-positive cells decreased in NP - and PP crypts compared to 6.5 h and 1 day after MTX treatment, but was still elevated compared to controls (Fig. 3C, *Appendix*). In both the NP - and PP crypts, the score of cleaved caspase-3-positive cells was comparable with control values on days 3 and 4. No differences in the score or position of cleaved caspase-3-positive cells were seen between the NP - and PP crypts, at each time point investigated. Further, there was no inter-animal variance in the score of caspase-3-positive cells at each time point investigated.

Enterocyte-specific gene expression

Enterocyte-specific mRNA expression was studied by *in situ* hybridisation using rat SI -, rat SGLT1 -, and rat l-FABP specific probes. SI -, SGLT1 -, and l-FABP mRNA was normally expressed in duodenal, jejunal, and ileal villus enterocytes (Fig. 4A and C, SGLT1 and l-FABP, respectively, *see Appendix*). At 6.5 h, and days 1 and 2 after MTX treatment no alterations in the enterocyte-specific mRNAexpression patterns were seen in any of the intestinal segments (not shown). However, on days 3 and 4 we observed dramatic alterations in enterocyte-specific mRNA expression patterns between the NP - and PP epithelium. Specifically, SI -, SGLT1 -, and l-FABP mRNA expression was decreased on day 3 in the NP villus epithelium in each intestinal segment, but not in the PP villus epithelium (not shown). On day 4 SI - and SGLT1 mRNA expression was even completely absent in the NP villus epithelium, but remained present at high levels in the PP villus epithelium (Fig. 4B, SGLT1, *Appendix*). Similar to SI - and SGLT1 mRNA, l-FABP mRNA remained present in the PP villus epithelium on day 4 after MTX treatment (Fig. 4C, l-FABP, *Appendix*). Additionally, many enterocytes of the NP villi were negative for l-FABP mRNA on day 4.

Enterocyte-specific protein expression was studied immunohistochemically using antibodies against SI, SGLT1, Glut2 and -5, and i- and l-FABP. SI -, SGLT1 - and Glut5 protein expression was normally confined to the brush border of villus enterocytes in NP - and PP epithelium of each intestinal segment (Fig. 4E, SI, *Appendix*). Glut2 protein was expressed at the basolateral membrane of enterocytes in NP - and PP villi in control duodenum, jejunum and ileum (Fig. 4G, *Appendix*). In contrast to the membrane-bound expression patterns of the markers described above, i- and l-FABP proteins were normally found in the cytosol of duodenal, jejunal and ileal villus enterocytes (Fig. 4I, l-FABP, *Appendix*). Similar to the mRNA expression patterns, no alterations in enterocyte-specific protein expression patterns were observed on 6.5 h and days 1 and 2 after MTX treatment in the NP epithelium or in the PP epithelium (not shown). On day 3 each of the enterocyte-specific protein markers appeared to be decreased in the NP villus epithelium of each intestinal segment, while the expression seemed to be unaffected in the PP villus epithelium. On day 4, the NP villus enterocytes were even negative for SI -, SGLT1 -, Glut2 and Glut5 protein (Fig. 4F and H, SI and Glut2, respectively, *Appendix*). Additionally, many NP villus enterocytes were negative for i-FABP protein (Fig. 4L, *Appendix*) as well as l-FABP protein (Fig. 4J and K, *Appendix*).

Goblet cell-specific gene expression

Goblet cell-specific gene expression patterns were studied using rat Muc2 - and rat TFF3 specific cRNA probes and antibodies. Muc2 - and TFF3 mRNA and protein were expressed by goblet cells in crypts and villi of the NP - and PP epithelium in control duodenum, jejunum and ileum (Fig.5A and E, Muc2 - and TFF3 protein, respectively, *see Appendix*). Following MTX treatment, goblet cells in each intestinal segment appeared to maintain Muc2 - and TFF3 mRNA expression in the NP epithelium (Fig. 5D, Muc2 mRNA) as well as PP epithelium (Fig. 5C, Muc2 mRNA, *Appendix*). Muc2 - and TFF3 protein expression were also maintained in the PP - and NP epithelium at day 4 (Fig. 5B and F, *Appendix*). Although goblet cells continued to express Muc2 - and TFF3 protein, the distribution pattern of goblet cells along the crypt-villus axis changed after MTX treatment in the NP epithelium, but not in the PP epithelium. Specifically, in the NP epithelium goblet cells were largely absent in crypts on day 2 after MTX treatment (not shown), but accumulated both in crypts and at villus tips on day 4 (Fig. 5B, D and F, *Appendix*).

Paneth cell-specific gene expression

Lysozyme was used as marker for Paneth cell-specific cell function. In controls lysozyme mRNA and protein was expressed in Paneth cells at the crypt base of NP - and PP epithelium of the duodenum, jejunum and ileum (Fig. 6A, mRNA, *see Appendix*). Additionally, also within immunocompetent cells of the PP lysozyme mRNA and protein expression was observed. No changes in lysozyme mRNA or protein expression patterns by Paneth cells occurred after MTX treatment in the NP - and PP epithelium. However on days 2 and 3, lysozyme mRNA and protein were maintained in the PP crypts and seemed up-regulated in NP crypts (Fig. 6B, mRNA, *Appendix*). Moreover, within the PP the number of immunocompetent cells expressing lysozyme mRNA and protein was strongly increased.

Discussion

In the present study we aimed to determine which mechanism(s) underlie the protection of the PP epithelium against MTX-induced damage. Therefore, we investigated if there were differences in epithelial proliferation and apoptosis between the NP - and PP epithelium after MTX administration. Additionally, as the morphology of the PP epithelium was relatively, but not completely unaffected after MTX treatment, we studied epithelial cell functions of the PP epithelial cells after treatment.

Morphological analysis revealed that MTX-induced damage was characterised by villus atrophy and flattening of crypt and villus cells of the NP epithelium. In contrast, the PP epithelium seemed relatively unaffected by MTX treatment. In several studies similar results were reported concerning the MTX-induced morphological damage to the normal small intestinal epithelium [3, 5, 24]. However, in none of these studies the effects of cytostatic drugs on the epithelial morphology of the PP epithelium have been described.

It is generally known that the sensitivity of tissues toward cytostatic agents depends primarily on the proliferation rate, *i.e.* high proliferation rate leads to high sensitivity. As the epithelial proliferation rate in the NP - and PP epithelium decreased from duodenum toward the ileum, one would expect the MTX-induced inhibition of epithelial proliferation to be most affected in the duodenum. Indeed, we observed that the duration of MTX-induced inhibition of epithelial proliferation in the NP and PP epithelium was the longest in the duodenum, and decreased from duodenum toward the ileum. These data are in line with our previous study in which we demonstrated that the MTX-induced inhibition of epithelial proliferation in the normal small intestine was least affected in the ileum [5]. Further, as the proliferation rate in the PP epithelium of each intestinal region was significantly higher than in the NP epithelium, we expected the MTX-induced inhibition of epithelial proliferation to be most pronounced in the PP epithelium. However, the opposite appeared to occur. Namely, the MTX-induced inhibition of proliferation was less pronounced, shorter in duration, or did not occur at all in the PP crypts. Similarly, Moore and Maunda reported that in mice, the mitotic activity in the PP crypts is higher than in the NP crypts [25, 26]. Furthermore, the apparent cell cycle time of epithelial cells in the PP crypts appeared to be insignificantly lower than the cell cycle time in the NP crypts. Interestingly, the latter authors also demonstrated that the PP crypts were less sensitive for radiation and cytostatic drug-induced damage than the NP crypts. It is well known that the response of cells to ionising radiation is influenced by the concentration of oxygen present at the time of radiation [26]. Therefore, asymmetries in the vascular supply in the gut as reported previously [27], might cause differences in oxygen concentrations between the PP - and NP crypts. Yet, in radiation experiments extra oxygen supply by breathing pure oxygen instead of room air or by using a hypoxic cell sensitizer did not sensitise PP crypts to radiation damage [25]. Oxygen need not be the only blood-borne factor unequally distributed between PP - and NP crypts, since Bhalla *et al.* observed a direct connection between capillaries draining the PP follicles and the crypt plexus of PP crypts [27]. Subsequently, it was suggested that humoral factor(s) from the PP might regulate proliferation within the PP crypts resulting in differences in proliferation kinetics between the PP - and NP epithelium. In the present study we demonstrated that the numbers of proliferating cells in the PP crypts differed from those in the NP crypts. Moreover, as the PP epithelium was largely unaffected after MTX treatment compared to the NP epithelium, the possible humoral factor(s) which regulate epithelial proliferation in the PP crypts also very likely protect the PP crypts against MTX-induced damage.

Analysis of MTX-induced damage revealed increased apoptotic cell numbers in each intestinal segment at 6.5 h and on days 1 and 2 after MTX in both NP - and PP crypts. No differences were seen in the number and position of apoptotic cells between the NP - and PP epithelium, at all timepoints investigated. However, because the variance in the number of caspase-3-positive cells between crypts per timepoint was large, we can not exclude that there are small differences between the number of apoptotic cells in NP - and PP crypts. These data suggest that the protection from damage of the PP epithelium after MTX treatment can be

accounted for by the differences in proliferation between the NP - and PP epithelium and not, or to a lesser extent accounted for by differences in epithelial apoptosis.

Studying enterocyte-specific cell functions we observed major differences between the NP - and PP epithelium in the duodenum, jejunum and ileum. After MTX administration we observed that each enterocyte-specific marker, *i.e.* SI, SGLT1, Glut2 and -5, and i- and l-FABP was down-regulated in the NP epithelium, but not in the PP epithelium. These data demonstrate a negative correlation between enterocyte-specific gene expression and the MTX-induced morphological damage. The down-regulation of enterocyte-specific gene expression in the NP epithelium implies enterocyte malfunctioning within this epithelium with regard to the degradation, absorption and transport of sugars and fatty acids. Furthermore, the retained proliferation and enterocyte-specific gene expression in the PP epithelium after MTX treatment suggest that maintenance of proliferation is a prerequisite for unperturbed enterocyte functioning after MTX treatment. Regarding the down-regulation of enterocyte-specific gene expression in the NP epithelium after MTX treatment, Tanaka *et al.* reported similar results for enterocyte-specific SI - and SGLT1 expression in the normal small intestinal epithelium of rats treated with 5-fluorouracil [28].

In contrast to the enterocyte-specific gene expression, goblet cell-specific gene expression (*i.e.* Muc2 and TFF3) appeared to be maintained after MTX treatment in the NP - as well as PP epithelium. Maintenance of Muc2 and TFF3 gene expression suggests an important role for goblet cells in the defence and repair of the small intestinal mucosa after MTX. Interestingly, several days after MTX injection goblet cells accumulated at the villus tips of the NP epithelium. These data are in line with our previous study in which we demonstrated that the goblet cells that accumulated at villus tips after MTX were selectively spared from extrusion [5].

Paneth cell-specific gene expression was maintained in the PP epithelium and seemed even up-regulated in the NP epithelium in response to MTX treatment. Moreover, the up-regulation of lysozyme also occurred in immunocompetent cells of the PP. Quantitation of lysozyme mRNA levels, as described in a recent study by our laboratory, showed a strong up-regulation of lysozyme mRNA during the first two days after MTX treatment [5]. In addition, Paneth cell hyperplasia in rat small intestine after sublethal doses of MTX was described previously [29]. These data in conjunction suggest that Paneth cells and also immunocompetent cells within the PP actively contribute to the protection of the small intestinal mucosa after MTX treatment.

In summary, the PP epithelium is protected from damage induced by MTX treatment. No differences in MTX-induced apoptosis between the NP - and PP epithelium seemed to occur. In contrast, proliferation was strongly inhibited after MTX treatment in the NP epithelium, whereas in the PP epithelium inhibition of proliferation was less pronounced or did not occur at all. Therefore, the protection of PP epithelium is based, at least partly, upon differences in the regulation of proliferation. MTX treatment induced a down-regulation of enterocyte-specific gene expression in the NP epithelium, but not in the PP epithelium. These data suggest maintenance of enterocyte functions in the PP epithelium after MTX treatment

with regard to the degradation, absorption and transport of sugars and fatty acids. Maintenance of Muc2 and lysozyme expression after MTX in both the NP - and PP epithelium suggest an important role for goblet cells, Paneth cells and immunocompetent cells of the PP in the mucosal defence after MTX administration. Additionally the maintained expression of TFF3 in the NP - and PP epithelium indicates that the mucosal repair capacity may not be affected after MTX treatment. Collectively these data indicate that maintenance of epithelial defence mechanisms and most importantly epithelial proliferation near PPs after MTX preserve enterocyte-specific functions such as nutrient degradation, absorption and transport. Therefore, identification of the factor(s) which control epithelial proliferation in the PP epithelium before and after MTX might be of relevance to develop clinical therapies to protect cancer patients from intestinal damage induced by chemotherapy.

Acknowledgements

We thank the following scientists for kindly providing the antibodies or cDNAs used in this study: Dr K. Y. Yeh for anti-rat SI antibodies, Dr P. G. Traber for rat SI cDNA; Dr B. Hirayama for anti-rabbit SGLT1 antibodies; Dr C. Burant for rat SGLT1 cDNA; Dr D. R. Yver for anti-rat Glut5 antibodies; Prof. Dr J. I. Gordon for anti-rat intestinal- and liver FABP antibodies, and rat intestinal - and liver FABP cDNAs; Dr D. K. Podolsky for WE9 (anti-human MUC2 antibodies), anti-rat TFF3 antibodies, and rat TFF3 cDNA; Dr J. H. Power for lysozyme cDNA.

References

1. Pinkerton CR, Cameron CH, Sloan JM, Glasgow JF, Gwevava NJ. Jejunal crypt cell abnormalities associated with methotrexate treatment in children with acute lymphoblastic leukaemia. J Clin Pathol 1982;35:1272-7.

2. Altmann GG. Changes in the mucosa of the small intestine following methotrexate administration or abdominal x-irradiation. Am J Anat 1974;140:263-79.

3. Taminiau JAJM, Gall DG, Hamilton JR. Response of the rat small-intestine epithelium to methotrexate. Gut 1980;21:486-92.

4. Trier JS. Morphological alterations induced by methotrexate in the mucosa of human proximal intestine. Gastroenterology 1962:295-305.

5. Verburg M, Renes IB, Meijer HP, Taminiau JA, Büller HA, Einerhand AWC, Dekker J. Selective sparing of goblet cells and paneth cells in the intestine of methotrexate-treated rats. Am J Physiol Gastrointest Liver Physiol 2000;279:G1037-47.

6. Renes IB, Verburg M, Bulsing NP, Büller HA, Dekker J, Einerhand AWC. The small intestinal epithelium near Peyer's Patches is protected against damage induced by the cytostatic drug methotrexate. Gastroenterology 2000;118:A433.

7. Van Klinken BJW, Dekker J, Büller HA, Einerhand AWC. Mucin gene structure and expression: protection vs. adhesion. Am J Physiol 1995;269:G613-27.

8. Dignass A, Lynch-Devaney K, Kindon H, Thim L, Podolsky DK. Trefoil peptides promote epithelial migration through a transforming growth factor beta-independent pathway. J Clin Invest 1994;94:376-83.

9. Mashimo H, Wu DC, Podolsky DK, Fishman MC. Impaired defense of intestinal mucosa in mice lacking intestinal trefoil factor. Science 1996;274:262-5.

10. Yeh KY, Yeh M, Holt PR. Differential effects of thyroxine and cortisone on jejunal sucrase expression in suckling rats. Am J Physiol 1989;256:G604-12.

11. Hirayama BA, Lostao MP, Panayotova-Heiermann M, Loo DD, Turk E, Wright EM. Kinetic and specificity differences between rat, human, and rabbit Na+- glucose cotransporters (SGLT-1). Am J Physiol 1996;270:G919-26.

12. Payne J, Maher F, Simpson I, Mattice L, Davies P. Glucose transporter Glut 5 expression in microglial cells. Glia 1997;21:327-31.

13. Cohn SM, Simon TC, Roth KA, Birkenmeier EH, Gordon JI. Use of transgenic mice to map cis-acting elements in the intestinal fatty acid binding protein gene (Fabpi) that control its cell lineage- specific and regional patterns of expression along the duodenal-colonic and crypt-villus axes of the gut epithelium. J Cell Biol 1992;119:27-44.

14. Sweetser DA, Hauft SM, Hoppe PC, Birkenmeier EH, Gordon JI. Transgenic mice containing intestinal fatty acid-binding protein-human growth hormone fusion genes exhibit correct regional and cell-specific expression of the reporter gene in their small intestine. Proc Natl Acad Sci U S A 1988;85:9611-5.

15. Tytgat KMAJ, Bovelander FJ, Opdam FJ, Einerhand AWC, Büller HA, Dekker J. Biosynthesis of rat MUC2 in colon and its analogy with human MUC2. Biochem J 1995;309:221-9.

16. Lindenbergh-Kortleve DJ, Rosato RR, van Neck JW, Nauta J, van Kleffens M, Groffen C, Zwarthoff EC, Drop SL. Gene expression of the insulin-like growth factor system during mouse kidney development. Mol Cell Endocrinol 1997;132:81-91.

17. Traber PG. Regulation of sucrase-isomaltase gene expression along the crypt-villus axis of rat small intestine. Biochem Biophys Res Commun 1990;173:765-73.

18. You G, Lee WS, Barros EJ, Kanai Y, Huo TL, Khawaja S, Wells RG, Nigam SK, Hediger MA. Molecular characteristics of Na(+)-coupled glucose transporters in adult and embryonic rat kidney. J Biol Chem 1995;270:29365-71.

19. Simon TC, Roth KA, Gordon JI. Use of transgenic mice to map cis-acting elements in the liver fatty acid-binding protein gene (Fabpl) that regulate its cell lineage- specific, differentiation-dependent, and spatial patterns of expression in the gut epithelium and in the liver acinus. J Biol Chem 1993;268:18345-58.

20. Suemori S, Lynch-Devaney K, Podolsky DK. Identification and characterization of rat intestinal trefoil factor: tissue- and cell-specific member of the trefoil protein family. Proc Natl Acad Sci U S A 1991;88:11017-21.

21. Yogalingam G, Doyle IR, Power JH. Expression and distribution of surfactant proteins and lysozyme after prolonged hyperpnea. Am J Physiol 1996;270:L320-30.

22. Cox KH, DeLeon DV, Angerer LM, Angerer RC. Detection of mrnas in sea urchin embryos by in situ hybridization using asymmetric RNA probes. Dev Biol 1984;101:485-502.

23. Nicholson DW, Ali A, Thornberry NA, Vaillancourt JP, Ding CK, Gallant M, Gareau Y, Griffin PR, Labelle M, Lazebnik YA, et al. Identification and inhibition of the ICE/CED-3 protease necessary for mammalian apoptosis. Nature 1995;376:37-43.

24. Xian CJ, Howarth GS, Mardell CE, Cool JC, Familari M, Read LC, Giraud AS. Temporal changes in TFF3 expression and jejunal morphology during methotrexate-induced damage and repair. Am J Physiol 1999;277:G785-95.

25. Moore JV, Maunda KK. Topographic variations in the clonogenic response of intestinal crypts to cytotoxic treatments. Br J Radiol 1983;56:193-9.

26. Maunda KK, Moore JV. Radiobiology and stathmokinetics of intestinal crypts associated with patches of Peyer. Int J Radiat Biol Relat Stud Phys Chem Med 1987;51:255-64.

27. Bhalla DK, Murakami T, Owen RL. Microcirculation of intestinal lymphoid follicles in rat Peyer's patches. Gastroenterology 1981;81:481-91.

28. Tanaka H, Miyamoto KI, Morita K, Haga H, Segawa H, Shiraga T, Fujioka A, Kouda T, Taketani Y, Hisano S, Fukui Y, Kitagawa K, Takeda E. Regulation of the PepT1 peptide transporter in the rat small intestine in response to 5-fluorouracil-induced injury. Gastroenterology 1998;114:714-23.

29. Jeynes BJ, Altmann GG. Light and scanning electron microscopic observations of the effects of sublethal doses of methotrexate on the rat small intestine. Anat Rec 1978;191:1-17.

Chapter 8

Summarizing discussion

Summarizing discussion

The effects of DSS on the colonic epithelium

DSS causes colitis and inhibits proliferation

The first part (Chapters 3-5) of this thesis deals with the colonic functions during acute inflammation induced by dextran sulfate sodium (DSS) treatment. In Chapter 3 we first characterized the DSS rat model with respect to clinical symptoms and morphological damage in relation to the various disease phases. DSS treatment appeared to induce body weight loss, loose stools, diarrhea and bloody stools. Morphologically, DSS-induced damage could be divided into 3 phase: 1. onset of disease, characterized by flattening of crypt cells and crypt atrophy/loss; 2. active disease, marked by crypt loss, loss of surface epithelium, and flattening of surface epithelium; and 3. regenerative phase, marked by crypt elongations and re-epithelialization of the surface mucosa. Furthermore, the DSS-induced damage was focal and most pronounced in the distal colon. Interestingly, in mice treated with DSS and in humans with ulcerative colitis (UC) similar clinical symptoms and pathological changes were observed [1, 2]. Yet, we would like to emphasize that the DSS colitis model described in this thesis represents acute colitis, whereas UC in humans is mostly chronic, with exacerbations and phases of remission.

DSS appeared to exert its effects on the colonic epithelium via inhibition of epithelial proliferation and induction of apoptosis. Similarly, *in vitro* DSS appeared to inhibit epithelial proliferation [3]. Additionally, *in vivo* DSS induced a decrease in the proliferative activity in the cecal epithelium of mice [4]. Collectively, these data suggest that the primary action of DSS on the epithelium is the inhibition of proliferation, thereby deranging epithelial homeostasis. Yet, the colonic epithelium responded to the DSS-induced inhibition of epithelial proliferation by a rapid hyper-proliferation and restitution. These data suggested that maintenance and restoration of epithelial barrier function is of primary importance during DSS colitis.

Effects of DSS on water and electrolyte transport

The question raises how does DSS treatment impact on epithelial functions like electrolyte and water absorption, fatty acid uptake and transport, and defense against pathogens and luminal agents? Therefore, in Chapters 3 and 4, we focussed on enterocyte and goblet cell functioning during DSS-induced colitis. Enterocyte specific expression of carbonic anhydrase I and -IV (CA I and -IV), sodium hydrogen exchanger-2 and -3 (NHE2 and -3), and intestinal fatty acid binding protein (i-FABP) was reduced in many normal-appearing surface enterocytes and in most of the flattened surface enterocytes during active disease. These data suggest down-regulation of specific enterocyte functions before and during epithelial restitution. In contrast enterocyte specific alkaline phosphatase (AP) activity, which is involved in endotoxin detoxification [5, 6], was maintained, or even up-regulated, independent of enterocyte morphology, implying that mucosal defense was maintained during DSS-induced colitis, even during epithelial restitution. Maintenance of processes like colonic electrolyte and nutrient

transport represent a major metabolic demand on most cells, especially under stress conditions like inflammation. Therefore, one could argue that down-regulation of these functions that are less essential for survival of the cells during DSS-induced colitis might be necessary to conserve sufficient energy for survival of the enterocytes. Moreover, this energy could be used to induce a phenotypic shift of the enterocytes preparing them for a pivotal role in epithelial restitution and mucosal defense. Supportive to this theory is the fact that the down-regulation of certain enterocyte-specific genes during and after DSS treatment are gene specific, *i.e.* the genes are down-regulated to various extents and/or at the different time points during/after DSS treatment. We would like to emphasize that the latter reasoning is highly speculative, yet studies in this direction seem to be warranted. *In vitro* studies concentrating on epithelial gene expression in wounded monolayers of confluent epithelial cells might give more insight and open possibilities to manipulate these processes.

Quantitative analysis also revealed a reduction in the expression of CA I and -IV, NHE2 and -3, and i-FABP during DSS-colitis. As i-FABP is likely to be involved in fatty acid uptake and/or transport, down-regulation of i-FABP implies that fatty acid uptake/transport is disturbed during DSS-colitis. Yet, further studies are necessary to delineate the role of i-FABP in fatty acid uptake and/or transport during health and disease. CA I, NHE2 and –3, and most likely also CA IV are involved in electrolyte and water absorption, therefore down-regulation of these genes during DSS-colitis suggests a critical role for these genes in the induction and perpetuation of the DSS-induced diarrhea. Studies in CA II deficient mice demonstrated an important role for CA I, but not for CA II, in basal and pH-stimulated colonic electrolyte absorption. Additionally, NHE3 deficient mice suffer from mild diarrhea and have intestinal absorption defects, demonstrating the importance of NHE3 in ion transport. However, it was recently shown that, next to NHE2 and -3, the Cl-dependent Na/H exchanger and the downregulated in adenocarcinoma (DRA) exchanger also contribute to colonic ion transport [7-9]. We can not exclude that these ion transporters are also down-regulated in the colon of DSS treated rats. Thus down-regulation of these genes might also contribute to the diarrhea associated with DSS treatment. Currently, no information is available on the expression levels of CAI and -IV and NHE2 and -3 in other experimental colitis models. In humans only one report has been published demonstrating a reduction in CA I levels during active UC [10]. However, in both human UC and in experimental colitis models electrolyte and water absorption are compromised, suggesting alterations in expression levels and activity levels of the respective CAs and NHEs. Furthermore, in the previous paragraph we speculated that enterocytes down-regulated specific genes, to prepare themselves for a critical role in epithelial restitution. At this point, we would like to put forward a second mutually inclusive possibility: CAs and NHEs might be specifically down-regulated to initiate watery diarrhea to expulse pathogens and noxious agents like DSS from the intestinal lumen, or to lower the amount of normal commensal bacteria. Normal commensal bacteria in the intestine can be detrimental under stress conditions like intestinal damage.

The epithelial response towards DSS: Augmented goblet cell activity

The goblet cell specific mucin (Muc2) and trefoil factor 3 (TFF3) expression was maintained, in flattened and normal appearing goblet cells. Moreover, Muc2 and TFF3-positive goblet cells accumulated in the surface epithelium during each disease phase. TFF3 expression, which is normally confined to the upper crypt region, was extended toward the crypt bottom. These findings seem to imply that epithelial protection and repair capacity are at least maintained during DSS colitis. However, in Chapter 3 we described DSS-induced loss of crypt and surface epithelium and thus loss of goblet cells. This seems to be a general phenomenon during colitis, implying decreased epithelial protection and repair. Therefore, it was essential to focus on the actual levels of expression of Muc2 and TFF3 in the colitis-affected proximal and distal colon. Analysis of these expression levels revealed maintenance or even an up-regulation of Muc2 and TFF3 expression levels in the proximal colon. Depending on the extent of DSS-induced loss of crypts and surface epithelium, Muc2 and TFF3 levels were either slightly decreased (as in Chapter 3) or maintained (as in Chapter 4) during active disease in the distal colon. This apparent contradiction can be explained by the difference in the DSS-induced extent of crypt and surface cell loss between the two independent experiments (*i.e.* ~50% loss of epithelium in the experiment described in Chapter 3 versus 40% loss of epithelium in the experiment described in Chapter 4). So, if we account for the DSS-induced loss of crypts and surface cells, it is likely that the absolute goblet cell numbers are decreased. This in turn suggests that the amount of Muc2 synthesis per goblet cell is increased during active colitis, however morphometric studies must be done to demonstrate changes in the relative goblet cell numbers during DSS-colitis. Intriguingly, these data indicate that the individual goblet cells that remain during DSS-colitis are able to compensate, at least to a certain extent, for the DSS-induced loss of goblet cells and thus loss of Muc2 synthesis. A similar reasoning can be applied to the TFF3 synthesis.

Besides the Muc2 and TFF3 expression levels we also determined the Muc2 and TFF3 secretion levels. The percentage of Muc2 secretion appeared to be maintained during each disease phase (Chapters 4 and 5). In conjunction with the maintained or increased Muc2 protein levels and excluding possible alterations in Muc2 sulfation, the retained Muc2 secretion levels suggest that the thickness of the mucus layer is at least maintained or even increased. In contrast, in humans MUC2 levels were significantly decreased in active UC compared to controls and UC in remission [11]. In part, this difference might be explained by the difference in type of colitis between DSS-induced colitis in rat and UC in human. The DSS-induced colitis is a relatively acute model, while UC in patients is chronic.

Next to the maintained or up-regulated TFF3 protein levels during DSS-colitis, the percentage of TFF3 secretion appeared to increase progressively (Chapter 4), indicating that the luminal TFF3 content is increased during each phase of DSS-induced colitis. Presently, information on TFF3 protein expression and secretion in other colitis models is lacking. Yet, TFF3 deficient mice had impaired mucosal healing and manifested poor epithelial regeneration after DSS treatment [12]. Rectal instillation of TFF3 was able to prevent the marked ulceration that occurred after DSS treatment in these TFF3 deficient mice. The up-ward

migration of epithelial cells to the crypt-villus junction appeared to be decreased in these TFF3 deficient mice. In concert with our findings, these findings suggest that TFF3 plays a pivotal role in epithelial protection and repair during acute DSS-induced inflammation and that the epithelial repair capacity is enhanced in this acute colitis model.

Sulfate on Muc2 may be important for protection during DSS-associated damage

Despite the increase/maintenance in Muc2 levels and Muc2 secretion levels, the DSS-induced epithelial damage was not prevented. Therefore, in Chapter 5 we compared Muc2 precursor synthesis, total Muc2 levels, Muc2 secretion levels, Muc2 sulfation, and secretion of sulfated Muc2 in the proximal and distal colon during DSS-induced colitis. Muc2 precursor synthesis levels, total Muc2 levels and the percentage secretion of Muc2 was at least maintained during each of the DSS-induced disease phases. Yet, focussing on Muc2 sulfation and secretion of sulfate-labeled Muc2, a decrease in sulfate incorporation into Muc2 and an increase in the secretion of sulfate-labeled Muc2 was observed in the proximal colon. This implies that the structure of Muc2 is altered during DSS-colitis in the proximal colon, and thus that the protective capacity of mucus layer is affected by DSS treatment. Similarly, Van Klinken *et al.* reported that in humans with active UC the sulfate incorporation into MUC2 decreased, while the secretion of sulfated MUC2 increased [13].

Sulfate is thought to confer resistance to enzymatic degradation of the mucus layer [14]. Therefore, higher Muc2 precursor synthesis levels and higher total Muc2 levels which are seen in the proximal colon, compared to the distal colon, might be a mechanism within the proximal colon to compensate for the increased sensitivity of Muc2 to enzymatic degradation. In the distal colon, the high sulfate content confers optimal resistance to enzymatic degradation. Hitherto information on colonic bacteria in relation to MUC2 sulfation in UC and DSS-colitis are lacking. As in both UC and in DSS-colitis damage is most pronounced in the distal colon studies concentrating on different types of colonic bacteria in relation to the sulfation of Muc2 in UC and DSS colitis seem to be warranted. In this way it may be possible to identify bacteria that influence Muc2 sulfation and protect Muc2 from degradation.

The DSS-induced damage model in the rat: Conclusions

In conclusion, in the first part of this thesis we have shown that, despite the fact that DSS-induced colitis in rat is rather acute compared to UC in human, there are strong similarities in morphological changes, epithelial hyper-proliferation and apoptosis [15-18]. Characterization of the DSS-model revealed that DSS primarily affects the colonic epithelium via inhibition of proliferation and the induction of apoptosis. DSS induced a down-regulation of enterocyte specific genes involved in pH regulation, ion transport, water uptake and fatty acid uptake and or transport. In contrast the enterocyte specific AP activity, which is involved in epithelial defense was maintained or up-regulated. Moreover, goblet cell specific genes involved in epithelial protection and repair were maintained or even upregulated during DSS-colitis. Finally, DSS affected the degree of Muc2 sulfation, which might have implications for the protective capacity of the mucus layer.

The effects of MTX on the small intestinal epithelium

MTX affects epithelial morphology, proliferation and apoptosis

The second part of this thesis (Chapters 6 and 7) describes the small intestinal functions after treatment with the cytostatic drug methotrexate (MTX). In Chapter 6 we first defined the MTX-rat model with respect to clinical symptoms and the effects of MTX on epithelial morphology. Single dose MTX-treatment resulted in body weight loss, loose stools, and mild diarrhea. Additionally, morphological analysis demonstrated that MTX-induced crypt loss, crypt and villus atrophy, accompanied flattening of crypt and villus cells in the small intestine. Similar clinical symptoms and morphological alterations were reported in the small intestine rat, mice and cancer patients treated with cytostatic drugs [19-22].

As MTX affects proliferation and apoptosis we analyzed the effects of single dose MTX treatment on epithelial proliferation and apoptosis from duodenum till ileum. In control tissue the epithelial proliferation rate decreased from duodenum toward the ileum. Previous studies revealed similar results in both rat and human intestine [19, 22]. It is generally known that the sensitivity of tissues toward cytostatic agents depends primarily on the proliferation rate, *i.e.* high proliferation rate leads to high sensitivity. Therefore, one would expect the MTX-induced inhibition of epithelial proliferation to be most affected in the duodenum. Indeed, we observed that the duration of MTX-induced inhibition of epithelial proliferation was the longest in the duodenum, and decreased from duodenum to the ileum. In each intestinal segment the MTX-induced inhibition in epithelial proliferation was followed by epithelial hyper-proliferation, conceivably to restore or maintain the epithelial barrier against noxious agents, bacteria and viruses.

Analysis of MTX-induced damage revealed increased apoptotic cell numbers in the epithelium of each intestinal segment after MTX treatment. No differences were seen in the number of apoptotic cells between the duodenum, jejunum, and ileum, at all timepoints investigated. However, because the variance in the number of caspase-3-positive cells between crypts per timepoint was large, we can not exclude that there are small differences in the number of apoptotic cells between the duodenum, jejunum and ileum. Overall these data suggest that MTX-induced damage can, at least in part, be ascribed to the effects of MTX on epithelial proliferation and epithelial apoptosis.

MTX specifically affects enterocyte-specific genes

It is generally known that MTX, its metabolites, and the folate by-products (dihydrofolate and 10-formyldihydrofolate), which are formed by the inhibition of the enzyme dihydrofolate reductase, not only inhibit DNA synthesis, but can also inhibit *de novo* purine synthesis [23, 24]. Thus, MTX treatment can affect the synthesis of RNA and thereby the synthesis of proteins. Therefore we analyzed enterocyte -, goblet cell -, and Paneth cell specific mRNA and protein synthesis in the entire small intestine after MTX treatment by means of *in situ* hybridization and (immuno) histochemistry. We observed that the enterocyte-specific sucrase-isomaltase

(SI) -, sodium glucose transporter1 (SGLT1) -, glucosetransporter2 and -5 (Glut2 and -5) -, and i- and liver (l-)FABP expression was down-regulated in flattened villus enterocytes, both at the mRNA and protein level after MTX treatment. In contrast, the expression of the house keeping gene ß-actin and enterocyte specific AP activity was maintained after MTX treatment. These results suggest that MTX, MTX metabolites and the dihydrofolate byproducts did not completely inhibit RNA synthesis or protein synthesis in enterocytes. Moreover, data tempt us to speculate that enterocytes specifically down-regulate certain genes possibly to reduce their metabolic need, and to prepare enterocytes for a critical role in epithelial restitution and defense. Generally, the down-regulation of SI, SGLT1, Glut2 and -5, and i- and l-FABP implies enterocyte malfunctioning within the small intestine with regard to the degradation, absorption and transport of sugars and fatty acids. Tanaka *et al.* reported similar results for enterocyte-specific SI and SGLT1 expression in the small intestinal epithelium of rats treated with 5-fluorouracil [25].

Goblet cells and their gene expression is spared under MTX-induced damage

Analysis of goblet cell -specific gene expression revealed maintained Muc2 and TFF3 expression after MTX treatment, suggesting an important role for goblet cells in the defense and repair of the small intestinal mucosa after MTX. Interestingly, several days after MTX injection goblet cells accumulated at the villus tips. These data are in line with our previous study in which we showed that the goblet cells that accumulated at villus tips after MTX were selectively spared from apoptosis and extrusion [26].

Similar to goblet cells, Paneth cells maintained their capacity to express specific genes, *i.e.* lysozyme, after MTX treatment. Moreover, in a recent study we quantitated lysozyme expression levels and demonstrated a strong up-regulation of lysozyme mRNA during the first two days after MTX treatment [26]. These data in conjunction suggest that Paneth cells actively contribute to the protection of the small intestinal mucosa after MTX treatment. Finally, comparing the effects of MTX on cell type-specific gene expression, *i.e.* down-regulation of enterocyte-specific genes and maintenance of goblet cell and Paneth cell specific genes, we conclude that enterocytes are relatively sensitive to MTX treatment, whereas goblet cells and Paneth cells are less sensitive.

MTX hardly affects the epithelium near the Peyer's Patches

Intriguingly, thorough analysis revealed that there not only appears a difference in sensitivity to MTX between the various cell types, but also between the epithelium adjacent to and overlying Peyer's patches (PP) and the epithelium more distantly, *i.e.* the so called 'non-patch' (NP) epithelium (Chapter 7). Namely, the epithelial morphology up to 2-3 crypt-villus units adjacent to and overlying the PP remained relatively intact after MTX-treatment when compared to the NP epithelium. Moreover, each of the enterocyte-specific markers, *i.e.* SI, SGLT1, Glut2 and -5, and i- and l-FABP, which were down-regulated in the NP epithelium after MTX (as described in Chapter 6), were maintained in the PP epithelium. Both in the NP and PP epithelium, goblet cells and Paneth cells maintained their capacity to express Muc2,

TFF3 and lysozyme after MTX. But only in the PP epithelium, goblet cells remained normally distributed along the crypt villus axis, whereas in the NP epithelium goblet cells accumulated in the crypt and surface epithelium on day 3 and 4 after MTX-treatment. The mechanisms involved in the protection of the PP epithelium were still unidentified. Therefore, we aimed to assess the mechanism(s) responsible for the protection of the PP epithelium from morphological damage after MTX treatment. Thereto, we investigated if there were differences in epithelial proliferation and apoptosis between the NP - and PP epithelium after MTX administration.

Similar to the proliferation rate in the NP epithelium, the epithelial proliferation rate in the PP epithelium decreased from duodenum toward the ileum. The duration of MTX-induced inhibition of epithelial proliferation in PP epithelium was the longest in the duodenum, and decreased from duodenum toward the ileum, similar to changes seen in the NP epithelium. Comparing the proliferation rate between the PP and NP epithelium we observed that the proliferation rate in the PP epithelium of each intestinal region was significantly higher than in the NP epithelium. Generally, a high proliferation rate leads to high sensitivity, therefore we expected the MTX-induced inhibition of epithelial proliferation to be most pronounced in the PP epithelium. However, the opposite appeared to occur. Namely, the MTX-induced inhibition of proliferation was less pronounced, shorter in duration, or did not occur at all in the PP crypts. Similarly, in mice, the mitotic activity in the PP crypts was higher than in the NP crypts [27, 28]. Additionally, PP crypts were less sensitive for radiation and cytostatic drug-induced damage than NP crypts [27, 28]. Extra oxygen supply did not sensitize PP crypts to radiation damage. Therefore, and because of the direct connection between capillaries draining the PP follicles and the crypt plexus of PP crypts [29], we suggest that humoral factor(s) from the PP might regulate proliferation within the PP crypts resulting in differences in proliferation kinetics between the PP - and NP epithelium. Subsequently, as the PP epithelium was largely unaffected after MTX treatment compared to the NP epithelium, the humoral factor(s) which are suggested to regulate epithelial proliferation in the PP crypts conceivably also protect the PP crypts against MTX-induced damage. From this it can be concluded that not only the proliferation rate of crypt cells, but also the (micro-)environment of proliferating crypt cells determines the sensitivity of the cells toward MTX treatment.

No differences were seen in the number and position of apoptotic cells between the NP - and PP epithelium, at all timepoints investigated. However, we can not rule out that there are differences, which remained unobserved because of the experimental approach used. Namely, we studied epithelial apoptosis at 6.5 h, and at days 1-4 after MTX. As apoptosis is a very rapid process, the measurement of apoptosis at more and shorter intervals after MTX-treatment would give more insight in eventual differences in the number of apoptotic cells between the NP - and PP epithelium. These data suggest that the protection from damage of the PP epithelium after MTX treatment can be accounted for by the differences in proliferation between the NP - and PP epithelium and not, or to a lesser extent accounted by differences in epithelial apoptosis. Taken together, the retained proliferation and enterocyte-specific gene expression in the PP epithelium after MTX treatment suggest that maintenance of proliferation

is a prerequisite for unperturbed enterocyte functioning after MTX treatment. Future studies should therefore be directed toward identification of the factor(s), which control epithelial proliferation in the PP epithelium before and after MTX. Such studies might be of relevance to develop clinical therapies to protect cancer patients from intestinal damage induced by chemotherapy.

The MTX-damage model in the rat: Conclusions

In conclusion, in the second part of this thesis we have shown that MTX-induced clinical symptoms and morphological alterations in rat small intestine is comparable to clinical symptoms and morphological alterations seen in mice and in humans treated with MTX. MTX inhibited epithelial proliferation and induced epithelial apoptosis. MTX induced a down-regulation of enterocyte specific genes involved in the digestion, uptake and transport of nutrients, suggesting enterocyte malfunctioning, which account for the observed malnutrition during anti-cancer therapy. Enterocyte-specific AP activity and Paneth cell specific lysozyme expression were maintained after MTX treatment, suggesting maintenance of epithelial defense. Additionally, goblet cell specific Muc2 and TFF3 expression was preserved after MTX treatment implying an important role for goblet cells in epithelial protection and repair mechanism after MTX. Finally, the difference in MTX sensitivity between the PP and NP epithelium is, at least partially, based on the distinct proliferation kinetics of the PP.

General remarks, conclusions, and future perspectives

Damage and damage control: Comparison of the DSS-model with the MTX-model

Comparing the effects of treatment of rats with DSS or with MTX reveals several remarkable similarities concerning the characteristics of the induced intestinal damage and the control of this damage. DSS is a toxic agent that inhibits proliferation, induces apoptosis, and elicits a strong inflammatory reaction. As a consequence, DSS treatment leads to loss of crypt and surface epithelium and ulcerations. The cytostatic agent MTX primarily inhibits proliferation and induces apoptosis, leading to loss of crypts and surface epithelium. MTX does not primarily induce an inflammatory reaction. The colonic epithelium and the small intestinal epithelium respond to these alterations in several ways. There are at least 3 main points of similarity in the response of the small intestinal and colonic epithelium, respectively. **Firstly, both colonic and small intestinal damage lead to flattening of epithelial cells lining the crypts and surface cuffs/villi implying the occurrence of epithelial restitution.** It is clear that epithelial restitution is of utmost importance to both maintenance of the epithelial barrier as well as restoration of the epithelial barrier. As such epithelial restitution can be divided in two fundamental different processes: 1) flattening of cells to **maintain** the epithelial barrier and 2) flattening of cells to **restore** the epithelial barrier. Maintenance of epithelial barrier occurs during inhibition of epithelial proliferation and induction of apoptosis, before ulcers are present. This process is seen during DSS treatment and after MTX treatment. Restoration of

the epithelial barrier takes place when ulcers are present, thus at the end of and after DSS treatment. Many *in vitro* and *in vivo* studies are designed to study epithelial restitution after the induction of a wound/ulcer. Thus these studies are designed to investigate only one part of the restitution process, namely the restoration of the epithelial barrier. As maintenance of epithelial barrier and restoration of epithelial barrier are essentially different processes it is likely that different types of growth factors are involved to stimulate these processes. Therefore, we plead for the design of studies that focus on the intestinal epithelium during the maintenance of the epithelial barrier next to studies that focus on the restoration of the epithelial barrier.

The flattening of epithelial cells coincided with the down-regulation of most of the enterocyte specific differentiation markers (*i.e.* SI, SGLT1, Glut2 and –5, and i- and l-FABP in the small intestine after MTX treatment, and CA I and -IV, NHE2 and -3 and I-FABP in the colon during/after DSS treatment). We hypothesize that down-regulation of these genes/functions that are less essential for survival of the cells during/after a severe insult is programmed, *i.e.* a hardwired genetic reaction of the epithelium, to conserve energy to survival of the cells and ultimately for survival of the organism. In this way the conserved energy can be used to induce a phenotypic shift of the enterocytes to prepare them for a critical role in epithelial restitution and mucosal defense. Supportive to this hypothesis is the fact the down-regulation of the differentiation markers by MTX and DSS is gene specific, *i.e.* the genes are down-regulated in different extent and/or at different time points. Furthermore, the maintenance of AP activity by the enterocytes in both epithelial damage models also supports the hypothesis described above. Consequently, this hypothesis should be tested by studying the processes of epithelial restitution (*i.e.* flattening of cell to maintain the epithelial barrier and flattening of cell to restore the epithelial barrier) in relation to epithelial gene expression in *in vitro* and in *in vivo* epithelial damage models. Those studies can give more insights and open possibilities to manipulate these epithelial processes.

The second response of the epithelium, which occurs after colonic and after small intestinal damage, is a rapid hyper-proliferation to restore epithelial barrier function. The hyper-proliferation after an epithelial insult is most likely a general mechanism of the small intestine as well as colon to restore epithelial barrier function, because it is seen in *in vitro* epithelial wound models [30-33], in several epithelial damage models [34-36], in both of our epithelial damage models, and in patients with UC [16, 37]. In the DSS colonic damage model epithelial hyper-proliferation is seen while DSS is still administered and only in severely damaged areas (*i.e.* in crypts adjacent to ulcerations). This is fundamentally different from the small intestinal damage induced by MTX, where hyper-proliferation is equally distributed along the entire epithelium.

The third response of the colonic and small intestinal epithelium to damage is maintenance of goblet cell-specific Muc2 and TFF3 expression after damage. Moreover, goblet cells accumulated in the surface/villus epithelium and/or in the crypts during/after DSS treatment and after MTX treatment. This indicates that goblet cells are selectively spared from apoptosis and extrusion and that epithelial cells preferentially differentiate along the goblet

cell lineage after severe epithelial damage. Supportive to this theory is the observed goblet cell accumulation/hyperplasia in the small intestine of nematode-infected mice and in rats treated with a zinc-deficient diet [38, 39]. Hence future studies should focus on factors regulating goblet cell differentiation.

As a consequence of the goblet cell accumulation in the surface/villus epithelium and/or the crypts during/after DSS treatment and after MTX treatment, the expression levels of goblet cell-specific Muc2 and TFF3 are maintained or even up-regulated. These data imply that goblet cells and in particular Muc2 and TFF3 are of critical importance to control and/or restore epithelial damage induced by DSS and MTX. That TFF3 has an important role in epithelial migration and the processes of epithelial restitution is clear. Namely, in the HT29 colonic carcinoma cell line recombinant TFF3 application resulted in perturbation of intracellular adhesion, and promotion of cell motility [40]. In TFF3 deficient mice migration of epithelial cells up the crypt is decreased [12]. Moreover, TFF3 deficient mice are more susceptible to DSS treatment and display impaired mucosal healing and manifested poor epithelial regeneration after DSS treatment [12]. Recently, it was reported that transgenic mice that overexpress rat TFF3 in the jejunum have reduced villus atrophy after indomethacin treatment compared to wild type mice [41]. This reduction of villus atrophy in TFF3 transgenic mice after indomethacin treatment was not related to effects of rat TFF3 on epithelial proliferation, migration or apoptosis. Taken together these data show that TFF3 plays a key role in epithelial protection and repair.

It is generally accepted that Muc2 plays a significant role in epithelial protection, yet studies proving this were lacking till the beginning of this year. The recently generated Muc2 deficient mouse opens the possibilities to test agents like MTX and DSS to clarify the exact role of Muc2 in epithelial protection in the small intestine and colon. Preliminary results indicate that the Muc2 deficient mice are indeed more susceptible to DSS treatment than their wild type littermates [42]. Moreover, because Muc2 deficient mice still express TFF3, this model gives the opportunity to study the role of TFF3 in epithelial protection apart from the combined protective effect of TFF3 and Muc2 as studied in wild type animals.

In summary, we conclude that both the small intestine and colon have at least 3 specific mechanisms to control epithelial damage after an insult: 1) epithelial restitution concomitant with down-regulation of most of the enterocyte-specific differentiation markers and maintenance/up-regulation of epithelial defense, 2) epithelial hyper-proliferation, 3) maintenance of goblet cell-specific Muc2 and TFF3 expression after damage in combination with goblet cell sparing and preferential differentiation into goblet cells. These epithelial responses after an intestinal insult are most likely genetically hardwired responses for survival of the intestine and ultimately for the survival of the organism. In other words the evolution has led to a 'concerted' reactions of the intestine after an epithelial insult, that together lead to the best result, *i.e.* survival of the organism.

References

1. Okayasu I, Hatakeyama S, Yamada M, Ohkusa T, Inagaki Y, Nakaya R. A novel method in the induction of reliable experimental acute and chronic ulcerative colitis in mice. Gastroenterology 1990;98:694-702.

2. Hamilton SR. Diagnosis and comparison of ulcerative colitis and Crohn's disease involving the colon. Churchill Livingstone, 1983.

3. Dieleman LA, Palmen MJ, Akol H, Bloemena E, Pena AS, Meuwissen SG, Van Rees EP. Chronic experimental colitis induced by dextran sulphate sodium (DSS) is characterized by Th1 and Th2 cytokines [In Process Citation]. Clin Exp Immunol 1998;114:385-91.

4. Tessner TG, Cohn SM, Schloemann S, Stenson WF. Prostaglandins prevent decreased epithelial cell proliferation associated with dextran sodium sulfate injury in mice. Gastroenterology 1998;115:874-82.

5. Poelstra K, Bakker WW, Klok PA, Kamps JA, Hardonk MJ, Meijer DK. Dephosphorylation of endotoxin by alkaline phosphatase in vivo. Am J Pathol 1997;151:1163-9.

6. Poelstra K, Bakker WW, Klok PA, Hardonk MJ, Meijer DK. A physiologic function for alkaline phosphatase: endotoxin detoxification. Lab Invest 1997;76:319-27.

7. Geibel JP, Rajendran VM, Binder HJ. Na(+)-dependent fluid absorption in intact perfused rat colonic crypts. Gastroenterology 2001;120:144-50.

8. Rajendran VM, Geibel J, Binder HJ. Characterization of apical membrane Cl-dependent Na/H exchange in crypt cells of rat distal colon. Am J Physiol Gastrointest Liver Physiol 2001;280:G400-5.

9. Jacob P, Rossmann H, Lamprecht G, Kretz A, Neff C, Lin-Wu E, Gregor M, Groneberg DA, Kere J, Seidler U. Down-regulated in adenoma mediates apical Cl-/HCO3- exchange in rabbit, rat, and human duodenum. Gastroenterology 2002;122:709-24.

10. Fonti R, Latella G, Caprilli R, Frieri G, Marcheggiano A, Sambuy Y. Carbonic anhydrase I reduction in colonic mucosa of patients with active ulcerative colitis. Dig Dis Sci 1998;43:2086-92.

11. Tytgat KMAJ, van der Wal JW, Einerhand AWC, Büller HA, Dekker J. Quantitative analysis of MUC2 synthesis in ulcerative colitis. Biochem Biophys Res Commun 1996;224:397-405.

12. Mashimo H, Wu DC, Podolsky DK, Fishman MC. Impaired defense of intestinal mucosa in mice lacking intestinal trefoil factor. Science 1996;274:262-5.

13. Van Klinken BJW, Van der Wal JW, Einerhand AWC, Büller HA, Dekker J. Sulphation and secretion of the predominant secretory human colonic mucin MUC2 in ulcerative colitis. Gut 1999;44:387-93.

14. Nieuw Amerongen AV, Bolscher JG, Bloemena E, Veerman EC. Sulfomucins in the human body. Biol Chem 1998;379:1-18.

15. Riddell RH. Pathology of idiopatic inflammatory bowel diseases. In: Kirsner JB, Shorter RG, eds. Inflammatory Bowel Diseases. Philadelphia: Lea Febiger, 1988:329-350.

16. Arai N, Mitomi H, Ohtani Y, Igarashi M, Kakita A, Okayasu I. Enhanced epithelial cell turnover associated with p53 accumulation and high p21WAF1/CIP1 expression in ulcerative colitis. Mod Pathol 1999;12:604-11.

17. Iwamoto M, Koji T, Makiyama K, Kobayashi N, Nakane PK. Apoptosis of crypt epithelial cells in ulcerative colitis. J Pathol 1996;180:152-9.

18. Strater J, Wellisch I, Riedl S, Walczak H, Koretz K, Tandara A, Krammer PH, Moller P. CD95 (APO-1/Fas)-mediated apoptosis in colon epithelial cells: a possible role in ulcerative colitis [see comments]. Gastroenterology 1997;113:160-7.

19. Taminiau JA, Gall DG, Hamilton JR. Response of the rat small-intestine epithelium to methotrexate. Gut 1980;21:486-92.

20. Devik F, Hagen S. Effects of X-rays and cytotoxic agents on the cell population of the crypts of the small intestine in mice. Cell proliferation kinetics after single administrations and effects of variations in multiple dose schedules. Virchows Arch B Cell Pathol 1973;12:223-37.

21. Altmann GG. Changes in the mucosa of the small intestine following methotrexate administration or abdominal x-irradiation. Am J Anat 1974;140:263-79.

22. Pinkerton CR, Cameron CH, Sloan JM, Glasgow JF, Gwevava NJ. Jejunal crypt cell abnormalities associated with methotrexate treatment in children with acute lymphoblastic leukaemia. J Clin Pathol 1982;35:1272-7.

23. Allegra JA. Antifolates. In: Chabner BA, Collins JM, eds. Cancer chemotherapy: Principles and Practice. Philadelphia: Lippincott, 1990:110-153.

24. Kamen BA, Cole PD, Bertino JR. Chemotherapeutic Agents: Folate Antagonists. In: Bast Jr. RC, Kufe DW, Pollock RE, Weichselbaum RR, Holland JF, Frei E, eds. Cancer Medicine. 5 ed. Hamilton: B. C. Decker INc., 2000.

25. Tanaka H, Miyamoto KI, Morita K, Haga H, Segawa H, Shiraga T, Fujioka A, Kouda T, Taketani Y, Hisano S, Fukui Y, Kitagawa K, Takeda E. Regulation of the PepT1 peptide

transporter in the rat small intestine in response to 5-fluorouracil-induced injury. Gastroenterology 1998;114:714-23.

26. Verburg M, Renes IB, Meijer HP, Taminiau JA, Büller HA, Einerhand AWC, Dekker J. Selective sparing of goblet cells and paneth cells in the intestine of methotrexate-treated rats. Am J Physiol Gastrointest Liver Physiol 2000;279:G1037-47.

27. Maunda KK, Moore JV. Radiobiology and stathmokinetics of intestinal crypts associated with patches of Peyer. Int J Radiat Biol Relat Stud Phys Chem Med 1987;51:255-64.

28. Moore JV, Maunda KK. Topographic variations in the clonogenic response of intestinal crypts to cytotoxic treatments. Br J Radiol 1983;56:193-9.

29. Bhalla DK, Murakami T, Owen RL. Microcirculation of intestinal lymphoid follicles in rat Peyer's patches. Gastroenterology 1981;81:481-91.

30. Dignass AU, Lynch-Devaney K, Podolsky DK. Hepatocyte growth factor/scatter factor modulates intestinal epithelial cell proliferation and migration. Biochem Biophys Res Commun 1994;202:701-9.

31. Dignass AU, Tsunekawa S, Podolsky DK. Fibroblast growth factors modulate intestinal epithelial cell growth and migration. Gastroenterology 1994;106:1254-62.

32. Dignass AU. Mechanisms and modulation of intestinal epithelial repair. Inflamm Bowel Dis 2001;7:68-77.

33. Jung S, Fehr S, Harder-d'Heureuse J, Wiedenmann B, Dignass AU. Corticosteroids impair intestinal epithelial wound repair mechanisms in vitro. Scand J Gastroenterol 2001;36:963-70.

34. Artis D, Potten CS, Else KJ, Finkelman FD, Grencis RK. Trichuris muris: host intestinal epithelial cell hyperproliferation during chronic infection is regulated by interferon-gamma. Exp Parasitol 1999;92:144-53.

35. Huang FS, Kemp CJ, Williams JL, Erwin CR, Warner BW. Role of epidermal growth factor and its receptor in chemotherapy-induced intestinal injury. Am J Physiol Gastrointest Liver Physiol 2002;282:G432-42.

36. Potten CS, Owen G, Roberts SA. The temporal and spatial changes in cell proliferation within the irradiated crypts of the murine small intestine. Int J Radiat Biol 1990;57:185-99.

37. Ierardi E, Principi M, Francavilla R, Passaro S, Noviello F, Burattini O, Francavilla A. Epithelial proliferation and ras p21 oncoprotein expression in rectal mucosa of patients with ulcerative colitis. Dig Dis Sci 2001;46:1083-7.

38. Garside P, Grencis RK, Mowat AM. T lymphocyte dependent enteropathy in murine Trichinella spiralis infection. Parasite Immunol 1992;14:217-25.

39. Nobili F, Vignolini F, Figus E, Mengheri E. Treatment of rats with dexamethasone or thyroxine reverses zinc deficiency-induced intestinal damage. J Nutr 1997;127:1807-13.

40. Liu D, el-Hariry I, Karayiannakis AJ, Wilding J, Chinery R, Kmiot W, McCrea PD, Gullick WJ, Pignatelli M. Phosphorylation of beta-catenin and epidermal growth factor receptor by intestinal trefoil factor. Lab Invest 1997;77:557-63.

41. Marchbank T, Cox HM, Goodlad RA, Giraud AS, Moss SF, Poulsom R, Wright NA, Jankowski J, Playford RJ. Effect of ectopic expression of rat trefoil factor family 3 (intestinal trefoil factor) in the jejunum of transgenic mice. J Biol Chem 2001;276:24088-96.

42. Van der Sluis M, Makkink MK, Sutmuller M, Büller HA, Dekker J, Augenlight LH, Velcich A, Einerhand AWC. MUC2 mucin Knockout mice are more susceptible to dextran sodium sulfate-induced colitis. Gastroenterology suppl; P194, T946.

Chapter 9

Samenvatting

Samenvatting

Het epitheel van dunne en dikke darm

In dit proefschrift zijn de effecten van het cytostaticum methotrexaat (MTX) en van de toxische stof dextraan sulfaat sodium (DSS) op het epitheel van respectievelijk de dunne en dikke darm beschreven. Het epitheel in zowel de dunne als de dikke darm heeft verschillende fysiologische functies, zoals de vertering en opname van voedingsstoffen, opname van ionen en water en bescherming tegen pathogenen, toxische stoffen en noxische stoffen. Hiertoe beschikt het epitheel over gespecialiseerde celtypen, die ontstaan uit stamcellen gelegen in de intestinale crypten. De gespecialiseerde cellen die worden beschreven in dit proefschrift zijn: enterocyten, gobletcellen (*i.e.* slijmbekercellen) en Paneth cellen.

Enterocyten in de dunne darm vervullen een centrale rol in de vertering, opname en transport van voedingstoffen, en produceren daartoe o.a. het enzym sucrase-isomaltase (SI), de natrium-glucose co-transporter 1 (SGLT1), glucose en fructose transporters 2 en –5 (Glut2 en –5) en de vetzuur-bindende eiwitten, fatty acid binding proteins (FABPs). In de dikke darm spelen enterocyten een rol in de opname van ionen en water waarvoor zij o.a. carbonic anhydrase I en -IV (CA I en -IV) en natrium waterstof transporter 2 en 3 (NHE2 en -3) tot expressie brengen. Daarnaast produceren enterocyten in de dunne darm en dikke darm het enzym alkalische fosfatase (AP), dat van belang is voor de detoxificatie van endotoxinen.

Gobletcellen zijn aanwezig in het dunne en dikke darmepitheel en produceren o.a. het secretoire mucine Muc2 en trefoil-peptide family factor 3 (TFF3). Muc2 is de structurele component van de beschermende slijmlaag. TFF3 speelt een voorname rol in epitheliale restitutie en induceert herstel van het epitheel na schade. Paneth cellen komen alleen voor in de dunne darm en produceren o.a. lysozym dat een belangrijk anti-bacteriële werking heeft.

Mucinen, het darmepitheel, inflammatoire darmziekten en experimentele colitis

De etiologie van de inflammatoire darmziekten, colitis ulcerosa (CU) en de ziekte van Crohn, is tot nu toe onbekend. Wel is het duidelijk dat deze ziekten mede veroorzaakt worden door verscheidene omgevings en genetische factoren zoals, 1) het immuun systeem, 2) microbiële factoren, en 3) de epitheliale barrière van de darm. Deze epitheliale barrière van de darm wordt gevormd door het epitheel en de daarmee geassocieerde slijmlaag. Mucinen worden gemaakt door het epitheel en zijn de bouwstenen van de slijmlaag. De dikte en beschermende eigenschappen van de slijmlaag worden dan ook bepaald door mucinen. Mogelijk zouden veranderingen in de structuur van en/of de expressie niveaus van mucinen een etiologische factor kunnen zijn in de pathogenese van IBD. In hoofdstuk 2 wordt de rol van het epitheel en de daarmee geassocieerde slijmlaag in IBD en in verscheidende experimentele colitis modellen bediscussieerd.

Recent is aangetoond dat, van de tot nu toe bekende mucinen (e.g. MUC1-2, MUC3A-B, MUC4, MUC5B-AC, MUC6-18), IBD geassocieerd is met genetische varianten van het membraan gebonden mucine MUC3A [1]. Het hebben van 1 of 2 allelen van het MUC3A gen met een afwijkend aantal 51-bp repeat eenheden is geassocieerd met colitis

ulcerosa. Genetische predispositie voor de ziekte van Crohn is gekoppeld aan nucleotide polymorfisme in de C-terminus van MUC3A [2]. In geen van de tot nu toe bekende andere mucine genen zijn mutaties of afwijkingen in allelen gevonden die gekoppeld zijn aan colitis ulcerosa of de ziekte van Crohn. Omdat MUC2 het meest prominente secretoire mucine is in de darm [3], is er in het bijzonder gezocht naar allel variaties in het MUC2 gen [4]. Er kon echter geen link worden gelegd met CU. Echter de biosynthese, de secretie en de sulfatering van MUC2 zijn sterk afgenomen in de actieve fase van CU [5, 6]. Dit impliceert dat de mucosale bescherming tijdens actieve CU is afgenomen. In experimentele colitis blijken er ook sterke veranderingen op te treden in de biosynthese, secretie en sulfatering van MUC2 [7]. Bovendien blijken cytokinen, enterale bacteriën en bacteriële componenten de synthese, secretie en sulfatering van MUC2 in cellijnen aanzienlijk te kunnen beïnvloeden [8-12]. Dit suggereert dat MUC2 een belangrijke rol speelt in de pathogenese van CU en in experimentele colitis-modellen.

DSS-geïnduceerde colitis: effecten op morfologie en epitheliale homeostase

De inductie van CU gaat in het algemeen niet gepaard met specifieke symptomen. Wanneer patiënten zich melden bij de arts is deze ziekte vaak in een gevorderd stadium en spreken we over actieve CU. Om de verschillende fasen van de ziekte, inclusief de inductie fase, te kunnen bestuderen hebben we gekozen om het DSS-geïnduceerde colitis model voor onze studies te gebruiken. In hoofdstuk 3 zijn de effecten van de toxische stof DSS op de dikke darm van de rat beschreven. De DSS-geïnduceerde colitis in de rat is gekarakteriseerd met betrekking tot klinische symptomen en het effect op het epitheel gedurende verschillende fases van de ziekte. DSS induceerde een afname van het lichaamsgewicht, dunne ontlasting, diarree en bloed in de ontlasting. Morfologisch hebben we de DSS-geïnduceerde colitis verdeeld in 3 fasen: 1) *inductie van de ziekte*, gekarakteriseerd door afplatting van crypt cellen, crypt atrofie en verdwijnen van crypten, 2) *actieve colitis*, gekarakteriseerd door verlies van crypten en oppervlakte epitheel en afplatting van oppervlakte epitheel, 3) *de regeneratie fase* gekarakteriseerd door crypt verlenging en re-epithelialisatie van de oppervlakte mucosa. DSS-geïnduceerde colitis is focaal en het distale colon is het sterkst aangedaan. In muizen behandeld met DSS en in patiënten met IBD treden vergelijkbare klinische symptomen en pathologische veranderingen aan het darmepitheel op.

De primaire actie van DSS op het epitheel is remming van de proliferatie en inductie van apoptose (geprogrammeerde celdood, Hoofdstuk 3), waardoor de epitheliale homeostase wordt verstoord. Het epitheel reageert hier op middels hyperproliferatie en afplatting van de cellen, *i.e.* epitheliale restitutie. Deze data impliceren dat herstel van de epitheliale barrière functie van primair belang is gedurende DSS-colitis. Bovendien is ook in patiënten met CU een toename van epitheliale proliferatie en apoptose waargenomen.

Effecten van DSS op enterocyt functies

Naast de effecten van DSS op de morfologie en de homeostase van het epitheel hebben we ons gericht op de bestudering van de effecten van DSS op de enterocyt-specifieke functies

(Hoofdstukken 3 en 4). Enterocyt-specifieke CA I en -IV, NHE2 en -3 expressie is bepaald als parameter voor water – en ion transport, intestinale (i-) FABP expressie als parameter voor vet opname/transport en AP activiteit als maat voor mucosale afweer. DSS behandeling induceerde een afname van CA I, -IV, NHE2, -3 en i-FABP expressie in enterocyten met een normale morfologie en in afgeplatte enterocyten. Dit suggereert een afname van specifieke enterocyt functies vòòr en gedurende epitheliale restitutie. Echter, AP activiteit bleef gehandhaafd en was onafhankelijk van enterocyt morfologie in elk van de DSS-geïnduceerde ziektefasen. Dit is een aanwijzing dat de mucosale afweer capaciteit van de mucosa gehandhaafd blijft gedurende DSS-colitis.

Kwantitatieve analyses op mRNA en eiwit niveau lieten ook een afname van CA I, -IV, NHE2, -3 en i-FABP in het proximale en distal colon zien. Dit laatste impliceert een defect in water en ion transport. Omdat DSS-colitis gepaard gaat met diarree suggereren deze data bovendien een kritische rol voor CA I, -IV, NHE2 en NHE3 in de DSS-geïnduceerde diarree.

Effecten van DSS op gobletcel functies: epitheliale bescherming en herstel

In hoofdstuk 3 en 4 zijn de gobletcel-specifieke functies tijdens DSS-colitis bestudeerd aan de hand van Muc2 en TFF3 expressie. Hierbij is Muc2 gebruikt als parameter voor epitheliale bescherming en TFF3 als parameter voor epitheliale herstel en restitutie. Ondanks de afplatting van het epitheel gedurende DSS-colitis blijven zowel Muc2 als TFF3 mRNA en eiwit expressie gehandhaafd. Muc2- en TFF3-positieve goblet cellen accumuleren in het oppervlakte epitheel gedurende elk van de DSS-geïnduceerde ziektefasen. TFF3, dat normaal in het bovenste deel van de crypten tot expressie komt, wordt gedurende actieve colitis zelfs gezien in de goblet cellen onder in de crypten. Gedurende de regeneratie fase blijken Muc2- en TFF3-positieve goblet cellen te accumuleren in de crypten. Deze data suggereren dat de bescherming en herstel van het epitheel, door respectievelijk Muc2 en TFF3, gehandhaafd blijven. Echter, zoals reeds is aangeven in hoofdstuk 2, 3 en 4, blijkt DSS behandeling ook het verlies van crypten en oppervlakte epitheel cellen te induceren.

Gezien het bovenstaande hebben we in hoofdstuk 3 en 4 naast Muc2 en TFF3 expressie niveaus de mate van epitheel verlies geanalyseerd. Tijdens iedere fase van de DSS-geïnduceerde colitis was de Muc2 en TFF3 expressie gehandhaafd of zelfs verhoogd, met name in het proximale colon. Afhankelijk van de mate van het DSS-geïnduceerde epitheel verlies waren Muc2 en TFF3 niveaus ofwel licht verlaagd (zoals in hoofdstuk 3) ofwel gehandhaafd (zoals in hoofdstuk 4) gedurende actieve colitis in het distale colon. Deze schijnbare tegenstrijdigheid kan worden verklaard door het verschil in de mate van DSS-geïnduceerde epitheel verlies tussen de 2 onafhankelijke experimenten (*i.e.* ~50% epitheel verlies in het experiment beschreven in hoofdstuk 3 ten opzichte van 40% epitheel verlies in het experiment beschreven in hoofdstuk 4). Deze gegevens geven geen uitsluitsel over veranderingen in het relatieve aantal goblet cellen gedurende DSS-colitis. Deze data geven echter wel aan dat de individuele goblet cellen die aanwezig blijven gedurende DSS-colitis, in

staat zijn om het verlies van epitheel/ goblet cellen, en dus van Muc2 en TFF3 expressie, tot op zekere hoogte te compenseren.

Muc2 en TFF3 zijn beide secretoire producten en worden dus gesecreteerd om hun functie te kunnen uitoefenen. Daarom is in hoofdstuk 4 de *ex vivo* secretie van Muc2 en TFF3 bepaald. In zowel het proximale als distale colon was het percentage Muc2 secretie gehandhaafd gedurende iedere fase van DSS-colitis. Het percentage TFF3 secretie bleek progressief toe te nemen gedurende iedere fase van DSS-geïnduceerde colitis in het proximale en distale colon. In samenhang met de handhaving van Muc2 en TFF3 mRNA en eiwit expressie niveaus door goblet cellen duiden deze data op handhaving van de goblet cel specifieke functies. Daarnaast suggereren deze data dat de epitheliale bescherming mogelijk wordt gehandhaafd en dat de capaciteit tot herstel/ restitutie van het epitheel toeneemt tijdens DSS-geïnduceerde schade.

Effecten van DSS op Muc2 biosynthese en structuur

Zoals reeds is beschreven in hoofdstuk 1 is de biosynthese, secretie en sulfatering van MUC2 afgenomen in patiënten met actieve colitis. In hoofdstuk 5 hebben we dan ook de biosynthese, secretie en sulfatering van Muc2 in DSS-geïnduceerde colitis geanalyseerd. In het proximale colon nam de Muc2 precursor synthese progressief toe gedurende de inductie fase en de actieve fase van DSS-colitis. Tijdens de regeneratie fase normaliseerde de Muc2 precursor synthese. In het distal colon was de Muc2 precursor synthese gehandhaafd tijdens de inductie en de actieve fase, terwijl deze toenam gedurende de regeneratie fase. Veranderingen in totale Muc2 expressie niveaus tijdens DSS-geïnduceerde colitis liepen parallel aan de veranderingen in Muc2 precursor synthese niveaus. Bovendien, bleef het percentage van Muc2 niveaus gehandhaafd in het proximale en distal colon gedurende iedere fase van DSS-colitis. Deze gegevens suggereren dat de bescherming van het epitheel en dus de barrière functie intact blijven in DSS-colitis.

Analyse van sulfaat incorporatie in Muc2 en secretie van gesulfateerd Muc2 laat zien dat de sulfaat incorporatie in Muc2 in het proximale colon afnam tijdens DSS colitis, terwijl de secretie van gesulfateerd Muc2 juist toenam. Dit impliceert dat gesulfateerd Muc2 preferentieel gesecreteerd wordt. Deze data suggereren dat de structuur van Muc2 verandert tijdens DSS colitis en dat mogelijk de beschermende capaciteit van Muc2 verandert. In het distale colon bleken deze veranderingen niet op te treden. Het uiteindelijke effect van de sulfateringsveranderingen van Muc2 tijdens DSS-geinduceerde colitis zal nader bestudeerd moeten worden.

DSS-geïnduceerde colitis in de rat: Conclusies

In het eerste deel van dit proefschrift hebben we laten zien dat DSS-geïnduceerde colitis sterke overeenkomsten vertoont met CU in patiënten wat betreft morfologische veranderingen, epitheliale proliferatie en apoptose. DSS bleek primair de epitheliale proliferatie te remmen en apoptose te induceren. Het epitheel reageerde hierop door middel van epitheliale hyperproliferatie en restitutie. DSS behandeling leidde tot een afname van de expressie van

genen betrokken bij water en ion transport en vetzuur opname/ transport. Echter, de enterocyt specifieke AP activiteit bleef gehandhaafd tijdens DSS-colitis, hetgeen suggereert dat de mucosale afweer intact blijft. De goblet cel-specifieke genen die van belang zijn in epitheliale bescherming en restitutie, in het bijzonder Muc2 en TFF3, bleven gehandhaafd of namen zelfs toe in DSS-colitis. Tot slot, DSS behandeling resulteerde in een afname van Muc2 sulfatering en een preferentiële secretie van gesulfateerd Muc2, dit zal mogelijk implicaties kunnen hebben voor de beschermende capaciteit van de slijmlaag.

MTX behandeling: Klinische symptomen en morfologische veranderingen
In het 2e deel van dit proefschrift zijn de effecten van het cytostaticum MTX op de morfologie, proliferatie, apoptose, en functies van het dunne darm epitheel in de rat beschreven (hoofdstukken 6 en 7). MTX behandeling leidde tot afname van het lichaamsgewicht, dunne ontlasting en milde diarree (Hoofdstuk 6). Morfologische analyse van het epitheel na MTX behandeling toonde verlies van crypten en crypt - en villus atrofie, dat gepaard ging met afplatting van epitheel cellen in de crypten en op de villi. Vergelijkbare klinische symptomen en morfologische veranderingen treden ook op in muizen en patiënten die worden behandeld met cytostatica.

Effecten van MTX op epitheliale proliferatie en apoptose
Het is algemeen bekend dat MTX aangrijpt op prolifererende cellen en apoptose kan induceren. In het MTX rat model is het effect van MTX op de epitheliale proliferatie en apoptose in de dunne darm beschreven (Hoofdstuk 6). In de normale (onbehandelde) dunne darm neemt de proliferatie van het epitheel af vanaf duodenum in de richting van het ileum. De gevoeligheid van weefsel voor cytostatica is primair afhankelijk van de proliferatie snelheid, d.w.z. een hoge proliferatie snelheid leidt tot een hoge gevoeligheid. Het is dus zeer aannemelijk dat de MTX-geïnduceerde remming van proliferatie het sterkst tot uiting komt in het duodenum. Inderdaad bleek dat de duur van proliferatie remming het langst was in het duodenum en dat dit afnam in de richting het ileum. In elk segment van de dunne darm werd de MTX-geïnduceerde remming van epitheliale proliferatie gevolgd door een toename van proliferatie en in het ileum zelfs door hyperproliferatie.

Naast de effecten op proliferatie bleek MTX ook apoptose te induceren in het dunne darmepitheel. Er werden geen verschillen gevonden in het aantal apoptotische cellen tussen het duodenum, jejunum en ileum. Het is echter mogelijk dat er subtiele verschillen zijn in het aantal apoptotische cellen tussen de verschillende intestinale segmenten, maar dat we deze subtiele verschillen niet hebben gedetecteerd vanwege de opzet van de experimenten en de detectie methode. In het algemeen kunnen we de MTX-geïnduceerde schade (morfologische veranderingen) onder andere toeschrijven aan de effecten van MTX op epitheliale proliferatie en apoptose.

Effecten van MTX op enterocyt functies

Naast het effect van MTX op DNA synthese, kunnen MTX, MTX metabolieten en de folaat producten die ontstaan bij de remming van het enzym dihydrofolaat reductase ook de *de novo* purine synthese remmen. Dit kan weer leiden tot de remming van zowel RNA als eiwit synthese. In hoofdstuk 6 hebben we dan ook de enterocyt specifieke functies bestudeerd na MTX toediening. Als parameters voor enterocyt functie(s) is de expressie van SI, SGLT1, Glut2 en –3, i- en l-FABP bepaald op RNA en eiwit niveau. Hiernaast is de AP activiteit bepaald als component van de mucosale afweer. MTX induceerde een afname van SI, SGLT1, Glut2 en –5 en i- en l-FABP expressie op zowel mRNA als eiwit niveau in de afgeplatte villus enterocyten. AP activiteit en ß-actine mRNA expressie bleven echter gehandhaafd. Deze data impliceren dat enterocyten de transcriptie van bepaalde genen specifiek kunnen remmen en dat in de enterocyt functies met betrekking tot de opname en transport van voedingsstoffen verstoord zijn na MTX behandeling. Aangezien de AP activiteit behouden bleef na MTX behandeling is het aannemelijk dat deze component van de mucosale afweer intact blijft na MTX.

Effecten van MTX op goblet cel en Paneth cel functies

In hoofdstuk 6 zijn de goblet cel en Paneth cel specifieke functies bestudeerd tijdens MTX-geïnduceerde schade in de dunne darm van de rat. Als parameter voor goblet cel functies is de expressie van Muc2 en TFF3 geanalyseerd. Lysozym fungeerde als maat voor Paneth cel functie. Na MTX behandeling behielden gobletcellen de capaciteit om Muc2 en TFF3 mRNA en eiwit tot expressie te brengen. Vanwege de rol van Muc2 en TFF3 in respectievelijk epitheliale bescherming en restitutie concluderen we dat deze goblet cel functies van cruciaal belang zijn na MTX behandeling.

Ook Paneth cellen bleken hun capaciteit met betrekking tot lysozym mRNA en eiwit expressie te behouden na MTX behandeling. Bovendien leek het aantal Paneth cellen en de expressie van lysozym toe te nemen. Deze gegevens suggereren dat na MTX behandeling de Paneth cell functie met betrekking tot de mucosale bescherming toeneemt.

Effecten van MTX op het epitheel geassocieerd met de Peyerse plaat

In de mucosa van de dunne darm zijn zogenaamde Peyerse platen (PPs; mucosale lymfeknopen) aanwezig. De morfologie van het dunne darmepitheel geassocieerd met PPs, *i.e.* 2-3 crypt villus eenheden naast de PP, leek gespaard te blijven na MTX behandeling (Hoofdstuk 7). Om inzicht te krijgen in het mechanisme die de MTX-geïnduceerde schade voorkomt in het PP-geassocieerde epitheel werd de epitheliale proliferatie en apoptose bestudeerd en vergeleken met die van het normale, 'non-PP-geassocieerde' epitheel. Voor en na MTX behandeling bleek de proliferatie van het PP-epitheel hoger dan in het non-PP-epitheel. Inhibitie van epitheliale proliferatie na MTX bleek niet of in mindere mate op te treden in het PP-epitheel. MTX induceerde een toename van apoptose in zowel het PP- en non-PP-epitheel, er werden echter geen verschillen in het aantal apoptotische cellen gevonden in deze

afzonderlijke epithelia. De bescherming van het PP-epitheel lijkt dus voornamelijk te zijn gebaseerd op verschil in proliferatie tussen het PP- en non-PP epitheel.

Epitheliale functies, d.w.z. enterocyt - , goblet cel - en Paneth cel functies, werden geanalyseerd om de mate van bescherming van het PP-epitheel te kunnen bepalen. De expressie van enterocyt markers SI, SGLT1, Glut2 en -5 en i- en l-FABP handhaafden zich in het PP-epitheel, maar namen sterk af in het non-PP epitheel. Deze data duiden erop dat de enterocyt functies na MTX behouden blijven in het PP-epitheel, maar niet in het non-PP-epitheel. Tot nu toe is/zijn de factor(en) die een rol spelen bij de handhaving van proliferatie en enterocyt functies in het PP-epitheel na MTX behandeling onbekend. De expressie van de goblet cel specifieke markers, Muc2 en TFF3, en de Paneth cel marker lysozym bleven na MTX toediening gehandhaafd in het PP- en het non-PP-epitheel. Dit betekent dat de epitheliale beschermings -, restitutie capaciteit en de mucosale afweer gehandhaafd blijven in zowel het PP-epitheel als het non-PP-epitheel.

Effecten van MTX op het darmepitheel: Conclusies

In het tweede deel van dit proefschrift hebben we weergegeven dat de MTX-geïnduceerde klinische symptomen en morfologische veranderingen vergelijkbaar zijn met de klinische symptomen en morfologische veranderingen in muizen en patiënten die behandeld worden met cytostatica. MTX induceerde een inhibitie van proliferatie en induceerde apoptose in het epitheel van de dunne darm. MTX behandeling resulteerde in een afname van enterocyt specifieke genen die betrokken zijn bij de digestie, opname en transport van voedingsstoffen. Enterocyt specifieke AP activiteit en Paneth cel specifiek lysozym expressie bleef gehandhaafd na MTX toediening. Dit suggereert dat de mucosale bescherming behouden blijft na MTX. Handhaving van goblet cell-specifieke Muc2 en TFF3 expressie impliceert dat goblet cellen een belangrijke rol spelen bij de bescherming en inductie van herstel na MTX behandeling. Het verschil in gevoeligheid voor MTX tussen het PP- en non-PP-epitheel is in ieder geval deels gebaseerd op de specifieke proliferatie kinetiek van het PP-epitheel. De identificatie van factor(en) die betrokken zijn bij bescherming van het PP-epitheel zal waarschijnlijk van belang kunnen zijn voor de ontwikkeling van therapieën ter bescherming van het darmepitheel na cytostatica toediening.

Schade en schade beperking: vergelijk van het DSS model met het MTX model

In hoofdstuk 8 is de respons van het epitheel op de DSS-geïnduceerde schade aan het colon vergeleken met de MTX-geïnduceerde schade aan de dunne darm. Zowel MTX behandeling als DSS behandeling induceert remming van epitheliale proliferatie. Daarnaast leidt DSS behandeling tot het ontstaan van ulcers. Om de schade te beperken en herstel te initiëren beschikt het colon en de dunne dunne darm over 3 specifieke mechanismen:

1) Afplatting van epitheel cellen gepaard gaande met **a)** verlies van specifieke enterocyt-functies door middel van afname van expressie niveaus van enterocyt-specifieke genen (*i.e.* SI, SGLT1, Glut2, Glut5, i-FABP en l-FABP in de dunne darm na MTX behandeling en CA

I, CA IV, NHE2, NHE3 en I-FABP in het colon tijdens en na DSS behandeling) en **b)** handhaving van epitheliale bescherming (d.w.z. handhaving van het enterocyt-specifieke AP activiteit).

2) Hyper-proliferatie van het epitheel.

3) Handhaving of zelfs verhoging van de epitheliale bescherming en herstel door middel van **a)** handhaving van Muc2 en TFF3 expressie door goblet cellen tijdens iedere fase van DSS- en MTX-geïnduceerde schade en **b)** selectieve sparing van goblet cellen en preferentiële differentiatie tot goblet cellen na schade inductie. Deze beide aspecten (3a en b) leiden tot handhaving of zelfs verhoging van Muc2 en TFF3 expressie niveaus.

In deze 2 fundamenteel verschillende schade modellen treden dus vergelijkbare epitheliale responsen op om de darmschade te beperken en herstel te initiëren. Deze epitheliale responsen zijn wellicht ingeprinte reacties in zowel de dunne darm als het colon, om de darm en daarmee het organisme te laten overleven in geval van darmschade. Een verdere ontrafeling van de betrokken mechanismen zijn van essentieel belang om de darmschade die optreedt bij CU en chemotherapie wellicht in de toekomst te kunnen beperken/voorkomen.

Referenties

1. Kyo K, Parkes M, Takei Y, Nishimori H, Vyas P, Satsangi J, Simmons J, Nagawa H, Baba S, Jewell D, Muto T, Lathrop GM, Nakamura Y. Association of ulcerative colitis with rare VNTR alleles of the human intestinal mucin gene, MUC3. Hum Mol Genet 1999;8:307-11.

2. Kyo K, Muto T, Nagawa H, Lathrop GM, Nakamura Y. Associations of distinct variants of the intestinal mucin gene MUC3A with ulcerative colitis and Crohn's disease. J Hum Genet 2001;46:5-20.

3. Tytgat KMAJ, Büller HA, Opdam FJ, Kim YS, Einerhand AWC, Dekker J. Biosynthesis of human colonic mucin: Muc2 is the prominent secretory mucin. Gastroenterology 1994;107:1352-63.

4. Swallow DM, Vinall LE, Gum JR, Kim YS, Yang H, Rotter JI, Mirza M, Lee JC, Lennard-Jones JE. Ulcerative colitis is not associated with differences in MUC2 mucin allele length. J Med Genet 1999;36:859-60.

5. Tytgat KMAJ, van der Wal JW, Einerhand AWC, Büller HA, Dekker J. Quantitative analysis of MUC2 synthesis in ulcerative colitis. Biochem Biophys Res Commun 1996;224:397-405.

6. Van Klinken BJW, Van der Wal JW, Einerhand AWC, Büller HA, Dekker J. Sulphation and secretion of the predominant secretory human colonic mucin MUC2 in ulcerative colitis. Gut 1999;44:387-93.

7. Makkink MK, Schwerbrock NJ, Van der Sluis M, Büller HA, Sartor RB, Einerhand AWC, Dekker J. Interleukin 10 Deficient Mice Are Defective in Colonic Muc2 Synthesis Both before and after Induction of Colitis by Commensal Bacteria. Gastroonterology, P-26, 254.

8. Campbell BJ, Rowe GE, Leiper K, Rhodes JM. Increasing the intra-Golgi pH of cultured LS174T goblet-differentiated cells mimics the decreased mucin sulfation and increased Thomsen-Friedenreich antigen (Gal beta1-3GalNac alpha-) expression seen in colon cancer. Glycobiology 2001;11:385-93.

9. Enss ML, Cornberg M, Wagner S, Gebert A, Henrichs M, Eisenblatter R, Beil W, Kownatzki R, Hedrich HJ. Proinflammatory cytokines trigger MUC gene expression and mucin release in the intestinal cancer cell line LS180. Inflamm Res 2000;49:162-9.

10. Gouyer V, Wiede A, Buisine MP, Dekeyser S, Moreau O, Lesuffleur T, Hoffmann W, Huet G. Specific secretion of gel-forming mucins and TFF peptides in HT-29 cells of mucin-secreting phenotype. Biochim Biophys Acta 2001;1539:71-84.

11. Gratchev A, Siedow A, Bumke-Vogt C, Hummel M, Foss HD, Hanski ML, Kobalz U, Mann B, Lammert H, Mansmann U, Stein H, Riecken EO, Hanski C. Regulation of the intestinal mucin MUC2 gene expression in vivo: evidence for the role of promoter methylation. Cancer Lett 2001;168:71-80.

12. Van Seuningen I, Pigny P, Perrais M, Porchet N, Aubert JP. Transcriptional regulation of the 11p15 mucin genes. Towards new biological tools in human therapy, in inflammatory diseases and cancer? Front Biosci 2001;6:D1216-34.

Dankwoord

Dankwoord

Elke grote onderneming verloopt niet zonder de hulp en ondersteuning van vele mensen. Dit proefschrift vormt geen uitzondering op deze regel. Al deze personen, te veel om allemaal te noemen, wil ik hierbij hartelijk bedanken voor de morele ondersteuning, technische hulp en gezelligheid. Toch wil ik nog een aantal mensen met name noemen.

Allereerst mijn directe begeleidster dr. Einerhand, beste Sandra, te allen tijde was je bereid om samen te brainstormen over het onderzoek, advies te geven en manuscripten na te kijken. Ik heb een enorme bewondering voor je betrokkenheid, je openheid en je enthousiasme voor het onderzoek. Vaak zaten we 's avonds laat nog in het lab achter de computer, omdat dit of dat nog even af moest. Goede herinneringen bewaar ik aan de congressen (ESPGHAN, AGA/DDW in de USA), wanneer we na een dag vol lezingen en posters tot 's avonds laat onze 'niewe' onderzoeksideeën bespraken. Ook hebben we ontzettend veel lol gemaakt en enorm gelachen na de congressen, tijdens onze woestijn en canyon trips. En niet te vergeten de gezellige bezoekjes aan de Arena om AJAX aan te moedigen. Bedankt voor alles! Enne.....gelukkig ben je geen ballerina geworden!

Dr. Dekker, beste Jan, in het begin was jij nauw betrokken bij mijn onderzoek als directe begeleider. Later volgde jij mijn project op iets meer afstand, doch niet met minder enthousiasme. Altijd was jij bereid om binnen een zeer korte tijd een manuscript te corrigeren en om vragen te beantwoorden over mucinen. Steevast kreeg ik na zo'n vraag een gedetailleerde en dus lange uitleg over mucinen, die eindigde met 'om een lang verhaal ingewikkeld te maken.....'. Je wordt niet voor niets 'DE MUCINE-MAN' genoemd! Je mening en eerlijkheid heb ik enorm gewaardeerd. Bedankt voor je betrokkenheid bij - en inzet voor mijn promotieonderzoek.

Prof. dr. Büller, beste Hans, als promotor volgde jij mijn project van een wat grotere afstand. Tijdens de werk/literatuurbesprekingen toonde je altijd een enorme betrokkenheid en enthousiasme voor ons onderzoek. Als bioloog heb ik veel geleerd van jouw klinische achtergrond en kijk op de verschillende aspecten van het wetenschappelijk onderzoek. Verder delen we samen één grote passie, namelijk AJAX. Dit leidde vaak tot kritische analyses (ahum) van de wedstrijden, spelers, coaches en..... Machlas! Bedankt!

Naast mijn copromotoren en promotor wil ik ook alle co-auteurs bedanken. Met name dr. Taminiau, beste Jan, jouw kennis van het methotrexaat-model vormde een belangrijke basis voor ons onderzoek. De studenten, Sacha Ferdinandusse, Marieke Jorritsma en Nathalie Bulsing heb ik mogen begeleiden tijdens hun stages. Bedankt voor jullie inzet. Danielle van Nispen, bedankt voor je technische ondersteuning tijdens het laatste jaar van mijn promotie onderzoek. We hebben samen hard gewerkt en ook veel lol gehad. Ik ben dan ook erg blij dat jij mijn paranimf wilt zijn. Mijn 'voorgangers', Kristien Tytgat, Jan-Willem van Klinken en Erik van Beers, bedankt voor al jullie adviezen. De huidige lichting promovendi, Melissa Verburg, Jeroen van de Bovenkamp, Jos Boshuizen, Barbara de Koning en Mireille Makkink, succes met jullie onderzoek en proefschriften. De andere (ex)leden van de KG&V, Helen Meijer, John Rossen, Anita Korteland (bedankt voor de vele cappuccino's en

alle technische ondersteuning), Rolien Raatgeep, Dicky Lindenbergh-Kortleve, Maria van der Sluis en Janneke Bouma, bedankt voor jullie hulp en gezelligheid. Mijn dank gaat uit naar iedereen van het laboratorium neurozintuigen (voormalig G2 en K2) in het AMC Amsterdam en het laboratorium kindergeneeskunde aan het Erasmus MC Rotterdam, voor zijn/haar inzet en het creëren van veel gezelligheid. In het bijzonder Theo Hoogenboezem, en nogmaals Dicky, Barbara en Rolien, dankzij jullie heb ik een vliegende start kunnen maken met mijn postdoc project. Paul Koppens, bedankt voor de computer ondersteuning. Wim Rietveld, de door jou ontworpen incubatie bakken en 2D-electrophorese systemen zijn en waren van essentieel belang voor het slagen van mijn experimenten. Verder Jules Meijerink en Arlène van Vliet, bedankt voor de koffie en de gezelligheid!

De Nijmeegse Rugby Club de Wasps ben ik dankbaar voor de broodnodige ont/inspanning die ze mij de afgelopen tijd hebben geboden. In het bijzonder alle Lady Wasps, dames bedankt enne..... dit jaar worden we kampioen!

Via this research project I also met Dr Van Seuningen, dear Isabelle, thanks for your friendship, support for my work and scientific discussions and everything else! I'm grateful for your peer reviewing of some of my manuscripts, before they were submitted. I'm looking forward to our collaboration! Mijn vriendinnen Linda Everse en Monique Bernsen. Lieve Linda en Monique, jullie hebben mij geleerd om echt te ontspannen (Swiss life-en). Vanaf het begin van mijn promotie-onderzoek (en ook al daarvoor) hebben jullie mij bij gestaan met raad en daad. Bedankt voor de vele wetenschappelijke discussies, gezellige momenten (zoals wandelen met de honden, vakantie in de Harz), hulp en bovenal jullie vriendschap. Thanks ladies!

Mijn familie, mijn broer Pierre en Wijnanda, ook al konden jullie mij af en toe niet volgen, toch toonden jullie veel interesse voor mijn werk. Mijn ouders, lieve paps en lieve mams, jullie waren en zijn er altijd voor mij. Dankzij jullie onvoorwaardelijke liefde en steun ben ik geworden wie ik nu ben. Zonder die rustige thuishaven zou het allemaal veel moeilijker zijn geweest. Bedankt!

Op naar de volgende uitdaging!

Ingrid

Curriculum vitae & Publications

Curriculum vitae

The author of this thesis was born on the 27th of April, 1970 in Zeist, The Netherlands. She spent her childhood years in Soesterberg. From August 1982 till June 1989, she attended the Rijks Scholengemeenschap Thorbecke in Amersfoort. In August 1989 she started to study Biology at the Utrecht University and passed her propadeutic exam in 1990. She fulfilled her MSc research projects at the Department of Experimental Zoology (Dr. J Peute, Dr RW Schulz), Utrecht University, and at the Department of Radiotherapy (Dr. IM Jürgenliemk-Schulz, Dr. DH Rutgers), Academic Hospital Utrecht and the Department of Functional Morphology (Dr. LA Everse), School of Veterinary Medicine, Utrecht. Additionally, a MSc research project was performed via the Erasmus Exchange program at the Laboratory of Applied Physiology of Aquatic Sciences, (Prof. dr. J Coimbra), University of Porto, Portugal, after which she graduated as MSc in Biology in August 1995. In October 1995, she joined the Research Group of Pediatric Gastroenterology & Nutrition (Dr. A.W.C. Einerhand, Dr. J. Dekker, Prof. dr. H.A. Büller) at the Academic Medical Center Amsterdam, where the work described in this thesis was started. In Februari 1998 the research group moved towards the Laboratory of Pediatrics at the Erasmus MC in Rotterdam, where the work was continued. From August 2001, she is employed as a Research Associate (post-doc) at the Laboratory of Pediatrics, Pediatric Gastroenterology & Nutrition (Dr. A.W.C. Einerhand, Prof. dr. H.A. Büller), Erasmus MC, Rotterdam, where she studies mouse small intestinal development before and after birth.

Publications

IB Renes, M Verburg, NP Bulsing, S Ferdinandusse, HA Büller, J Dekker and AWC Einerhand. Protection of the Peyer's patch-associated crypt and villus epithelium against methotrexate-induced damage is based on its distinct regulation of proliferation. *Journal of Pathology,* 198:60-68 (2002).

IB Renes, M Verburg, DJPM Van Nispen, JAJM Taminiau, HA. Büller, J Dekker, and AWC Einerhand. Epithelial proliferation, cell death, and gene expression in experimental colitis: *alterations in carbonic anhydrase I, mucin MUC2, and trefoil factor 3 expression. Int J Colorectal Dis,* 17(5):317-26 (2002).

IB Renes, M Verburg, DJPM Van Nispen, JAJM Taminiau, HA Büller, J Dekker and AWC Einerhand. Distinct epithelial responses in experimental colitis: *implications for ion uptake and mucosal protection. Am J Physiol,* 283:G169-G179 (2002).

IB Renes, JA Boshuizen, DJPM Van Nispen, NP Bulsing, HA Büller, J Dekker and AWC Einerhand. Alterations in Muc2 biosynthesis and secretion during dextran sulfate sodium-induced colitis. *Am J of Physiol,* 282:G382-G389 (2002).

AWC Einerhand, IB Renes, MK Makkink, M Van der Sluis, HA Büller, J Dekker. Role of mucins in inflammatory bowel disease: Important lessons from experimental models. Eur. J Gastroenterol Hepathol, 14:757-765 (2002).

MK Makkink, NJM Schwerbrock, M Mähler, JA Boshuizen, IB Renes, M Cornberg, HJ Hedrich, AWC Einerhand, HA Büller, S Wagner, ML Enss, and J Dekker. Fate of goblet cells in experimental colitis. *Dig Dis Sci,* 46:2286-2297 (2002).

M Verburg, IB Renes, HP Meijer, S. Ferdinandusse, M Jorritsma, HA Büller, AWC Einerhand, J Dekker. Carbohydrate and amino acid metabolizing enzymes are specifically repressed during methotrexate-induced villus atrophy in the small intestine of the rat. *J Histochem Cytochem, in press.*

M Verburg, IB Renes, HP Meijer, JAJM Taminiau, HA Büller, AWC Einerhand, J Dekker. Selective sparing of goblet cells and Paneth cells in the intestine of methotrexate-treated rats. *Am J Physio*l, 279:G1037-G1047 (2000).

J Dekker, BJW Van Klinken, KMAJ Tytgat, GR Van den Brink, JHB Van de Bovenkamp, M Verburg, IB Renes, HA Büller, AWC Einerhand. Regulation of Mucin Expression in the Gastrointestinal Tract. In: Digestive mucus, from research to clinical implications. Bara J, Christen Y, Droy-Lefaix MT, eds, Irvinn Editions, Neuilly-sur-Seine, France, pp19-32 (2000).

BJW Van Klinken, AWC Einerhand, LA Duits, MK Makkink, KMAJ Tytgat, IB Renes, M Verburg, HA Büller, J Dekker. Gastrointestinal expression and partial cDNA cloning of murine Muc2. *Am J Physiol,* 276: G115-G124 (1999).

LA Everse, IB Renes, IM Jürgenliemk-Schulz, DH Rutgers, MR Bernsen, HFJ Dullens, W Den Otter, and JJ Battermann. Local low-dose Interleukin-2 induces systemic immunity when combined with radiotherapy of cancer. A preclinical study. *International Journal of Cancer,* 72:1003-1007 (1997).

IM Jürgenliemk-Schulz, IB Renes, DH Rutgers, LA Everse, MR Bernsen, W Den Otter, and JJ Battermann. Anti-tumor effects of local irradiation in combination with peritumoral administration of low doses of recombinant interleukin-2 (rIL-2). *Rad Oncol Invest,* 5:54-61 (1997).

RW Schulz, IB Renes, MA Zandbergen, W van Dijk, J Peute, and HJTh Goos. Pubertal development of male African Catfish (*Clarias gariepinus*): Pituitary ultrastructure and responsiveness to GnRH. *Biology of Reproduction*, 53:940-950 (1995).

Appendix

Color plates

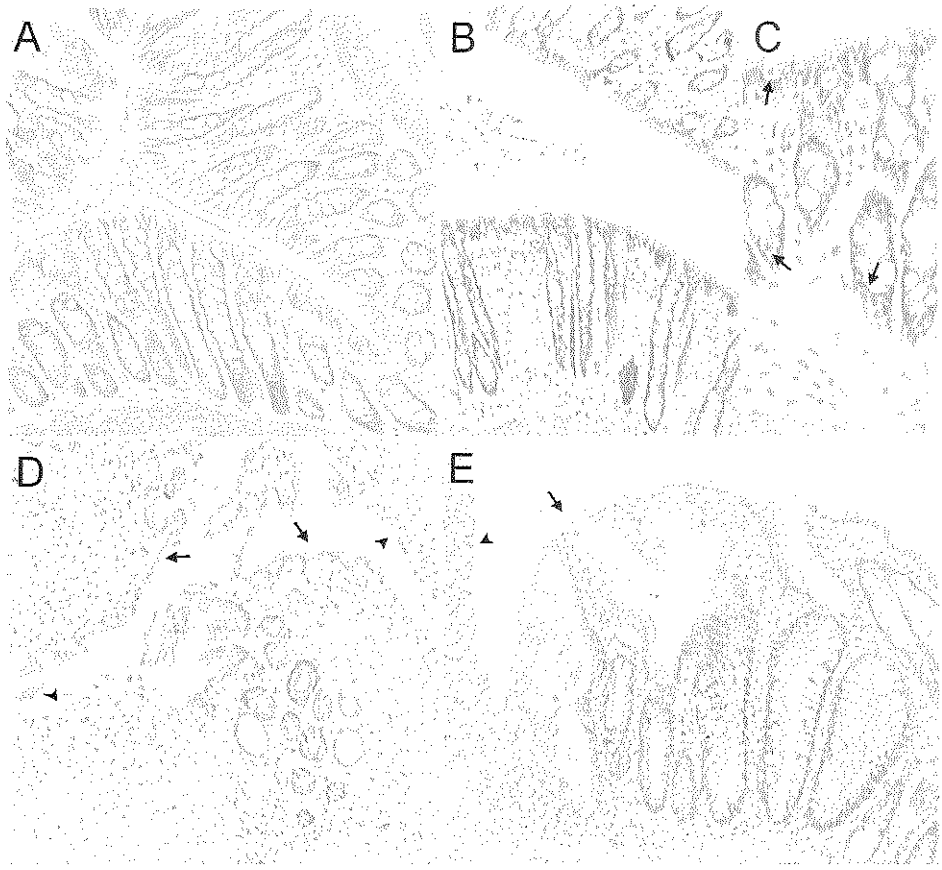

Chapter 3, Figure 2. Epithelial morphology and apoptosis before, during and after DSS treatment. HE-staining of the distal colon. Morphology of controls (A), after 2 days (B and C), and after 7 days of DSS treatment (D). Distal colon at day 28, 21 days after the end of DSS administration (E). Apoptotic cells are indicated by arrows (C). Flattened surface epithelium and erosions are indicated by arrows and arrowheads, respectively (D and E).

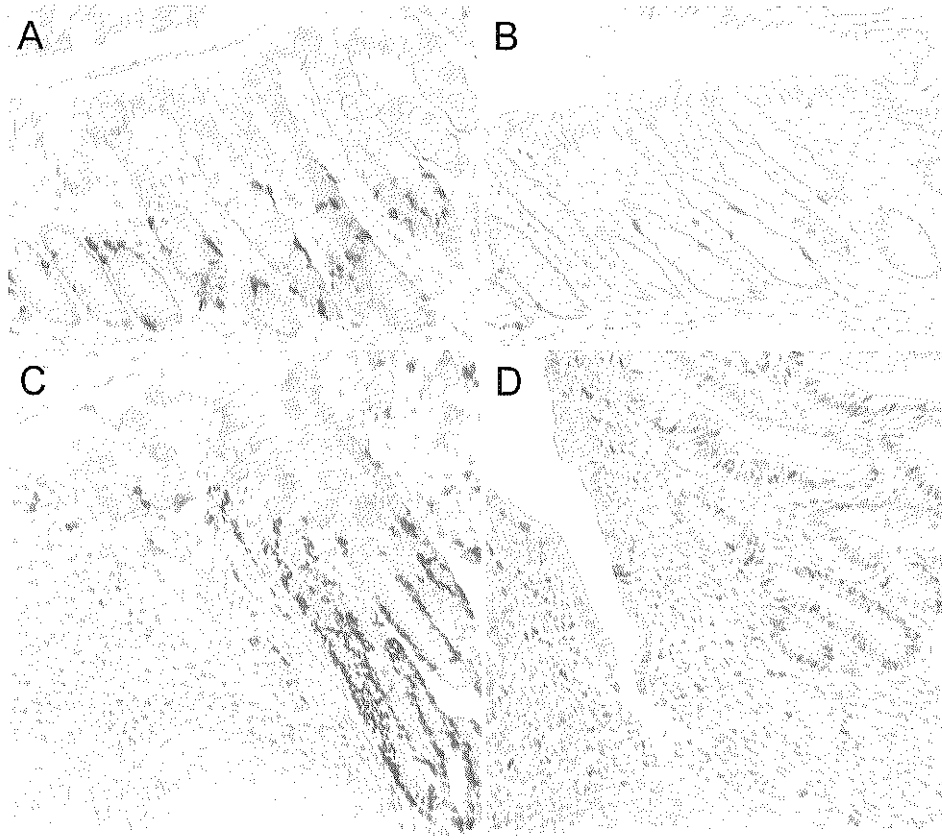

Chapter 3, Figure 3. Effect of DSS treatment on epithelial proliferation as measured by BrdU incorporation into the distal colon. BrdU-positive epithelial cells were confined to the lower half of the crypts in control tissue (A). The number of BrdU-positive cells was decreased at day 2 in distal colon (B) as compared to control tissue. Continuation of DSS treatment resulted in a strong increase in the number of BrdU-positive cells in the proximity of ulcerations in the distal colon on day 7 (C). Note that BrdU-positive cells were seen from crypt base to almost the surface epithelium. On day 28, 21 days after the last DSS administration, elevated levels of BrdU-positive cells were still observed near ulcerations in the distal colon (D).

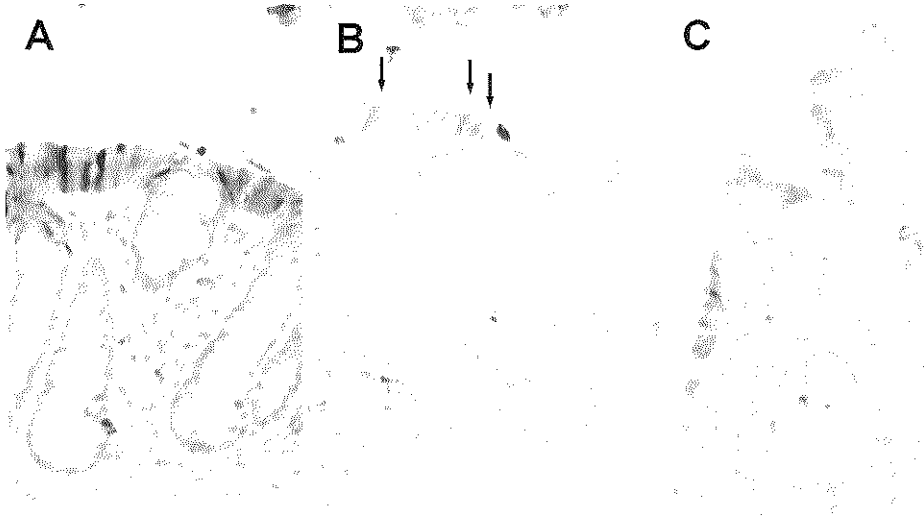

Chapter 3, Figure 4. Effects of DSS on surface enterocytes in the distal colon. Surface enterocytes were identified by CA I expression in the colon of control rats (A), after 7 days of DSS treatment (B) and on day 28 during the recovery phase (C). The CA I-positive cells during active disease (day 7) are indicated by arrows (B).

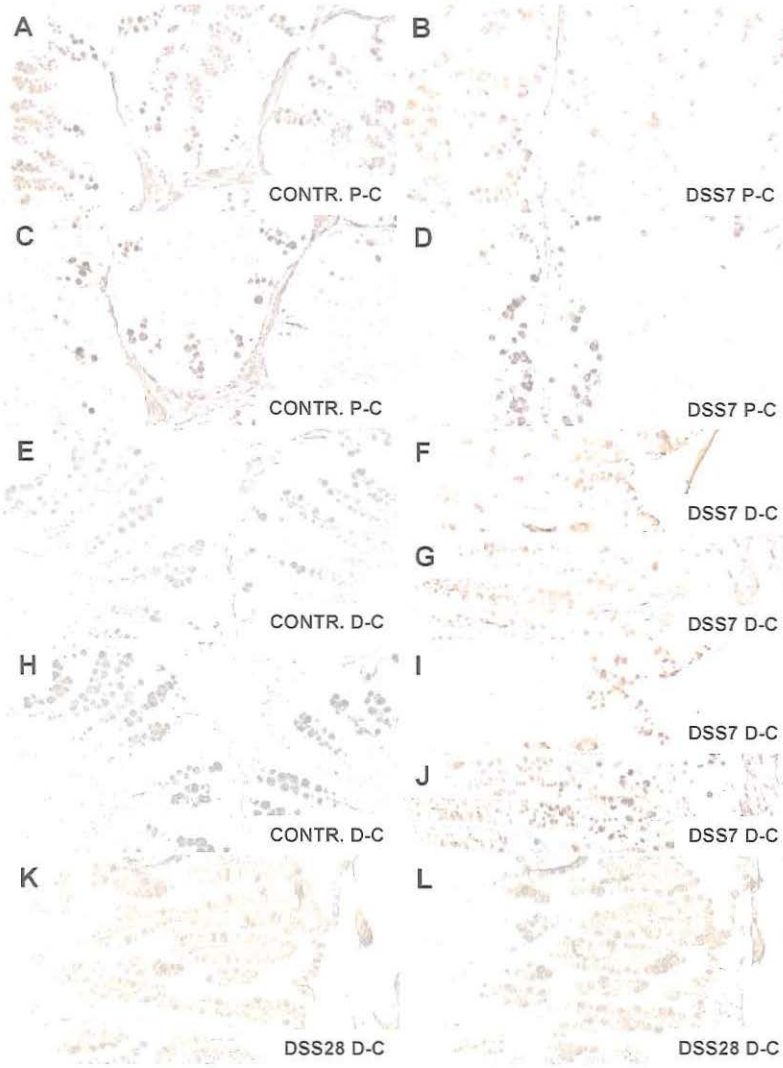

Chapter 3, Figure 6. Effects of DSS on goblet cells in the proximal and distal colon. Goblet cells in the proximal colon (A-D) and distal colon (E-L) were identified by detection of Muc2 - (A, B, E-G and K) and TFF3 expression (C, D, H-J and L). Goblet cells in control tissue (A, C, E and H), after 7 days of DSS treatment (B, D, F, G, I and J), and on day 28, 21 days after the end of DSS administration (K and L). Note the accumulation of goblet cells in the surface epithelium of the proximal colon on day 7 (B and D), the expression of TFF3 at the bottom of the crypts in the distal colon on day 7 (J), the accumulation of goblet cells in the surface epithelium on day 7 (F and I) and day 28 (K and L), and the large goblet cells in the elongated crypts on day 28 (K and L). Contr., control; pc, proximal colon;dc, distal colon; DSS7, day 7 of DSS treatment; DSS28, day 28 *i.e.* 21 days after the end of DSS treatment.

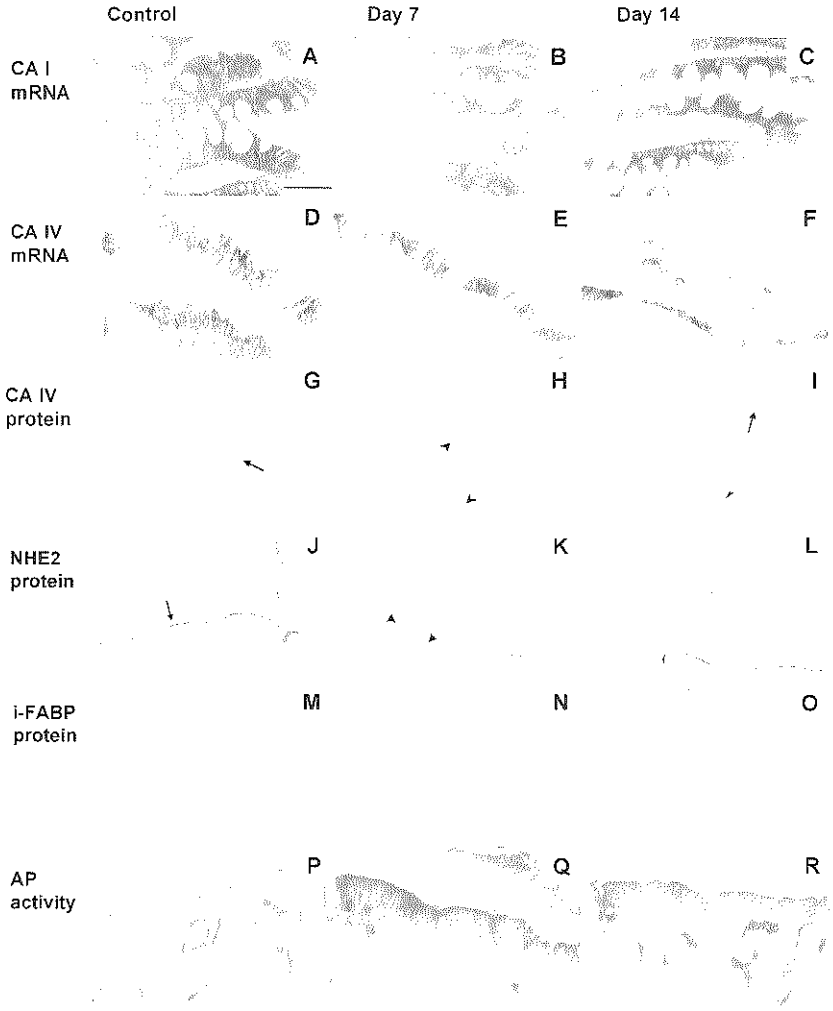

Chapter 4, Figure 1. Localization of enterocyte-specific gene expression during DSS-induced colitis. Expression of enterocyte-specific genes in controls (A, D, G, J, M, P), at day 7 of DSS treatment (B, E, H, K, N, Q), and at day 14 (C, F, I, L, O, R). CA I mRNA expression in the proximal colon (A-C); CA IV mRNA expression in the distal colon (D-F); CA IV protein expression in the distal colon (G-I); NHE2 protein expression in the distal colon (J-L); i-FABP protein expression in the proximal colon (M-O); AP activity in the proximal colon (P-R). Arrows indicate normal/normal appearing surface epithelium positive for CA IV protein (G and I) and NHE2 (J) protein. Large arrowheads indicate flattened surface epithelium negative for CA IV protein (H) and NHE2 (K) protein. Small arrowheads indicate flattened surface epithelium positive for CA IV protein (I) and NHE2 protein (L). Sections in panel J-L were counterstained with hematoxylin. Bar in panel A represents 39 μm, magnifications of panel A-R are similar.

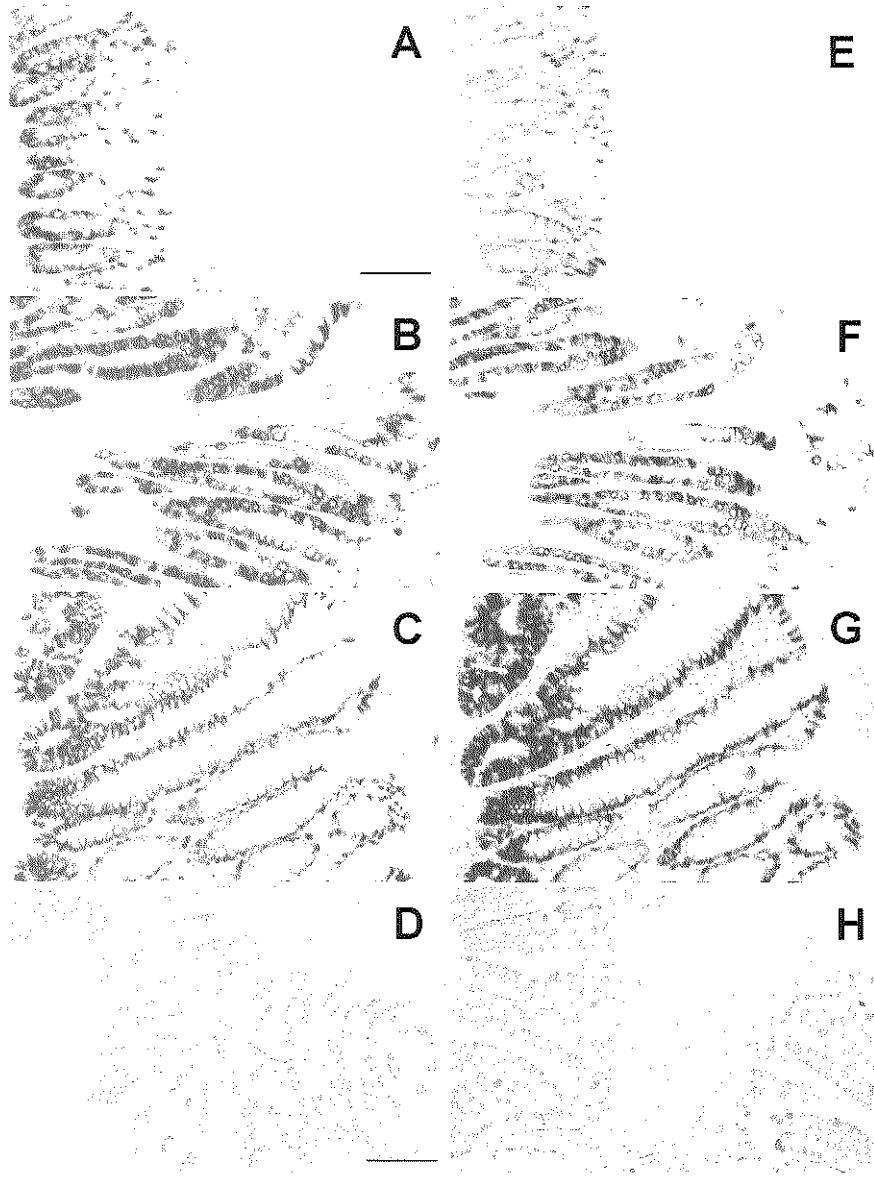

Chapter 4, Figure 4. Localization of goblet cell-specific gene expression during DSS-induced colitis. Expression of Muc2 mRNA (A-C) and protein (D and H), TFF3 mRNA (E-G) in the distal colon of controls (A, D and E), at day 7 of the DSS treatment (B and F), and at day 14 (C, G, and H). Sections used for immunohistochemistry were counterstained with hematoxylin (D and H). Note the accumulation of Muc2-positive goblet cells in the elongated crypts and surface epithelium at day 14 (H). Bar in panel A represents 110 μm, magnifications of panel A-C and E-G are similar. Bar in panel D represents 215 μm, magnifications of panel D and H are similar.

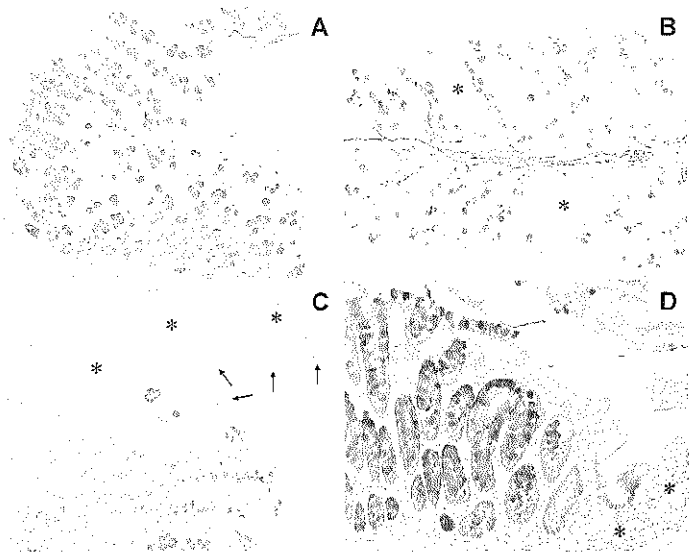

Chapter 5, Figure 1. Epithelial damage during and after DSS treatment. Muc2 staining of goblet cells in the distal colon using the WE9 monoclonal antibody and hematoxylin as counterstain. Morphology of control tissue (panel A), during onset of disease (day 2, panel B), active disease (day 7, panel C), and the regenerative phase (day 14, panel D). Areas with crypt loss and ulcerations are indicated by asterisks and arrows, respectively.

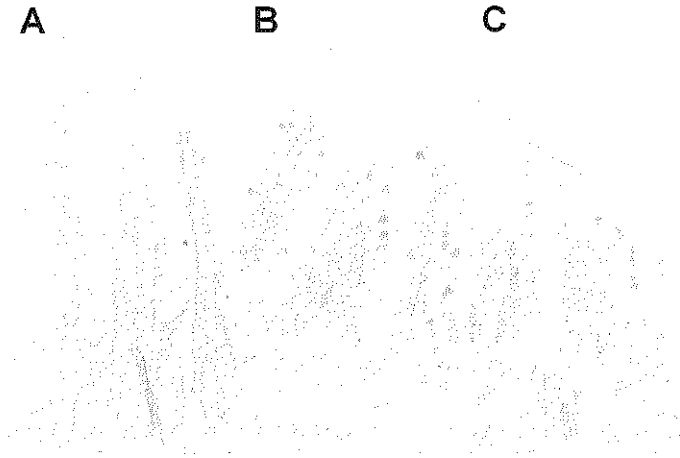

Chapter 6, Figure 1. Morphology of the jejunal epithelium before and after MTX-treatment. Alcian Blue-Nuclear Fast Red staining. A, control; B, day 2 after MTX; C, day 4 after MTX. Crypt atrophy (B), villus atrophy and flattening of crypt - and villus epithelial cells (C) were observed after MTX treatment.

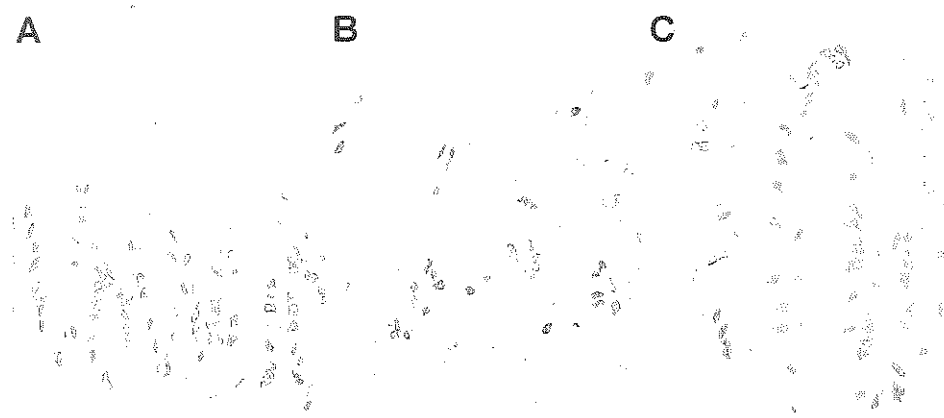

Chapter 6, Figure 3. Epithelial proliferation in the ileum. A, control; B, day 2 after MTX; C, day 4 after MTX. Note that the number of BrdU-positive cells was strongly decreased at day 2 after MTX (B), and increased at day 4 (C).

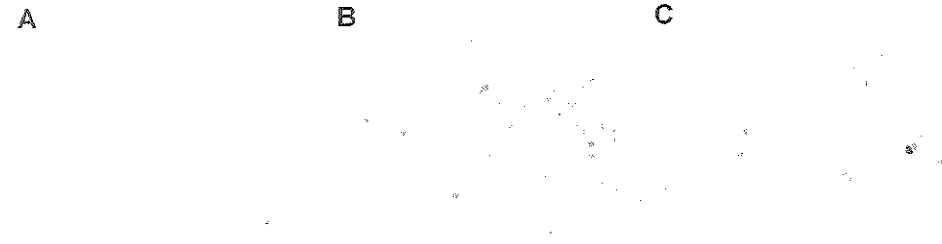

Chapter 6, Figure 4. MTX-induced apoptosis in the jejunum. A, control rat; B, 6.5 h after MTX; C, day 2 after MTX. Caspase-3-positive cells were present 6.5 h and 2 days after MTX in the crypt epithelium.

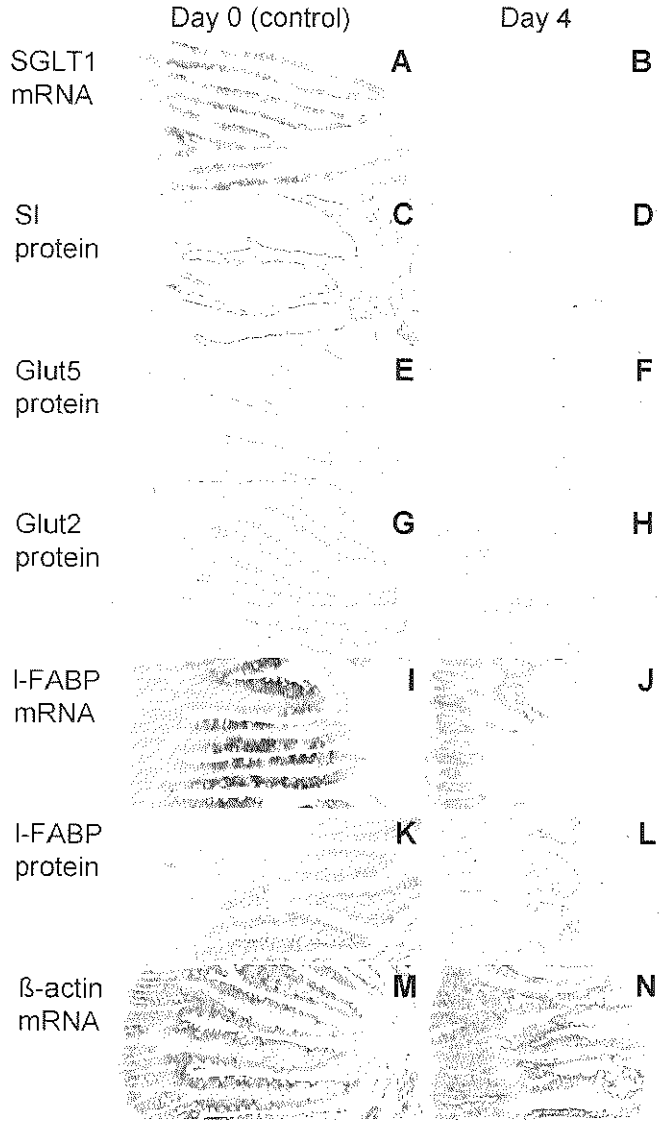

Chapter 6, Figure 5. Effects of MTX on enterocyte-specific gene expression in the small intestinal epithelium. A, C, E, G, I, K, M: control epithelium; B, D, F, H, J, L, N: epithelium on day 4 after MTX; A, B, E, F, G, H: duodenum; C, D, I, J, K, L, M, N: jejunum. SGLT1 mRNA (A), SI protein (C), Glut5 protein (E), Glut2 protein (G), and I-FABP mRNA (I), I-FABP protein (K), and ß-actine mRNA (M) were expressed in the small intestinal epithelium of controls. Four days after MTX, SGLT1 mRNA (B), SI protein (C), Glut5 protein (F) Glut2 protein (H), and I-FABP mRNA (J) and protein (L) were not expressed or less expressed in the villus epithelium. Note that ß-actine mRNA was still detectable at high levels at day 4 after MTX (N).

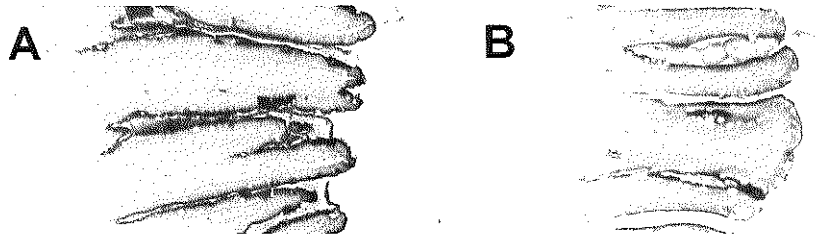

Chapter 6, Figure 6. Enterocyte-specific in situ alkaline phosphatase (AP) activity in the jejunum before and after MTX treatment. AP-activity in controls (A) and at day 4 after MTX (B). Note that enterocytes remained their capacity to synthezise active AP after MTX treatment.

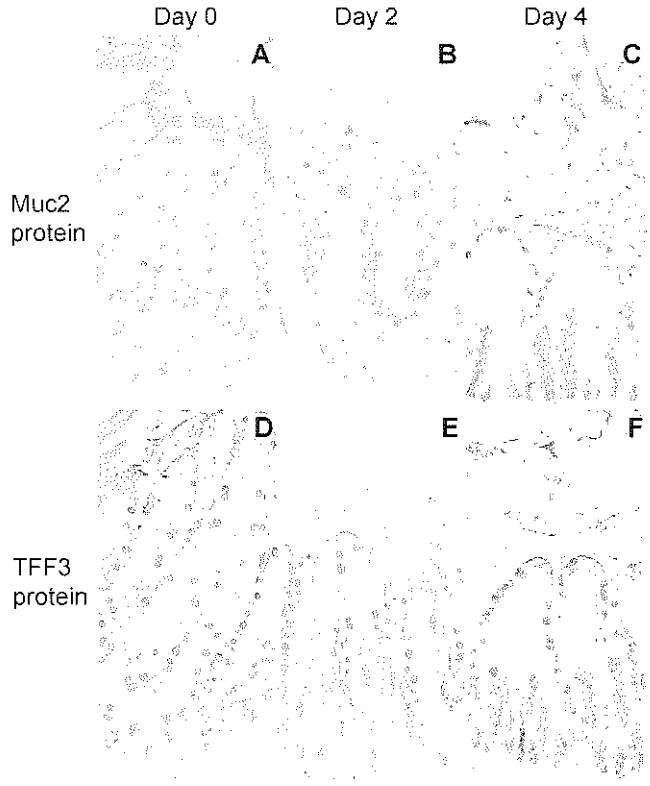

Chapter 6, Figure 7. Effects of MTX treatment on goblet cell-specific gene expression in the jejunal epithelium. A and D, controls; B and E, day 2 after MTX; C and F, day 4 after MTX. In control rats, Muc2 protein (A) and TFF3 protein (D) were normally expressed by goblet cells in the crypts and along the villi. At day 2, goblet cells in the crypts were flattened but continued to express both Muc2 protein (B) and TFF3 protein (E). At day 4 after MTX, goblet cells positive for Muc2 protein (C) and TFF3 protein (F), and accumulated in the crypts and at the tips of the villi.

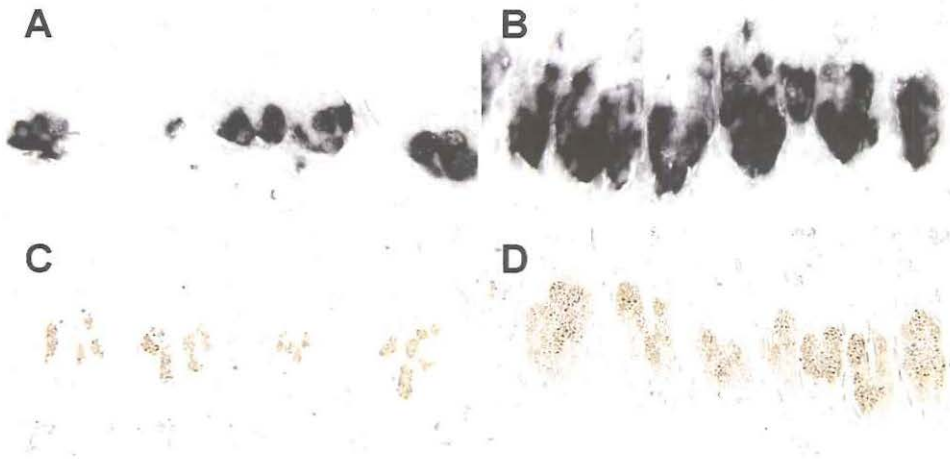

Chapter 6, Figure 8. Effects of MTX on Paneth cell-specific gene expression in the ileum. A and C, controls; B and D, day 2 after MTX. Lysozyme mRNA (A) and protein (C) were normally expressed by Paneth cells in the crypts. At day 2 after the number of Paneth cells, and both lysozyme mRNA (B) and protein (D) seemed to be up-regulated.

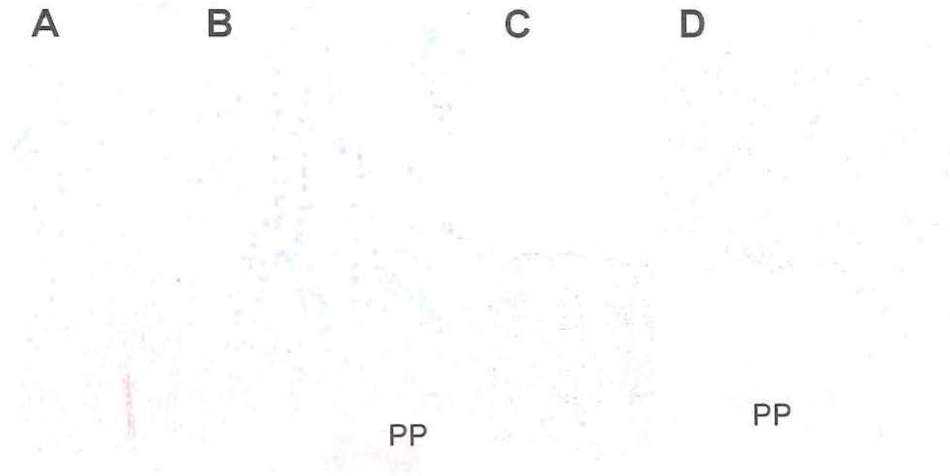

Chapter 7, Figure 1. Morphology of the normal jejunal epithelium (*i.e.* 'non-patch (NP) epithelium) and the jejunal epithelium near and lining Peyer's patches (PP) (*i.e.* PP epithelium) before and after MTX-treatment. Alcian Blue-Nuclear Fast Red staining. A and B: jejunum of control rat; C and D: jejunum 4 days after MTX treatment. Villus atrophy and flattening of crypt - and villus epithelial cells were observed in the normal intestinal epithelium, *i.e.* 'non-patch' (NP) epithelium on day 4 (C). The epithelium up to 2-3 crypt-villus units next to and lining Peyer's patches (PPs), *i.e.* the PP epithelium appeared to be spared from damaged (D).

Chapter 7, Figure 3. MTX-induced apoptosis in the normal intestinal epithelium (*i.e.* 'non-patch' (NP) epithelium) and the epithelium near and lining Peyer's patches (PP) (*i.e.* PP epithelium). A: jejunum of control rat; B: jejunum 6.5 hrs after MTX; jejunum 2 days after MTX. Caspase-3-positive cells were present 6.5 hrs and 2 days after MTX in the NP - and PP epithelium. Some crypts are indicated with asterisks.

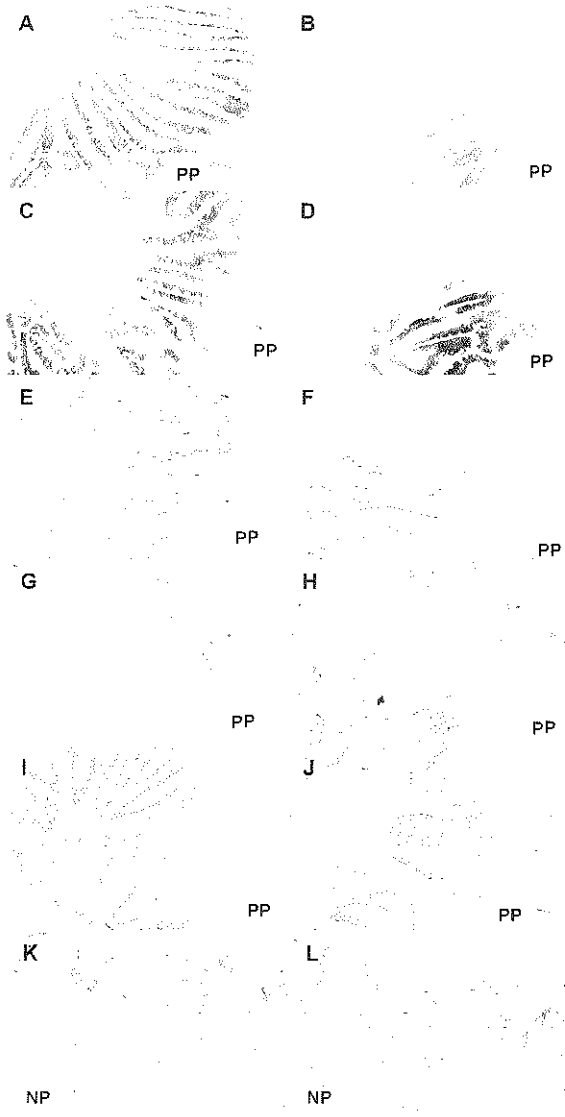

Chapter 7, Figure 4. Effects of MTX on enterocyte-specific gene expression in the normal intestinal epithelium (*i.e.* 'non-patch (NP) epithelium) and the epithelium near and lining Peyer's patches (PP) (*i.e.* PP epithelium). A, C, E, G, I: jejunum of controls; B, D, F, H, J, K, L: jejunum on day 4 after MTX. SGLT1 mRNA (A), l-FABP mRNA (C), SI protein (E), Glut2 protein (G), and l-FABP protein (I) were expressed in the NP - and PP epithelium in controls. Four days after MTX, SGLT1 mRNA (B), l-FABP mRNA (D), SI protein (F), Glut2 protein (H) and l-FABP protein (J) were expressed at high levels in the PP epithelium, but were not expressed or less expressed in the NP epithelium. L-FABP protein (K) and i-FABP protein (L) were expressed in the PP epithelium and in some cells of the NP epithelium at day 4.

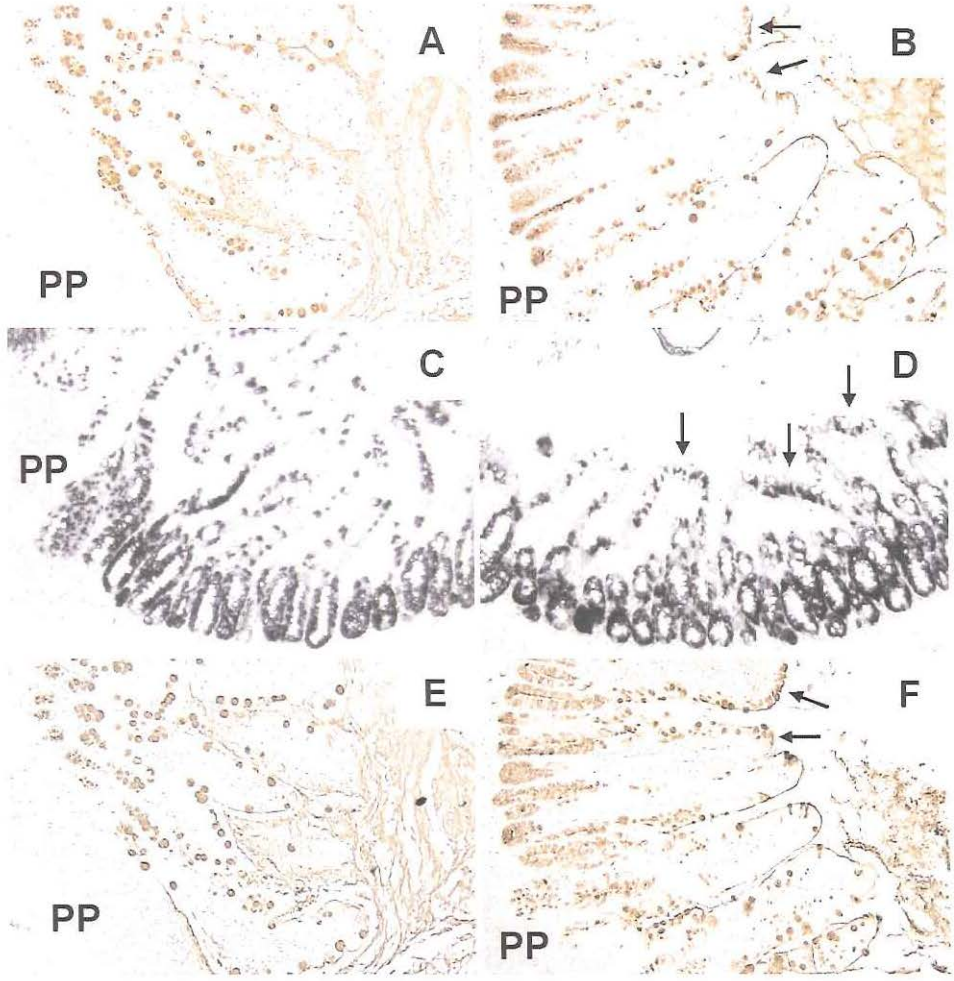

Chapter 7, Figure 5. Effects of MTX treatment on goblet cell-specific gene expression in the 'non-patch' (NP) epithelium and the epithelium near and lining Peyer's patches (PP). A and E: rat control jejunum; B, C, D, and F, rat jejunum 4 days after MTX treatment. Muc2 protein (A) and TFF3 protein (E) were normally expressed by goblet cells in both the PP - and NP epithelium. Four days after MTX treatment, goblet cell-specific Muc2 mRNA was maintained both in the PP epithelium (C) and NP epithelium (D). Muc2 protein (B) and TFF3 protein (F) expression were also maintained in the PP - and NP epithelium at day 4. Note that in the NP epithelium goblet cells seemed to accumulate at the villus tips (arrows).

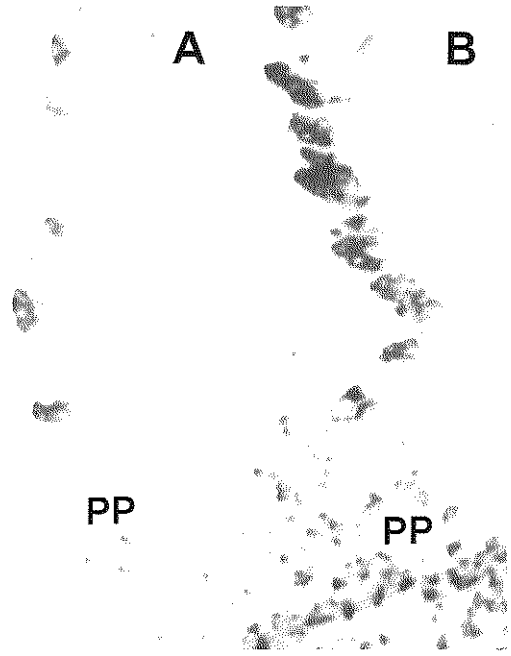

Chapter 7, Figure 6. Effects of MTX on Paneth cell-specific gene expression in the 'non-patch' (NP) epithelium and the epithelium near and lining Peyer's patches (PP). Lysozyme mRNA was expressed by Paneth cells in the NP - and PP epithelium, and by immunocompetent cells within the PP (A). Two days after MTX treatment lysozyme mRNA seemed to be up-regulated in the NP - and PP epithelium and in immunocompetent cells within the PP.